NTNU – Trondheim
Norwegian University of
Science and Technology

Optimization of NMR Data Utilization on Valhall - a Brown Chalk Oilfield

Katrine Ropstad Ånensen

Petroleum Geoscience and Engineering
Submission date: June 2015
Supervisor: Tom Aage Jelmert, IPT

Norwegian University of Science and Technology
Department of Petroleum Engineering and Applied Geophysics

ACKNOWLEDGEMENT

I would like to thank my supervisor Tom-Aage Jelmert, Professor at the Norwegian University of Science and Technology (NTNU), department of Petroleum Engineering and Applied Geophysics, for help and comments during the work.

I would also like to thank BP Norway for giving me the opportunity to write this thesis, for providing me with the subject and the data, and for the support.

At last, a special thanks to Nils-Andre Aarseth and Boris D'arcy, petrophysicists at BP, for comments, guidance and proofreading throughout the work of the thesis. Your help has been very valuable and highly appreciated.

Katrine Ropstad Ånensen

Stavanger, June 2015

SUMMARY

The Valhall field started production in 1982 and has been producing since. A vast amount of data has been gathered and interpreted since then. Because of its complexity, there are still many questions left unanswered. Some are questions related to the water flooding system; in-fill wells are drilled, and logging data detects unexpected water. Where does the water come from and why? Others are related to the confidence in estimated target parameters such as water saturation, porosity and permeability. Can this data contribute to increase the confidence in them? Valhall is a brown chalk field. It is a complex, mature field and consists of tight, fractured chalk. Successful reservoir management requires good understanding of the reservoir and the data.

The Nuclear Magnetic Resonance is a fairly old technology and is well understood. It has a great potential of providing useful information along the wellbore. Data have been acquired from the reservoir but the applications in the Valhall reservoir management has not been exploited to its full potential. It has been used as a secondary source of porosity and saturation and used if no other source of such information has been available.

The objective of the present study is to optimize the utilization of NMR data on Valhall through investigation of the current applications and possible additional applications. Investigations are done on the data quality, porosity, fluid saturations, permeability and the possibility of improving the understanding of water flooding. Moreover parameters are optimized to better fit conventional logs. Its applicability for well placement and Geosteering are discussed. The results lead to the conclusion that data is useful, trustworthy, and recommended for use in future operations. The extra information NMR provides regarding bound and movable water is added value and very useful in waterflood surveillance. NMR data provides important information about key reservoir properties.

SAMMENDRAG

Valhallfeltet startet produksjonen i 1982 og har produsert siden. En enorm mengde data har blitt samlet inn og tolket siden den gang. På grunn av sin kompleksitet er det enda mange ubesvarte spørsmål igjen. Noen spørsmål er relatert til vannfløммingssystemet; innfyllingsbrønner blir boret, og målingsutstyr oppdager overraskende at det er vann til stede. Hvor stammer dette vannet fra og hvorfor? Andre spørsmål er relatert til troverdigheten til beregnede parametere som vannmetning, porøsitet og permeabilitet. Kan denne type data bidra til å øke tilliten til dem? Valhall er et brunt krittfelt. Det er et kompleks og modent felt som består av tett men oppsprukken krittbergart. Suksessfull reservoarforvaltning krever god forståelse av reservoaret og av dataene.

Kjernemagnetisk resonans (NMR) er en nokså gammel teknologi og velforstått. Denne teknologien har et stort potensiale for å gi nyttig informasjon på kontinuerlig vis langs brønnbanen. Slike målinger har blitt innsamlet fra reservoaret men har ikke blitt anvendt i sitt fulle potensiale i forvaltningen av reservoaret. De har blitt brukt som en sekundær kilde for porøsitet og vannmetning hvis intet annet har vært tilgjengelig.

Formålet til denne studien er å optimalisere anvendelsen av NMR data fra Valhall-feltet gjennom å undersøke nåværende bruksområder og andre mulige anvendelser. Undersøkelser ble gjort på datakvalitet, porøsitet, væskemetninger, permeabilitet og muligheten for å øke forståelsen av vannfløмming. Videre ble parametere optimert til å bedre overlappe de tradisjonelle loggene. Dens anvendbarhet for brønnplassering og Geosteering er diskutert. Resultatene leder til den konklusjon at disse målingene er meget nyttige, pålitelige og anbefalt brukt i videre arbeid. Den ekstra informasjonen NMR gir angående bundet og mobilt vann gir merverdi og er veldig nyttig i vannfløммingsovervåkningen. NMR gir viktig informasjon om reservoarets nøkkelegenskaper.

TABLE OF CONTENTS

TABLE OF FIGURES

1 INTRODUCTION

Nuclear Magnetic Resonance is a lithology-independent logging principle based on magnetic interaction of hydrogen nuclei. It provides porosity, permeability and fluid saturations as well as pore size distribution. No other logging tool is able to provide this diversity of reservoir properties all at once. More complex analysis also provides fluid characterization, wettability and capillary pressure curves amongst others.

Valhall is an *Upper Cretaceous* chalk field situated in the southernmost part of the Norwegian North Sea. Production has been ongoing for several decades, since 1982. Baker Hughes' MagTrak has been run-while-drilling in five wells. It is their Logging-While-Drilling NMR tool. It has the benefit of giving real-time data as the well is being drilled and there are no matrix or borehole effects. In addition, core studies have been conducted but these are few and not from the same wells as the log data.

The motivation for this study is to investigate the usefulness, robustness and further applications of NMR data in order to improve the comprehension of the reservoir and decrease uncertainties related to reservoir management. After the logging job is complete the service company executing the job will produce a report complete with the measured data. This data and the applications are the subject of this investigation. The emphasis will lie on specific issues which have been encountered within the field management and will provide answers to questions that so far remain unanswered.

This will be carried out through analysis of data from five wells containing newer NMR data. The software Techlog (from Schlumberger) will mainly be used. The analysis will focus on data confidence and areas of utility. How confidently can the data be used for porosity and saturation calculations when other sources are unavailable? Can NMR support the waterflood surveillance? Does NMR give reliable permeability estimations? Can NMR be used to improve Geosteering? These are the kind of questions this study will attempt to answer.

2 NUCLEAR MAGNETIC RESONANCE LOGGING

This chapter is partly taken and modified from the specialization project written by the author (Ånensen, 2014) and aims to give the reader a good understanding of the principals behind the NMR data and analysis.

2.1 PHYSICS

Nuclear magnetism is a nuclei's response to an imposed external magnetic field. Many atomic nuclei have magnetic momentum and spin, notably those with an odd number of protons, neutrons or both. The nucleus spins around the magnetic field's orientation. The spinning of all the nuclei produces a magnetization to occur which is measurable by the logging tool. Most of the different nuclei found in the downhole formations do not give strong enough signals that can be measured with a NMR logging tool. The hydrogen atom, with its one proton, has a relatively large magnetic moment and produces a strong signal. Most of the hydrogen atoms in the formation are present in the formation fluids. There are also other hydrogens, but they are locked in a crystal lattice and have smaller magnetic momentum because they have a restricted ability to spin. This is not measurable for the logging tools. Thus the signal measurement is only sensitive to the formation fluids. (Coates et al., 2000)

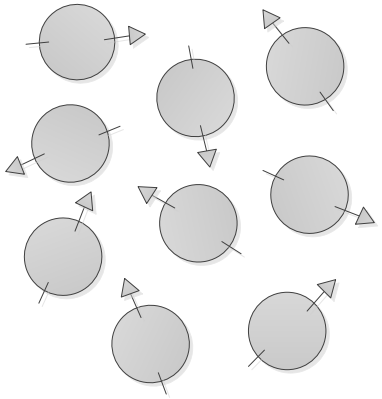

FIGURE 1: PROTONS RANDOMLY ORIENTATED IN ABSENCE OF EXTERNAL MAGNETIC FIELD

The protons act as small bar magnets randomly oriented in absence of an external magnetic field as seen in Figure 1. They then have a net magnetization equal to zero. In order to make a NMR measurement, a permanent static magnetic field $\mathbf{B_0}$ must first be applied to polarize the protons. $\mathbf{B_0}$ will exert a torque on the protons so that they align along with $\mathbf{B_0}$ and spin, a movement called precession. Precession is the movement of a spinning object. The object

spins because a torque is applied to it. This makes the axis of the spinning object to be oriented perpendicular to the torque.

The protons precess around the axis of $\mathbf{B_0}$, illustrated by Figure 2, with a frequency f called the Larmor frequency, given by equation (1):

$$f = \frac{\gamma B_0}{2\pi} \tag{1}$$

γ is the gyromagnetic ratio, which is a measure of the strength of the nuclear magnetism. For hydrogens $\frac{\gamma}{2\pi} = 42.58\,{}^{MHz}/_{Tesla}$. Equation (1) shows that the Larmor frequency is proportional to the magnitude of the static magnetic field. The strength of the magnetic field is position dependent and will decrease away from the source. This implies that the Larmor frequency also is position dependent. Due to the tool's geometry the crucial parameter is the radial distance from the source. So by changing the frequency, different depths of investigation (DOI) can be obtained.

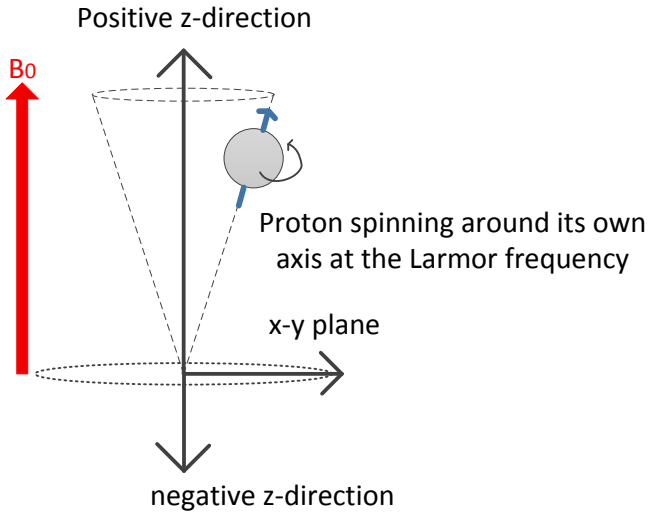

FIGURE 2: ILLUSTRATION OF A PRECESSING PROTON

According to the theories of quantum mechanics a proton is forced into one of two energy states when it is exposed to an external magnetic gradient field. This is a high energy or a low energy level. The energy state depends on the orientation of the precessional proton; if the orientation is the same as the external magnetic field, $\mathbf{B_0}$, it is the low energy state. The opposite direction means high energy state. This splitting is called the Zeeman splitting (Coates et al., 2000) and is the cause of the bulk magnetization $\mathbf{M_0}$. $\mathbf{M_0}$ is defined as the net magnetic moment per unit volume and is given by Curie's law as (Eq.2)

$$\boldsymbol{M_0} = N\frac{\gamma^2 h^2 I(I\gamma+1)}{3(4\pi^2)kT_K}\boldsymbol{B_0} \quad (2)$$

Here N is the number of nuclei per unit volume. k is the Boltzmann's constant, T_K is temperature (in Kelvin), h is Planck's constant, and I is the spin quantum number of nucleus. The macroscopic magnetization M_0 is measurable and proportional to the number of protons (N), the magnitude of $\mathbf{B_0}$ and the inverse of the absolute temperature (T_K).

The polarization of protons, the process of aligning the protons in $\mathbf{B_0}$, does not happen instantaneously. It grows exponentially with a time constant called T_1, the longitudinal relaxation time. The relation is given by Equation 3:

$$M_z(t) = M_0(1 - e^{\frac{-t}{T_1}}) \quad (3)$$

The $M_z(t)$ is the magnetization magnitude at time of exposure t, and z is the direction of $\mathbf{B_0}$. M_0 is the final and maximum magnetization in the given magnetic field. The longitudinal relaxation time constant T_1 varies with the environment of the proton. It takes more time to polarize hydrogens in water and light oils compared to heavier, more viscous oils.

To obtain an NMR measurement an oscillating magnetic field ($\mathbf{B_1}$) is applied perpendicular to $\mathbf{B_0}$ in order to tip the protons from the longitudinal direction to a transverse plane. This is illustrated in Figure 3. The frequency of this oscillating magnetic field must equal the Larmor frequency of the protons relative to $\mathbf{B_0}$. Then protons at the low-energy state may then absorb energy provided by $\mathbf{B_1}$ and jump to the high-energy state. It causes the protons to precess in phase with one another. This is called Nuclear Magnetic Resonance (NMR). When the oscillating magnetic field, $\mathbf{B_1}$, is turned off, the protons begin to dephase. That is, the net magnetization will decrease and the protons will no longer be in resonance. This decay in magnetization is what the logging tool measures. The decay is exponential, so it happens very fast and is called free induction decay (FID). The time constant related to FID is the transverse relaxation time T_2, and it is in generally in the order of a few tens of microseconds. The FID is caused by inhomogeneities in the magnetic field. These are due to the magnetic field gradient and to certain molecular processes. (Coates et al., 2000)

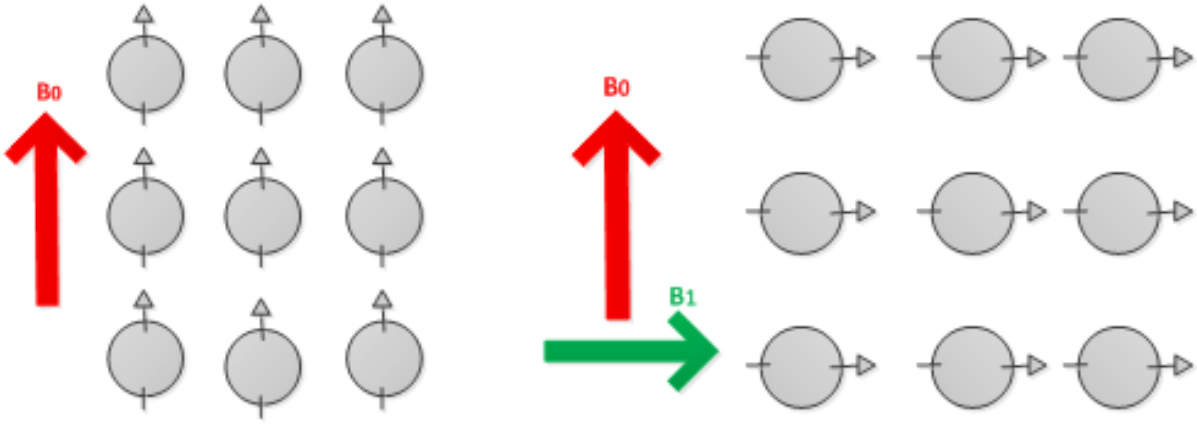

FIGURE 3: POLARIZED PROTONS ALIGNED WITH B_0 (TO THE LEFT), PROTONS TIPPED BY B_1 TO THE TRANSVERSE PLANE (TO THE RIGHT)

2.2 RELAXATION MECHANISMS

Proton relaxation is caused by several mechanisms happening simultaneously. There are three mechanisms that each contributes to the dephasing process. (Coates et al., 2000)

The two relaxation types; longitudinal (related to T_1) and transverse (related to T_2) relaxation, are caused by magnetic interactions between protons. When their only energy loss is to the surroundings, it is called the longitudinal relaxation (T_1). When transverse relaxation (T_2) is occurring, the loss of energy to the surrounding is accompanied by the process of dephasing. Hence, T_2 is always equal to or less than T_1.

Of the three processes that contribute to proton relaxation, the first one is the bulk relaxation which is the intrinsic relaxation property of the fluid. Fluid properties such as viscosity, chemical composition and environmental conditions (e.g. temperature and pressure) govern this mechanism. Figure 4 illustrates a water-filled pore space that undergoes relaxation, both surface and bulk relaxation.

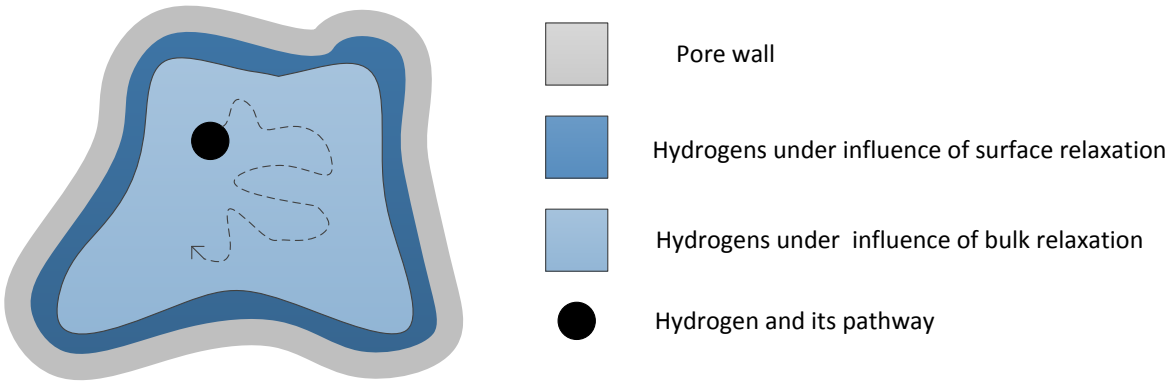

FIGURE 4: SCHEMATIC DEMONSTRATING THE BULK AND SURFACE RELAXATION MECHANISMS

The relaxation processes work in parallel so the equations for the T_1 and T_2 relaxations are given by Equation 4 and 5:

$$\frac{1}{T_1} = \frac{1}{T_{1,bulk}} + \frac{1}{T_{1,surface}} \tag{4}$$

$$\frac{1}{T_2} = \frac{1}{T_{2,bulk}} + \frac{1}{T_{2,surface}} + \frac{1}{T_{2,diffusion}} \tag{5}$$

Each of the three mechanisms is defined as functions of various parameters. The relative importance of these three mechanisms depends on the type of pore fluid, the pore size, wettability and the strength of surface relaxation. Both the bulk fluid and the surface relaxation processes affect T_1 and T_2 relaxation, but diffusion only affects the T_2 relaxation.
The bulk relaxation times (given in seconds) for water, oil and gas are given by

$$\text{Water: } T_{2,bulk} \cong T_{1,bulk} \cong 3\left(\frac{T_K}{298\eta}\right) \tag{6}$$

$$\text{Gas: } T_{2,bulk} \cong T_{1,bulk} \cong 2.5 * 10^4 \left(\frac{\rho_g}{T_K^{1.17}}\right) \tag{7}$$

$$\text{Dead oil: } T_{2,bulk} \cong T_{1,bulk} \cong 0.00713\frac{T_K}{\eta} \tag{8}$$

T_K is the absolute temperature in Kelvin, ρ_g is the gas density (gm/cm^3) and η is the fluid viscosity given in centipoise.

The surface relaxation occurs at the interface between the fluid and the grain surface. The relaxing strength of the grain surface depends on the mineralogy. As an example, chalk has a much weaker surface relaxivity than quartz (Timur, 1972). In the fast diffusion limit, i.e the pores are small enough and the surface mechanisms slow enough that a typical molecule crosses the pore many times before it relaxes, (Kenyon, 1997) the surface relaxation times are given by:

$$\frac{1}{T_{2,surface}} = \rho_2 \left(\frac{S}{V}\right)_{pore} \quad (9)$$

$$\frac{1}{T_{1,surface}} = \rho_1 \left(\frac{S}{V}\right)_{pore} \quad (10)$$

$\rho_{1,2}$ is the $T_{1,2}$ surface relaxivity, the relaxing strength of the grain surfaces. $(S/V)_{pore}$ is the ratio of pore surface to volume. This is a way of measuring pore size. If pores are assumed to be spherical, the surface-to-volume ratio is 3/r, r being the sphere radius.

Diffusion in the presence of magnetic field gradients and only affects the transverse relaxation time T_2. It is given by Equation 11

$$\frac{1}{T_{2,diffusion}} = \frac{D(\gamma * G * TE)^2}{12} \quad (11)$$

D is the molecular diffusion coefficient, γ the gyromagnetic ratio of a proton, G the field-strength gradient (G/cm), and TE (ms) is the inter-echo spacing used in the CMPG sequence. Thus, the diffusion effect is dependent on the echo spacing time TE of the acquisition which is a principle applied in many interpretations.

Inserting into Eq. (4) for T_1 and Eq. (5) for T_2 relaxation gives the entire expression for T_1 and T_2

$$\frac{1}{T_1} = \frac{1}{T_{1,bulk}} + \rho_1 \left(\frac{S}{V}\right)_{pore} \quad (12)$$

$$\frac{1}{T_2} = \frac{1}{T_{2,bulk}} + \rho_2 \left(\frac{S}{V}\right)_{pore} + \frac{D(\gamma G\, TE)^2}{12} \quad (13)$$

2.3 THE MEASUREMENT

In order to measure the magnitude of M(t), the magnetization must be flipped or pulsed down to the transverse x-y plane or even to the –z-direction, see figure 2. A pulsating magnetic field, perpendicular to $\mathbf{B_0}$, must be applied to flip M with a predetermined angle θ of for a certain amount of time τ. This relationship is given by Eq. 14:

$$\theta = \gamma B_1 \tau \tag{14}$$

Usually it is π /2 (90°) or π (180°) pulses. This is what $\mathbf{B_1}$ does when it is applied to the polarized proton population. The simplest manipulation is to pulse M down to the y' axis (90°). The inhomogeneity of the static magnetic field $\mathbf{B_0}$ makes M(t) dephase quickly.

Carr, Purcell, Meiboom and Gill (CPMG) (Coates et al., 2000) introduced a method to negate the effects of this inhomogeneity and this enables the investigation of the transverse magnetization decay (T_2). This is called a CPMG pulse sequence. It consists of the polarization of the nuclei by the static magnetic field $\mathbf{B_0}$. Then, after a certain amount of time, called Wait Time (TW), a 90° pulse is applied and followed by a series of 180°pulses separated by a constant time called echo spacing (TE). An illustration of the sequence is given in Figure 5. The grey blocks represent the $\mathbf{B_1}$ pulses and the continuous green curves the magnetization. At the peak of these curves, the protons are in resonance. The tool measures these points which are illustrated by the green dashed line.

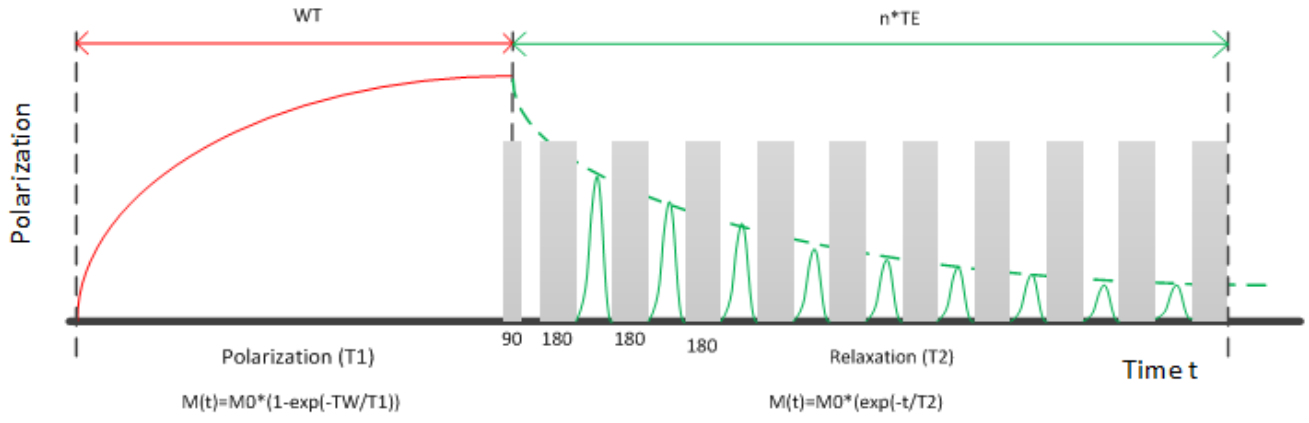

FIGURE 5: ILLUSTRATION OF THE ACQUISITION OF A CPMG-SEQUENCE

The 180° pulses repolarize the protons and make them go back into phase with one another, but for each echo the total magnitude decreases. This is because of irreversible molecular diffusion. The process of turning these echoes into an exponentially decaying curve is done by Fourier-transforming each echo into a spectrum, and then taking the area under the spectrum curve as a point (as a function of time) in the decay curve. Figure 6 is demonstrating how the magnetization decay will be measured.

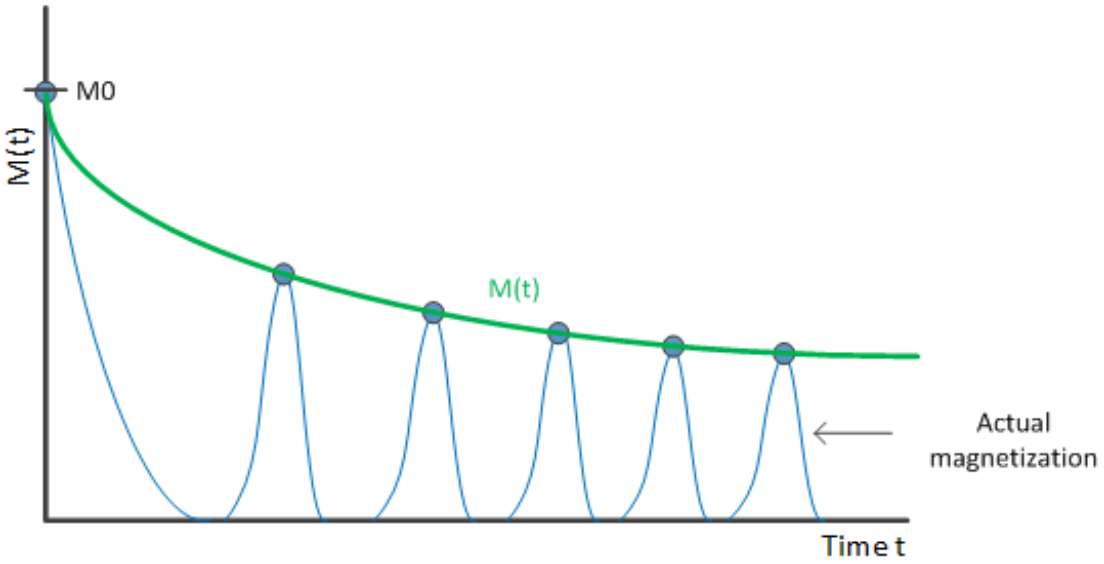

FIGURE 6: MAGNETIC RESPONSE OF PROTONS, THE ACQUIRED DATA IS THE GREEN LINE

The magnetization decay can be expressed as:

$$M(t) = M_0 e^{\frac{-t}{T_2}} \tag{15}$$

To do a T_1 measurement, a series of CPMG sequences with different Wait Times (TW) must be done. This is very time consuming and requires a rather slow logging speed (or Rate of Penetration if NMR data is acquired during drilling).

2.4 ACQUISITION

2.4.1 TOOL

The MagTrak tool is the LWD version of Baker Hughes' Magnetic Resonance Tools. It is the main tool used on Valhall for NMR acquisition. Figure 7 illustrates the main features of the tool. It comes in two sizes; 4 ¾ inches and 6 ¾ inches for use in hole sizes from 5 ¾ to 9 7/8 inches. The tool is centralized and placed at the end of the BHA, far away from the bit. The distance reduces the motion effects that considerably influence the quality of the NMR measurements. In addition there are two Low Motion Stabilizers on the BHA, one on each end of the MagTrak sensor sub. They aim to prevent excessive tool motion and aid the centralization of the tool. The entire sensitive volume should be in the formation and not in the borehole for reliable measurements. On the sensor sub the emitting and receiving coil, the antenna, has strong, permanent magnets placed on each side. The permanent magnets provide the static magnetic field $\mathbf{B_0}$ that polarizes the formation before the Radio Frequency (RF) pulses are applied. Its field gradient is 2.0 G/cm=2mT/m which is considered as a constant gradient field over the sensitive volume.

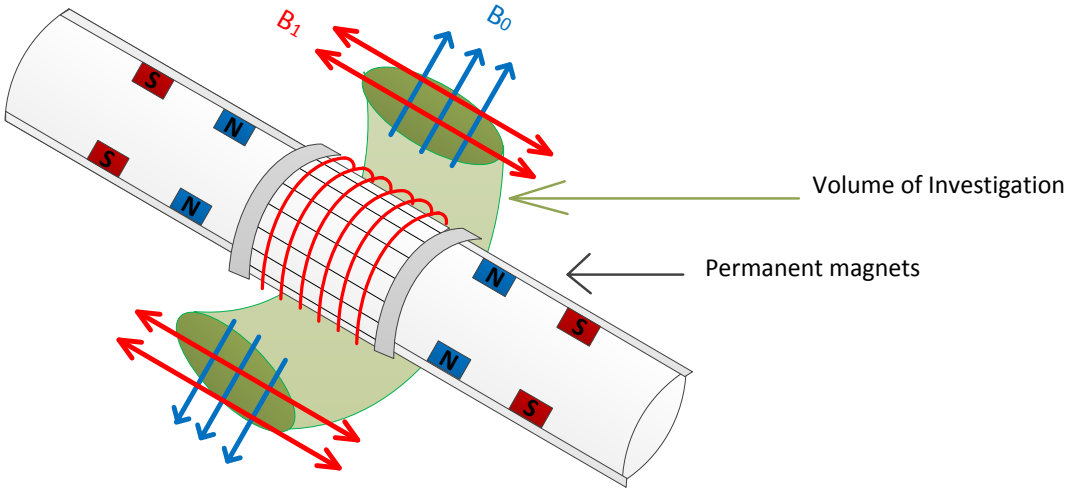

FIGURE 7: SCHEMATIC OF THE MAGTRAK TOOL

The volume of investigation is torus shaped with a diameter of 12 inches giving a Depth Of Investigation (DOI) of approximately 2 inches in a 8 ½ inch borehole. The static vertical resolution is 70mm (2.8inches) while during drilling it is 1.4ft given a ROP of 50ft/hr. During drilling the vertical resolution depends on the Rate Of Penetration (ROP) and on the size of the stacking window (or Running Average). The necessary size of the stacking window depends in the Signal-to-Noise ratio (S/N) and data quality. The accuracy is ±1 Porosity Unit (pu).

There are some tool limitations on pressure and temperature. The downhole temperature should not exceed 150ºc (300ºF) and the BHP should not exceed a hydrostatic pressure of 25 000psi (1725 bar).

The MagTrak is power supplied by an internal turbine driven by the mud flow and is therefore independent from any power supply from other BHA sections. It has an internal independent alternator which reduces power consumption and current fluctuations that increase the SNR (Signal to Noise Ratio) and the data quality. The data is mainly stored on a downhole memory device due to the large amount of bytes needed. It can also be transmitted by mud pulse telemetry for real-time acquisition, but with a poorer vertical resolution.

There are two standard acquisition modes; “PoroPerm” (PP) and “PoroPerm + Light HydroCarbon” (PP+LHC) mode. The “PoroPerm” mode provides total porosity, fluid volumetrics and permeability index (a qualitative measurement of the permeability). The “PP+LHC” mode provides, including what is given by the “PP” mode, light hydrocarbon saturation. The tool has a low magnetic field gradient; in the order of 2G/cm. This makes the assumption of a constant magnetic field across the volume of investigation reasonable. Due to this, the measurements are free from diffusion “artifacts”. But this takes away the possibility of using this feature in Diffusion Coefficients for Fluid Characterization.

The MagTrak tool has an implemented “casing detection” feature in order to prevent it from transmitting the RF pulses whilst inside the casing which would destroy the permanent magnets.

Table 1 summarizes the main technical specifications.

TABLE 1: MAGTRAK SUMMARY

MagTrak Tool Summary		
Max. Temperature	150 300	°c °F
Max. Pressure	25 000 1 725	psi bar
Tool sizes available	4 ¾ 6 ¾	inches inches
DOI (8 ½'' borehole)	2	inches
Vertical Resolution	Depends on Signal to Noise Ratio and ROP	
Field Magnetic Gradient	2	G/cm

2.4.2 CALIBRATION

The main calibration process is done in a calibration tank at the service company's workshop before shipping the tool to the rig site. The tool is calibrated against a container of water, 100% porosity at a temperature close to the downhole temperature. Then protective shields are put on the permanent magnets for covering and protection.

The calibration procedure consists of a frequency sweep and a master calibration. The frequency sweep aims to find at which frequency the gain (relative voltage gain in the system) is largest and then set the tool to operate at this frequency. The master calibration aims to determine the amplitude of the CPMG pulses and relations for power and stimulated-echo corrections.

At the rig site, while the shields still are covering the magnets, the tool communication functionality is checked. The tool is not powered up until it is covered with drilling mud downhole. This prevents high frequency radio pulses at the drilling floor which can cause damages to equipment and to people.

The borehole itself is prepared by running a ditch magnet to clean the hole for magnetic particles impeding good measurements.

2.5 NOISE AND NOISE REDUCTION

The NMR signal is in general very weak. Distinguishing signal from noise is therefore difficult and the raw Signal-to-Noise (S/N) is very poor. Signal noise consists amongst other factors of electronic offset, ringing and random noise.

Noise originates from different sources. This could be vibration in the antenna (ringing) or from the bit, tool motion or poor calibration.

In order to remove some of the noise, a method called Phase Alternated Phase Sequence (PAPS) is applied. Two CPMG sequences are acquired 180 degrees out of phase. The effect is to reverse the sign of the echo data.

At 0 degree phase; $echoes = signal + ringing + offset$

At 180 degree phase; $echoes = -signal + ringing + offset$

So by subtracting and dividing by two;

$$PAPS = \frac{(signal + ringing + offset) - (-signal + ringing + offset)}{2} = true\ signal \tag{16}$$

In the pre-processing the two echo trains are subtracted, and divided by two, as illustrated by Figure 8. This is to cancel out electronic offsets and ringing effects. Ringing is the signal seen at longer times and is caused by vibration in the antenna due to the polarization pulse.

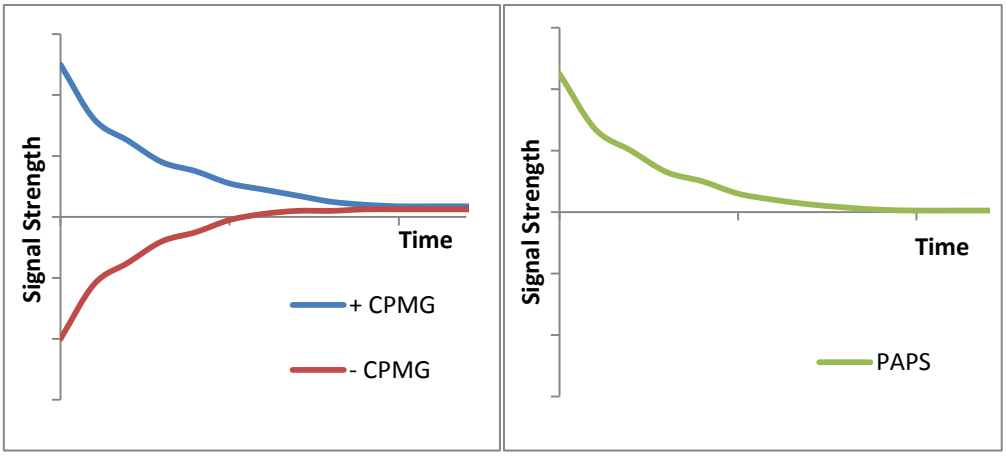

FIGURE 8: POSITIVE (+) AND NEGATIVE (-) CPMG COMBINED TO A PAPS

The PAPS removes electronic offset and ringing effects but not random noise. Stacking and averaging several echo trains reduce the level of random noise. The number of echoes needed to produce a stacked and averaged echo train is called a running average (RA). It is illustrated by Figure 9. However this reduces the vertical resolution of the measurement. An optimal number of RA is a function of S/N and vertical resolution. It is desirable to get a high S/N ratio but without compromising the vertical resolution.

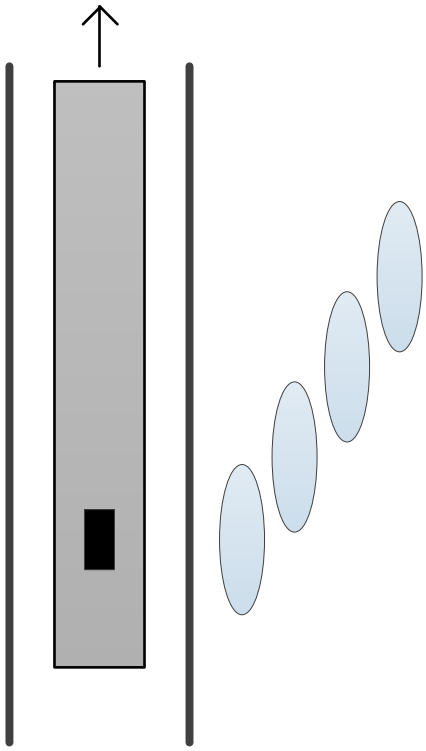

FIGURE 9: SCHEMATIC ILLUSTRATING RUNNING AVERAGE

3 THE VALHALL FIELD

This chapter gives an introduction to the Valhall field. Some general information first, then some reservoir geology and finally the challenges encountered in terms of reservoir management. Figure 10 is a map of the field which indicates where the wells in focus are.

3.1 GENERAL INFORMATION

The Valhall field was discovered in 1975. It is situated 290 km offshore southwestern Norway, in the southernmost corner of the Norwegian Continental Shelf. The field started producing oil in October 1982. It is an over-pressured and under-saturated Upper Cretaceous chalk oil field. The main reservoir formation is the Tor Formation where 90 % of the reserves are located. The Hod Formation is the secondary reservoir. Other Cretaceous formations such as Magne and Ekofisk are present in some places but do not contain any significant volumes. All the more recent producer wells are horizontal.

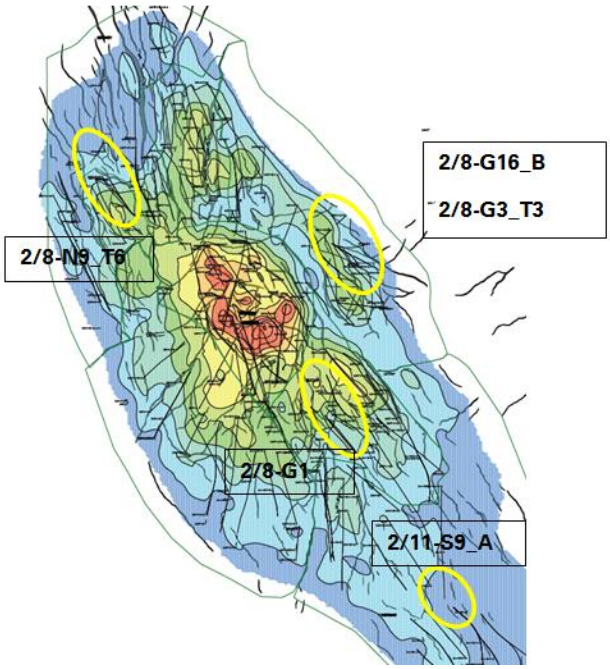

FIGURE 10: HYDROCARBON PORE VOLUME MAP OF VALHALL. THE FIVE WELLS IN THE STUDY ARE MARKED BY YELLOW CIRCLES

Subsidence and reservoir rock compaction is a principal issue in the reservoir development. Solids production was seen early on and cores indicated high compaction potential. The reservoir has compacted and this contributes to the oil production as an extra reservoir drive mechanism. It also decreases the expected life of wells due to shear failure and casing collapse and leads to seabed subsidence which makes the platforms sink. This compaction also induces arching in the overburden and causes the stress regimes to change which makes drilling challenging.

Water Injection was approved in 2000 as a measure for increased recovery, maintaining reservoir pressure and hence trying to prevent further subsidence. The injection started in 2003 and has been implemented more over the years.

The Valhall Life of Field Seismic (LoFS) system was installed in 2003 to assist the monitoring of production and injection. Four Component (4C) ocean bottom seismic (OBS) arrays were installed and cover an area of approximately 45 km^2. The LoFS data helps defining new well targets, overburden integrity and reservoir modeling. Surveys are conducted once or twice per year. Over the central crest there is a shallow gas cloud which masks the seismic over this particular area. This increases the importance of the wellbore data coming from these wells as they are the main source of information.

3.2 THE GEOLOGY

3.2.1 CHALK

Chalk is a biogenic carbonate rock composed of small shells of coccolithosphores with a diameter less than 4 micrometers. Fragments of planktonic foraminifera and larger fossils like bryozoa also occur. It is classified by the Dunham classification for carbonate sedimentary rocks as a mudstone. Compared to other carbonate rocks it is quite homogeneous with respect to pore size. It was deposited during the Cretaceous. These coccolithosphores are planktons with hard carbonate shells that were floating in the upper part of the sea and sank down to the sea bed when they died. The shells were deposited, buried and partially crushed and compacted in the process. The chalk mainly consists of micron sized calcite shells as showed in Figure 11, and very little clay minerals. (Glennie, 1998)

In the North Sea the chalks are situated in the southern part of the Norwegian Continental Shelf. The three main formations are Ekofisk, Tor and Hod Formations (Fm.). The Ekofisk and Tor Fm. have a very high porosity (up to nearly 50%) whereas the Hod Fm. has a slightly lower porosity (approximately 30%). The high porosities were preserved during diagenesis because of the early development of high pore pressure. The formations are very tight due to the small pore size and throats. The permeability ranges from tens of millidarcies down to one millidarcy.

There are two main facies; autochthonous coccoliths and reworked (redeposited), allochthonous coccoliths. The latter is masses of carbonate sediments that have been transported away in the form of a current flow due to gravity. This redeposition gives an upward fining sequence with good sorting. Thus, the best reservoir quality is at the bottom of these sequences. This is not a straightforward classification without core and is not much used.

3.2.2 PRIMARY RESERVOIR: TOR

The primary reservoir formation, Tor Fm., is a fractured chalk with porosity ranging from 30-50% and matrix permeability between 1 and 10 millidarcies. Most of the porosity values lie within 30 to 40 % but goes as high as 50 % on the crest of the structure. Its thickness varies from 0 to 80 meters. The thin zones generally have a skim of high porosity chalk that is overlaying a dense hardground. In these dense zones there was a low net sedimentation and the depositional environment was close to storm wave level. Connate water saturations in Tor Fm. typically are less than 5%.

3.2.3 SECONDARY RESERVOIR: HOD

The Hod Formation is divided into three parts; Lower, Middle and Upper Hod. Most of the Hod Fm. is laminated and bioturbated chalk with clay content of 10-30% (Andersen, 1995). The porosity usually ranges from 30-38% and the matrix permeability 0.1-3 md. The Hod Fm. has smaller pores than the Tor Fm. and thus more connate water. In general there is not much hydrocarbons present in this formation.

3.3 CHALLENGES AND UNCERTAINTIES

Despite the discovery of the field in 1975 and over 40 years of data recovery from the field, a large number of uncertainties remain regarding understanding and managing the field. It is a highly complex field experiencing reservoir compaction (and seabed subsidence). For this and other reasons water injection has been implemented. The reservoir chalk is highly porous and a very tight formation, but natural fractures and faults enables fluid flow and hydrocarbon production. A surrounding aquifer is also present but it is not well understood.

The water aquifer is present below and around the reservoir. The water table does not advance equally everywhere and this makes it hard to understand its behavior. When drilling, unexpectedly high water saturation zones are encountered. This reveals questions regarding the water's provenance. Is it injected sea water coming through a permeability highway or a fracture system, or is it formation water? As injection implementation moves forward and the number of infill-wells increases, this becomes a frequent issue.

The permeability estimations are highly uncertain. They derive from a core porosity-permeability relationship with great scatter. The chalk is very tight with permeability in the range of 1-10 md. The chalk is also fractured, and this system of fractures enables the flow of fluids.

The seismic data indicate that solution gas is present. The distribution across the field is not known. This is because the pressure drops and this makes the gas come out of solution. If the pressure is increased sufficiently by injection the gas goes into solution again.

These are some of the challenges related to this field. In general there are uncertainties related to all data acquisition and must be considered.

4 DATA QUALITY CONTROL

Quality Control is essential to the interpretation. Poor quality data gives unreliable interpretations. Therefore that data must be recognized and marked. Several parameters indicate the data quality during the logging job. The T_2-distribution curve is one of many outputs. The NMR end product from the service company comprises several other things such as NMR-porosity (total and effective), saturations, Bulk Bound Fluid Volume, permeability etc.

4.1 DATA QUALITY CONTROL INDICATORS WHILE DRILLING

There are several data quality indicators which are recorded during the logging procedure.

Chi is a measure of the fit between the calculated decay curve and the recorded echo amplitude. It is given in porosity units (pu) and should not exceed a value of approximately 2.0. This parameter is usually included in the NMR dataset. Sudden spikes could indicate tool problems.

Gain is another QC parameter and is a continuous calibration function downhole. A small signal is sent to a test loop on the antenna and the Gain is measured to be the ratio of the induced signal amplitude divided by the test coil signal amplitude. The Gain will be a function of temperature and mud conductivity and should never be zero. Sudden spikes in the Gain could also indicate tool problems.

There are also indicators which alerts the service company onsite representative of tool failure and poor quality data. The tool is powered by a downhole turbine so it is dependent on a proper, undisturbed mud flow. These will be recorded in the logging report.

4.2 POST DATA QUALITY CONTROL

After the logging job the data is processed and inverted by Laplace-transform from a decay time to a transverse relaxation time (T_2) distribution. The inversion process is a critical step for the data. After the inversion the T_2-distribution the consistency with other log curves, if available, must be confirmed.

The NMR data should be checked against other logs to assure that the data are coherent with each other. The changes in the different logs should be consistent. The GR log should also correlate quite well with the Clay Bound Water (CBW) volume, represented by the very short T_2-relaxation times. Furthermore, the NMR-derived porosity should be crossplotted with the Density-derived porosity and other porosity measurements if available. These should give the same porosity values with an accuracy of 1 pu. Poor borehole conditions usually give a large difference. This can be seen on the Density Image Log by a thick low-density interval in the upper part of the wellbore. There are examples of this presented later on.

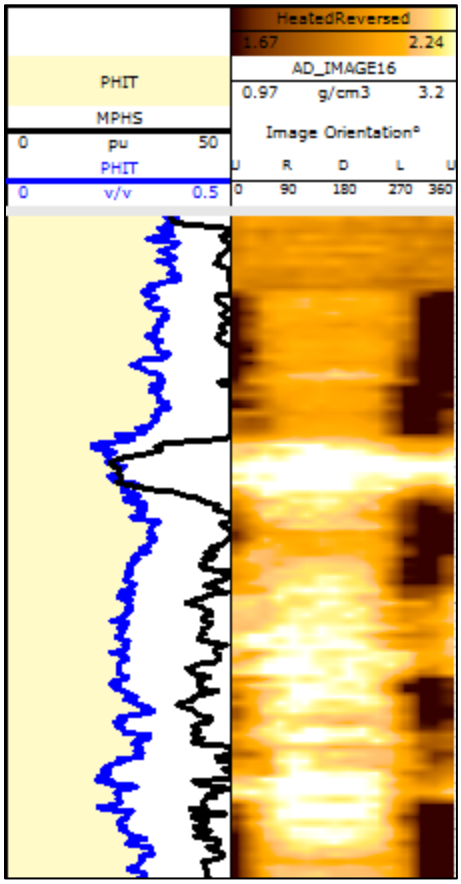

FIGURE 11: EXAMPLE OF A TYPICAL BOREHOLE ENLARGEMENT

If there are two or more runs over the same interval these must be compared. Comparison may reveal invasion, borehole degradation or other time-dependent changes.

In order to make the post-logging QC process standard in the workflow, a Techlog-template has been defined which is given in Appendix B. Here the most frequent conventional logging parameters are present, as well as T_2-relaxation, NMR-derived porosity and others in order to assure the NMR data quality before proceeding to the interpretation part of the workflow. The proposed standard work flow is given in the format of a flow chart in Appendix D.

The QC process consists of removing data where the tool failed. When the data is imported to Techlog, there is no data over the sections where the tool failed but the software automatically interpolates the data points to give a straight line. If there are multiple runs these should be compared to each other to look for time-dependent changes. Furthermore the data must be classified into poor, medium and good quality data. The quality can be represented by coloured flags. This is done by looking for poor borehole condition indications such as unrealistically high NMR- porosity or low-density stripes on the density image log. If there are no apparent reason for strange behavior of the T_2-distribution it should be flagged yellow.

Figure 12 illustrates a good example of what should be flagged as questionable data quality. There are no apparent reasons for this strange T_2-distribution and it will therefore be classified with the color yellow.

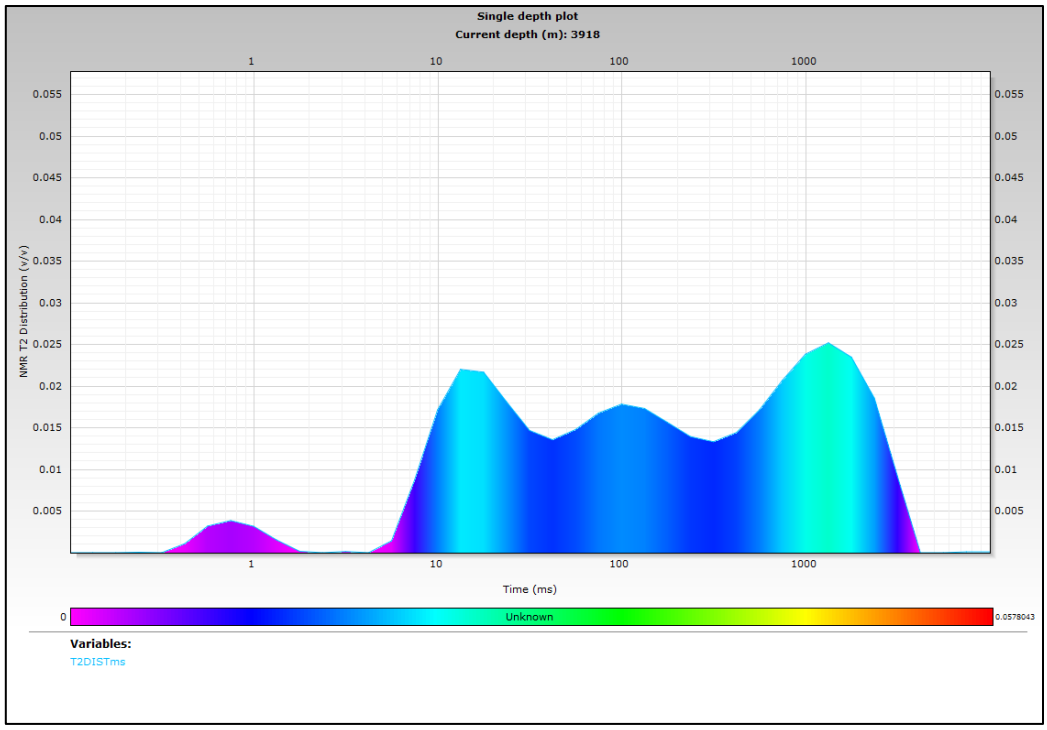

FIGURE 12: EXAMPLE OF NOISY AND QUESTIONABLE DATA

5 NMR-DERIVED POROSITY

NMR-porosity is an essential part of the NMR end product. It provides a lithology-independent porosity from a non-nuclear logging tool. It provides several types of porosity. This chapter discusses the robustness of the NMR-porosity and comparison with the Density-derived total porosity.

5.1 METHOD

The simplest porosity provided is the total porosity. Porosity is classified into different groups by applying pre-defined T_2-cutoff values. These may represent micro-, meso- and macro- sized pores or other types of classifications.

Another possible porosity classification is to distinguish the porosity by its fluid content. Capillary Bound Water (CBW), Bound Fluid Volume (BFV) and Free Fluid (FFI) porosities are the most frequent. The underlying assumption is that the smallest pores only contain capillary bound water, larger pores contain bound water and then the largest pores contain free, movable fluid. This method is widely used for saturation and permeability calculations which will be discussed later on.

In order to obtain reliable porosity measurements all the hydrogen atoms must be fully polarized. Otherwise the NMR-porosity will underestimate the porosity. This is usually taken into account when planning the job.

When the inversion is done, the resulting T_2-distribution gets the amplitude given in incremental porosity units. This requires a porosity calibration, which usually is a water-filled tank (100% porosity).

The total porosity is the integration of the T_2-distribution curve. This enables the porosity classifications. By selecting cutoffs, the total porosity is separated into different groups. Figure 13 illustrates principle of cutoffs, here by defining all the porosity below the cutoff (red line) as porosity containing bound fluid and the rest as porosity containing free, movable fluid.

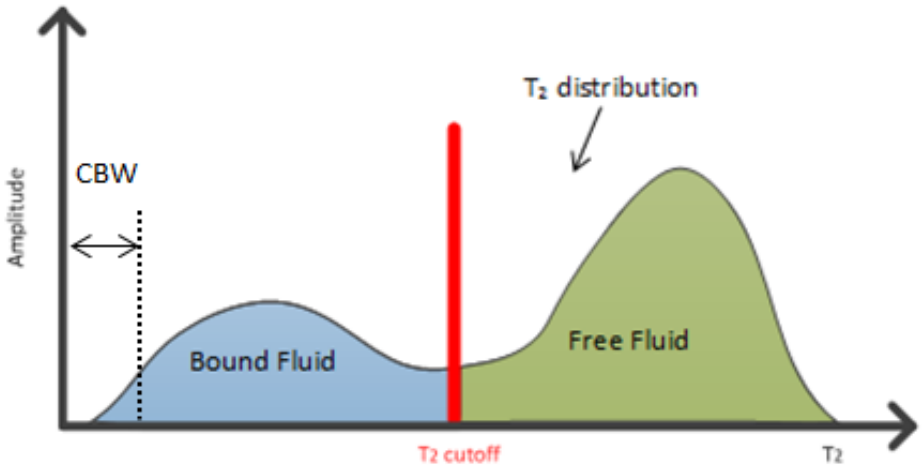

FIGURE 13: ILLUSTRATION OF DEFINITION OF FLUID TYPES BY APPLYING CUTOFFS

The original cutoff values are 3.3 ms for CBW and 92 ms for BFV. The BFV cutoff value is an industry standard for carbonate rocks.

The Density-derived porosity is assumed correct for the entire field. It is calculated by iterating the three equations below in order to obtain equilibrium between porosity, water saturation and total fluid density. It has been calibrated against core porosity as well to increase its reliability.

$$\rho_{bulk} = \rho_{matrix} * (1 - \varphi) + \rho_{fluid} * \varphi \quad (17)$$

$$S_W^n = \frac{a * R_W}{\varphi^m * R_t} \quad (18)$$

$$\rho_{fluid} = S_w * \rho_{water} + (1 - S_w) * \rho_{hydrocarbon} \quad (19)$$

In the investigation of the reliability of the NMR-derived porosity, the NMR-derived porosity is crossplotted against the Density-derived porosity.

5.2 RESULTS AND DISCUSSION

The NMR- and density-porosity were crossplotted, first all the wells together, then for each well and each formation (Tor, Magne and Hod, all wells together) to look for lithological dissimilarities. The crossplotting did not go further into detail regarding formation members due to insufficient amount of points in each member.

Figure 14 is an overall crossplot of all the data points from all the five wells in this study. Figure 15 is the same plot but has a color scale that indicates the data density. The regression line (in blue) is very close to unity slope line (in red) with a slope of 1.07. The cluster of data points are lying within an interval of 30-40% porosity which is where one expect to find most of the porosities. There the regression line appears to overlap the unity slope line. This supports the reliability of NMR as a porosity tool because it shows similar porosity values as the Density-porosity within the porosity range expected for the field. One may also conclude that the formation is fully polarized.

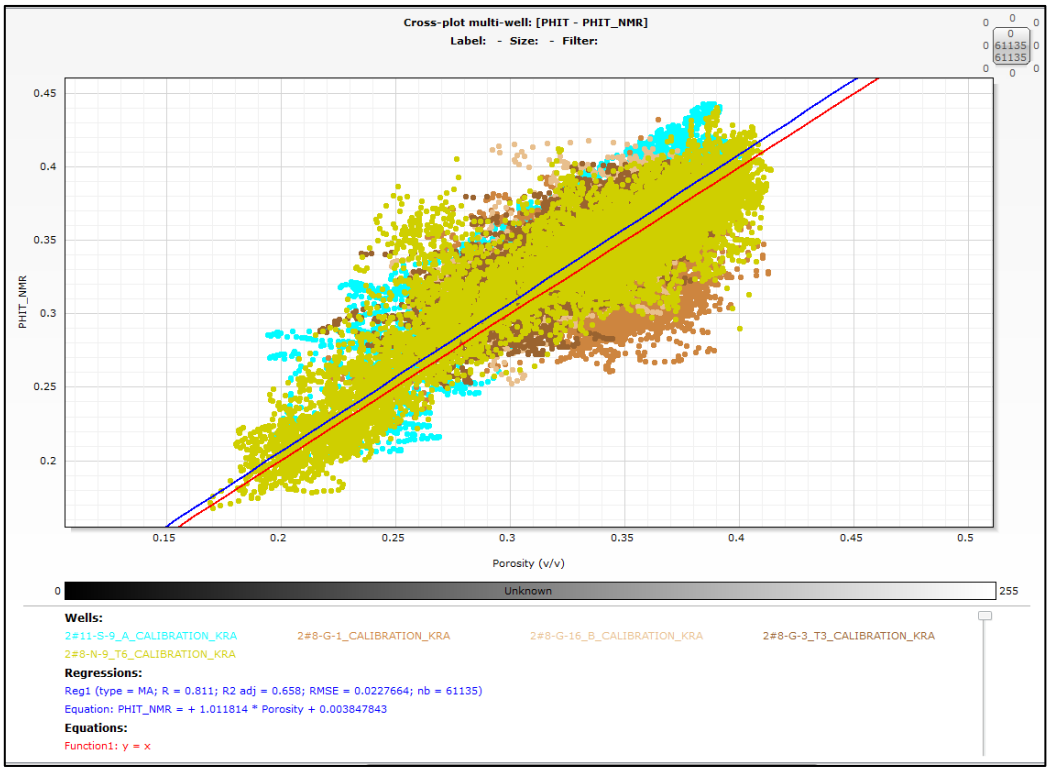

FIGURE 14: CROSSPLOT OF DENSITY-POROSITY (X-AXIS) VS. NMR-POROSITY (Y-AXIS)

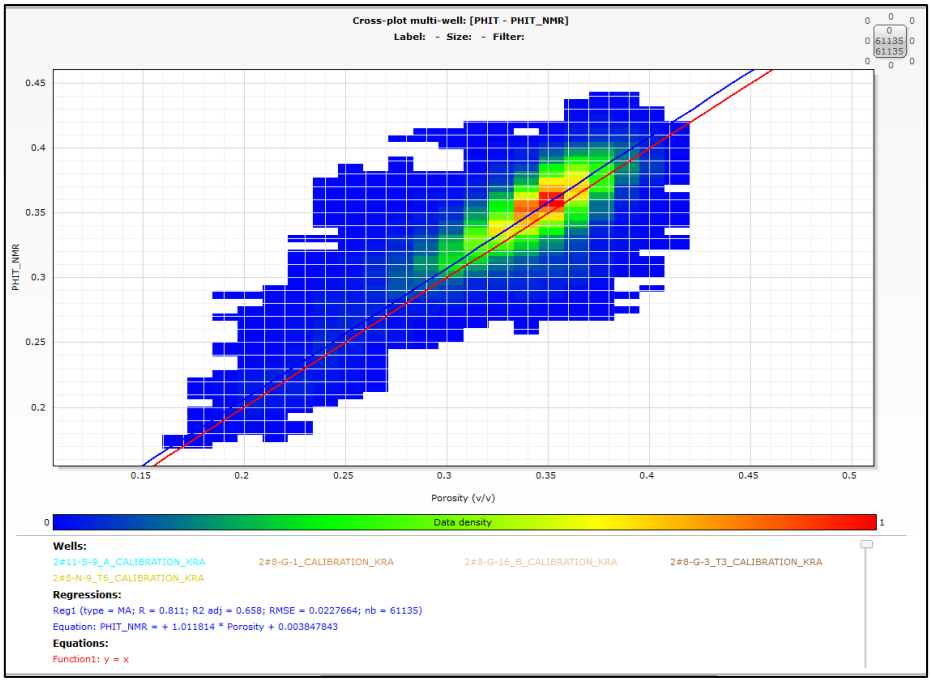

FIGURE 15: CROSSPLOT OF DENSITY-POROSITY (X-AXIS) VS. NMR-POROSITY (Y-AXIS), COLOR SCALE INDICATES DATA DENSITY

Further, an investigation on the necessity of formation dependent correction factor was conducted. It was concluded that such a factor was not needed. On Figure 16-18 below the data points have been separated into formations. These did not either show any significant difference in the porosity interval of 30-40% from the global crossplot. This observation is valid for all the three formations.

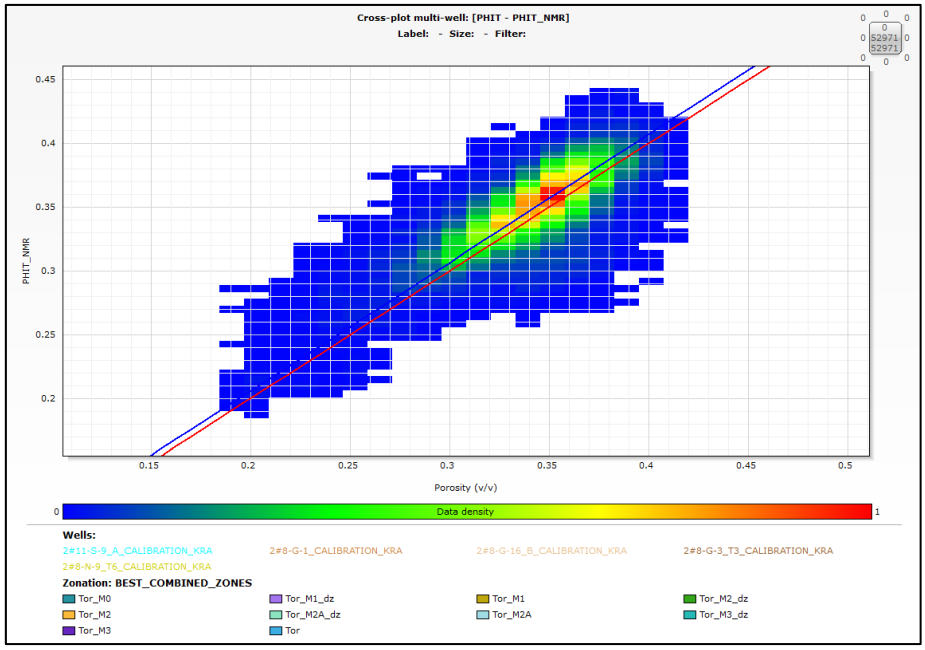

FIGURE 16: TOR FM. ONLY, CROSSPLOT OF DENSITY-POROSITY (X-AXIS) VS. NMR-POROSITY (Y-AXIS). COLOR SCALE INDICATES DATA DENSITY

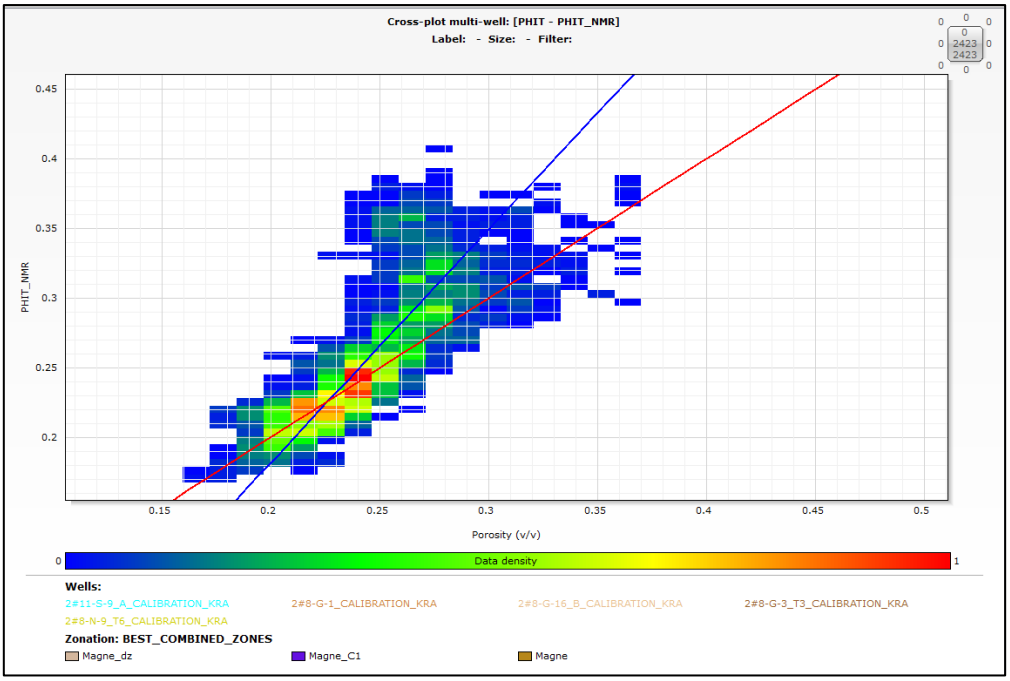

FIGURE 17: MAGNE FM. ONLY, CROSSPLOT OF DENSITY-POROSITY (X-AXIS) VS. NMR-POROSITY (Y-AXIS). COLOR SCALE INDICATES DATA DENSITY

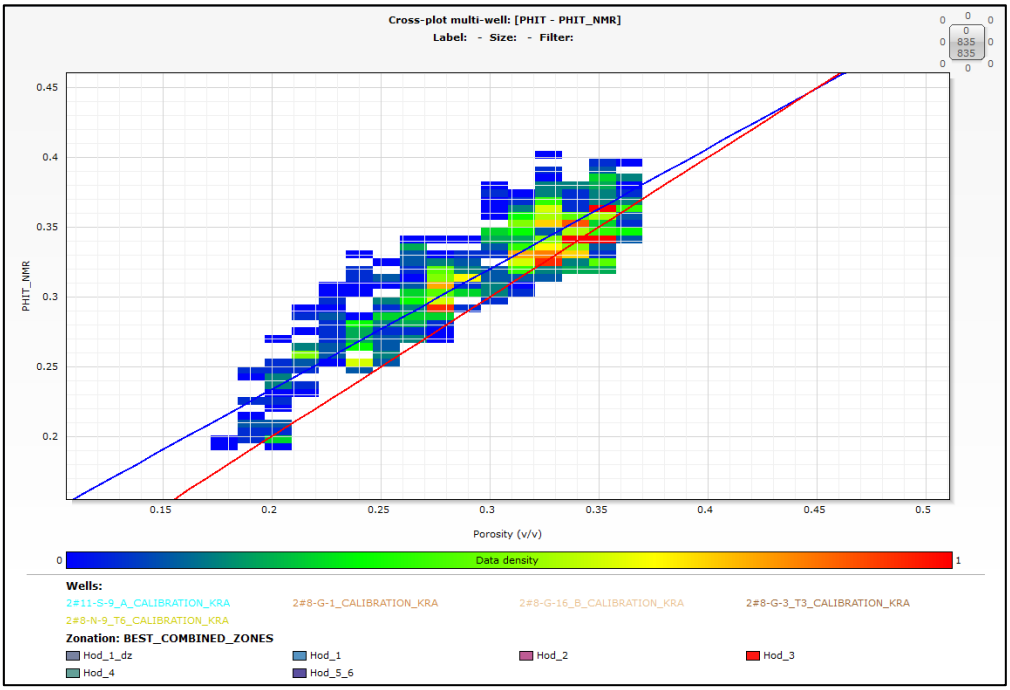

FIGURE 18: HOD FM. ONLY, CROSSPLOT OF DENSITY-POROSITY (X-AXIS) VS. NMR-POROSITY (Y-AXIS). COLOR SCALE INDICATES DATA DENSITY

Figure 19 shows a problem related to the data quality which in this case was classified by a red flag.

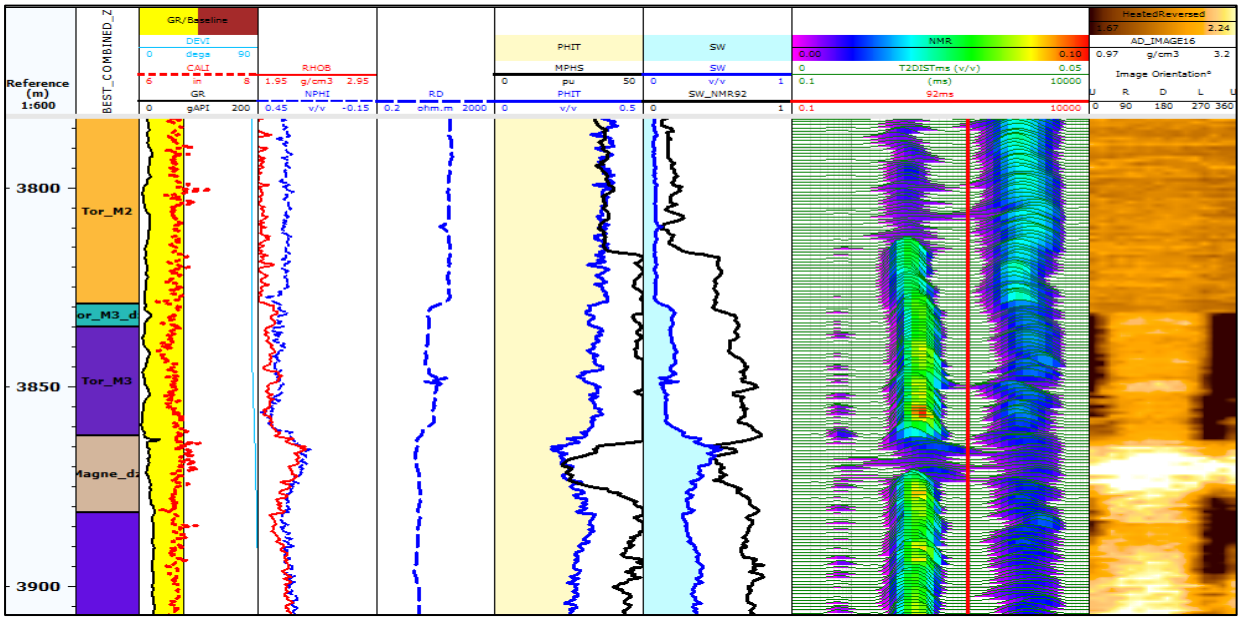

FIGURE 19: WELL 2/8-G1, EXAMPLE OF HOLE WASHOUT (DENSITY IMAGE LOG, TRACK 7)

The Density-Image log clearly shows washouts in the upper part of the wall in the horizontal section. It does not appear clearly on the (sonic) Caliper log (borehole diameter). This is because the sonic caliper which measures in all directions, only takes the average borehole diameter. The NMR also gives average measured values of the volume of investigation. It is a toroid shaped volume, a donut, around the borehole. When a part of the wellbore is enlarged this will increase the output porosity simply because in that area the local porosity is 100% and completely fluid filled. This is illustrated by Figure 20. The average porosity will then be considerably larger than the true porosity.

The washout areas are filled with drilling fluids. In all these intervals the same high amplitude signal is seen at 10 ms. Because there have not been any NMR-measurements of the mud nor the mud filtrate it is reasonable to think it is approximately 10 ms.

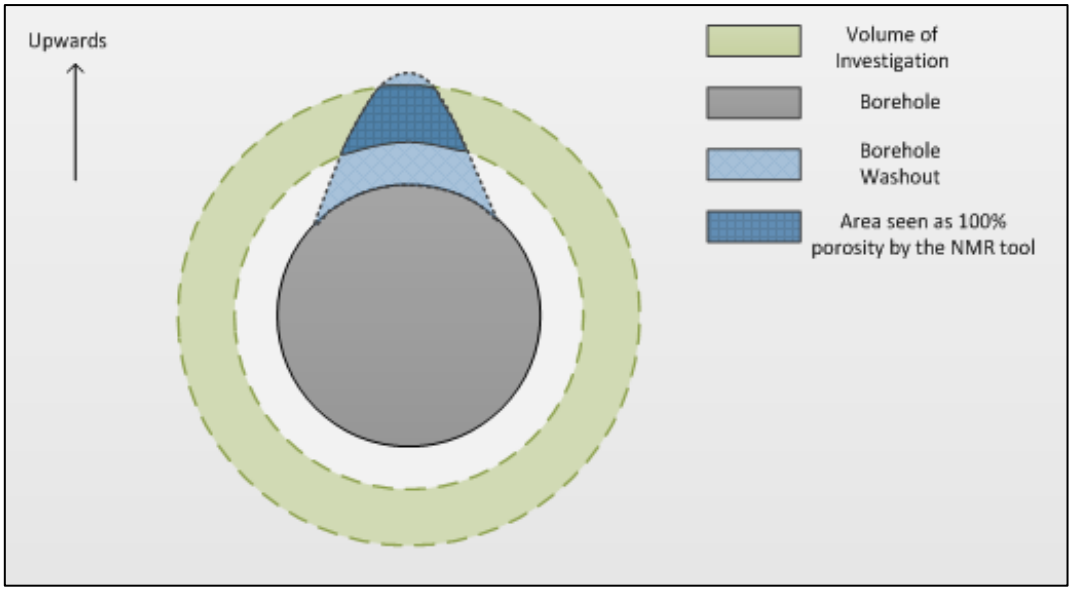

FIGURE 20: ILLUSTRATION OF WHY THE NMR-POROSITY IVERESTIMATES IN POOR BOREHOLE CONDITIONS

These poor borehole conditions prevent the possibility of using NMR as a porosity tool but they are easily detectable.

In the Valhall field, with all its wellbore stability issues, the risk of losing the drillstring is considerable. Therefore nuclear tools are in some cases not run. This means that the NMR measurement is an equivalent option to the nuclear Neutron-Density tool as a porosity tool and could replace the Neutron-Density tool.

6 FLUID SATURATION

Since 1942 the Archie Equation has been the traditional equation for estimating water saturation in clean formations. NMR has also the ability to provide an estimate of water saturation when the fluid properties allow it. There are different methods, the most common one being the constant cutoff. Varying cutoff will also be tested as a measure of optimizing the application.

6.1 NMR-DERIVED WATER SATURATION

Chalks have high porosities and small uniformly distributed pore sizes. When water-filled, the chalk will exhibit a T_2-peak at values less than approximately 100 ms. The light oil that fills the pores in the formation has a long bulk relaxation time. Because the chalk is water-wet, the oil will not be in contact with the pore wall and only experience bulk relaxation. This means that the T_2-distribtion is expected to clearly separate into two T_2-peaks.

Previous studies show that partially saturated cores exhibit a bi-peak distribution regardless of the pore size distribution (Mao et al. 2007). The amplitudes to the right will be only from the hydrocarbons and the amplitudes at lower T_2-values (to the left) will be from the formation water. If there then is a clear separation between the two peaks, porosities can be grouped into hydrocarbon-filled and water-filled porosity by a cutoff value and compute saturations. This is a very simplistic way of computing saturations because it does not take into consideration gas presence or mud filtrate invasion. Even so it seems to provide quite reliable results. The water saturation may then be computed by the following equation:

$$S_{w,NMR} = \frac{water\ filled\ porosity}{total\ porosity} \tag{20}$$

A more detailed grouping is dividing the water into capillary bound, bound and movable water. This is illustrated by Figure 21. In most of the intervals drilled and logged from the five wells of this study, the amount of water is very little and is assumed to bound water. This applies predominately to the Tor Fm. where most of the hydrocarbons are. In Magne and Hod Fm. movable water is also assumed to be present but due to the smaller pores there will be more bound water here than in the Tor Fm.

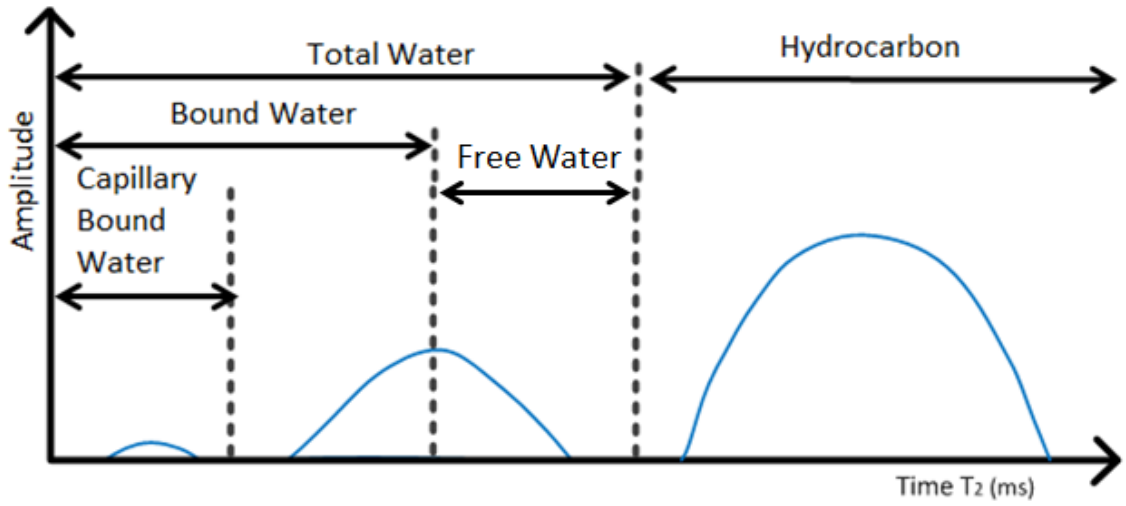

FIGURE 21: SCHEMATIC ILLUSTRATING HOW CUTOFF VALUES DEFINE TYPES OF FLUID

The saturation depends only on the pre-defined cutoff-value. It is classifying the various types of fluid and must be chosen wisely. From the service company's NMR report there was no consistency in what Hydrocarbon Cutoffs were used for the wells. Values from 92 to 250 ms were used. As for the Bound Fluid cutoff 92 ms was used. This is an industry standard for carbonates. There is no HCC industry standard because the T_2-response of hydrocarbons strongly depends on its composition.

Figure 22 illustrates the importance of correctly setting the cutoff. If the cutoff is erroneous, like in the figure (red line) some of the fluid will be misinterpreted and taken for the wrong fluid phase. The water saturation is then under- or overestimated. When the two peaks demonstrate such a clear separation the cutoff should lie right in the middle of the two T_2-peaks.

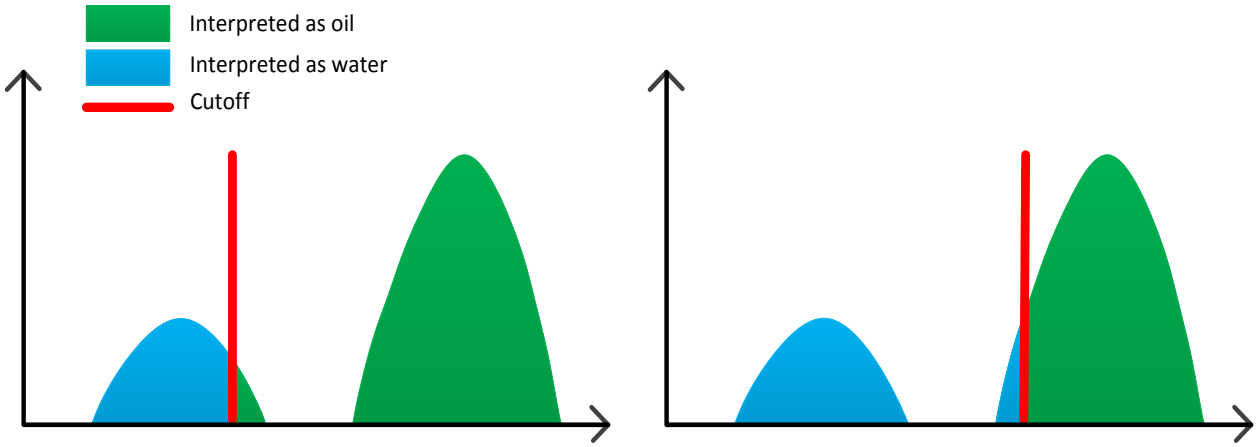

FIGURE 22: ILLUSTRATION OF THE IMPORTANCE OF A PROPER HYDROCARBON CUTOFF

6.2 WATER SATURATION USING THE CONSTANT CUTOFF METHOD

The first part of the water saturation study was to investigate whether constant cutoff values used to define the porosities and saturations was a reliable method. Constant values of 250, 200 and 92 ms were tested. The values were chosen on the basis of what had already been used in the NMR MagTrak end products delivered from the service company.

Computing the water saturation with a cutoff of 250 ms and comparing this with the Archie-water saturation showed that the NMR water saturation generally was overestimated. The same calculations using a 200 ms cutoff showed a somewhat better match. The 92 ms cutoff case is crossplotted with Archie-saturation in Figure 23 and it was the best. The 92 ms is in general situated more in the middle of the oil and water signal than 200 and 250 ms in the T_2-distribution. The 200 and 250ms cutoff had a tendency of defining some oil signal as water (illustrated by Figure 22, on the right side).

Despite this, the 92 ms cutoff overestimates the water saturation with an average of 10 pu over various intervals. This is mainly where Archie's equation indicates that there is very little water. Where it indicates higher values the NMR-derived saturation matches better. Over other intervals, even in the same well, it gives the same saturations as Archie's equation.

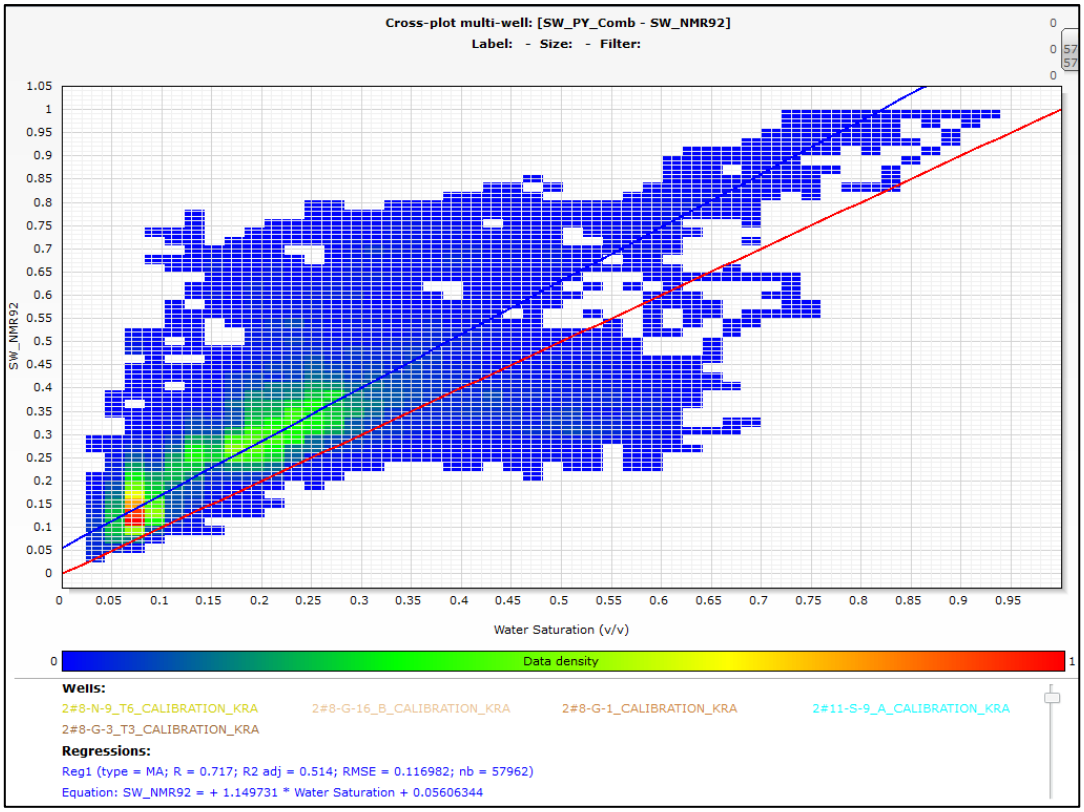

FIGURE 23: CROSSPLOT OF ARCHIE SW (X-AXIS) VS. NMR-SW (Y-AXIS), CONSTANT CUTOFF (92 MS)

There could be several explanations for these discrepancies. Some of the overestimation can alternatively be explained by the pre-defined hydrocarbon cutoff value. The oil signal moves slightly and thus the constant cutoff may define some of the oil as water. This is however not a reasonable explanation for most of the overestimation. The 92 ms cutoff rarely cut into the oil signal. Therefore one can conclude that the amplitudes at the lower part of the T_2-distribution must be too strong compared to the Archie-saturation.

One other possible explanation is mud filtrate invasion. The MagTrak depth of investigation is shallow, only 2 inches (approximately 5 cm). Although the wells are all drilled with OBM the OBM response appears to be around 10 ms and not to mix in with the oil signal as one would have expected. The composition of the OBM; it contains 20-30% water, solids and emulsifiers. This was discussed further into detail in Chapter 4 “NMR-derived Porosity”. Observation of small amplitudes at 10 ms is done in several places as well. This occurs often together with amplitudes at 20 ms which gives a tri-peak distribution and suggests invasion meaning that the NMR-derived water saturation in reality gives flushed zone saturation.

6.3 VARYING CUTOFF

Even if the previous chapter stated that a constant cutoff of 92 ms was relatively good water saturation predictor compared to Archie-derived saturation it also revealed that it misses a significant amount of water in some parts, mainly in Tor Fm. where Archie predicted much water. This is due to the varying position of the fluid signal along the wellbore. The constant cutoff lacks the ability to follow it and does therefore not distinguish between the fluid signals as they move. This fluctuation can be caused by several things like lithology, mud filtrate invasion, wettability, gas etc. Figure 24 displays the log curves. In track 3 the constant cutoff saturation method (black curve) exhibits its limitation.

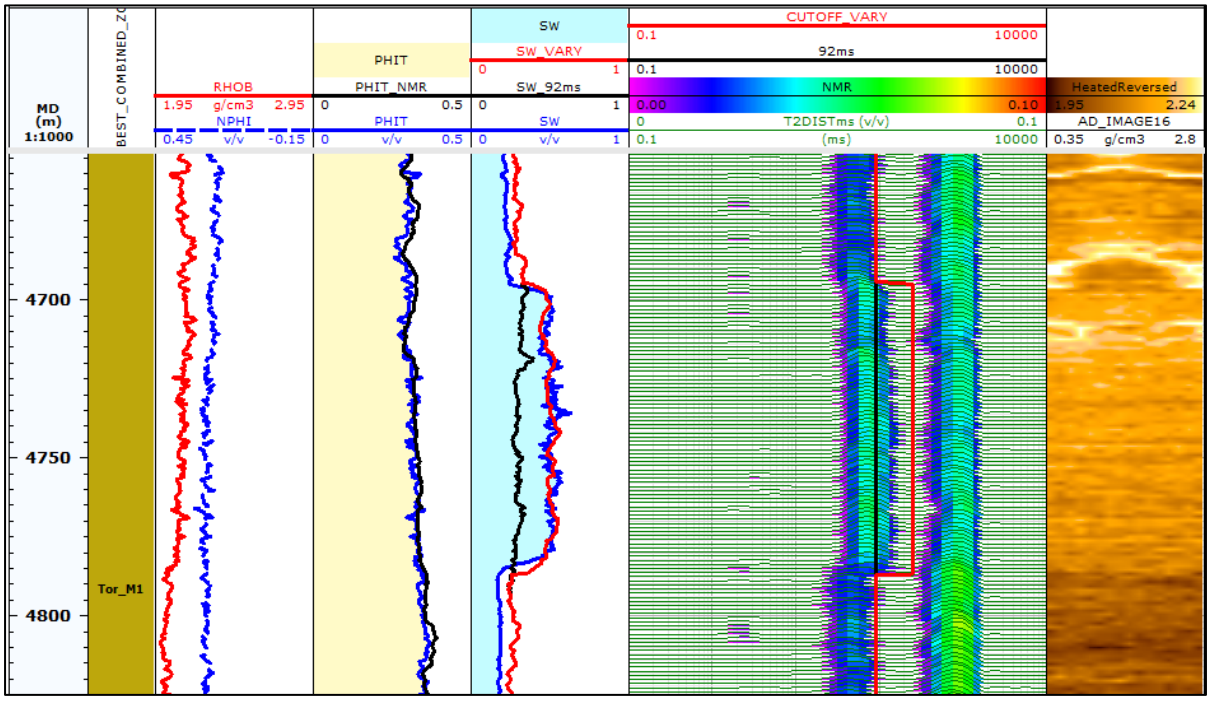

FIGURE 24: WELL 2/8-G3_T3: EXAMPLE OF WHY A VARYING CUTOFF IS NECESSARY

In order to capture these movements the method of variable cutoff has been tested. First a log curve (CUTOFF) was created with a value of 92 ms. The water saturation computation was then carried out and compared to the Archie equation. If there were any specific deviations, the cutoff value over that area was modified to 250 ms. This value was chosen for several reasons. Firstly because it has been used both by the service company and in NMR core reports and secondly because it fits in the trough between the two T_2-peaks. Howard et al. (2001) also applied a method using varying cutoffs in saturation estimations on the Ekofisk

field, a chalk field near Valhall. They found that a simple cutoff was sufficient to distinguish the two fluid phases and adjusted it by visual inspection if necessary.

For the five wells containing MagTrak NMR data only three were subject to any cutoff modifications. The water saturation was computed after having modified the cutoff value and compared with the Archie-saturation. Comparison of how well the two methods correspond to the Archie-saturation was also done and the varying cutoff showed as expected that this method was better. In track 3 and 4 the red curve (varying method) overlays the black line (constant value of 92 ms).

Figure 25 is the crossplot of the Archie (x-axis) and NMR-derived (y-axis) saturations. The varying cutoff method has been applied for the NMR-technique. Figure 26 displays the same crossplot but with a colour scale indicating the data density.

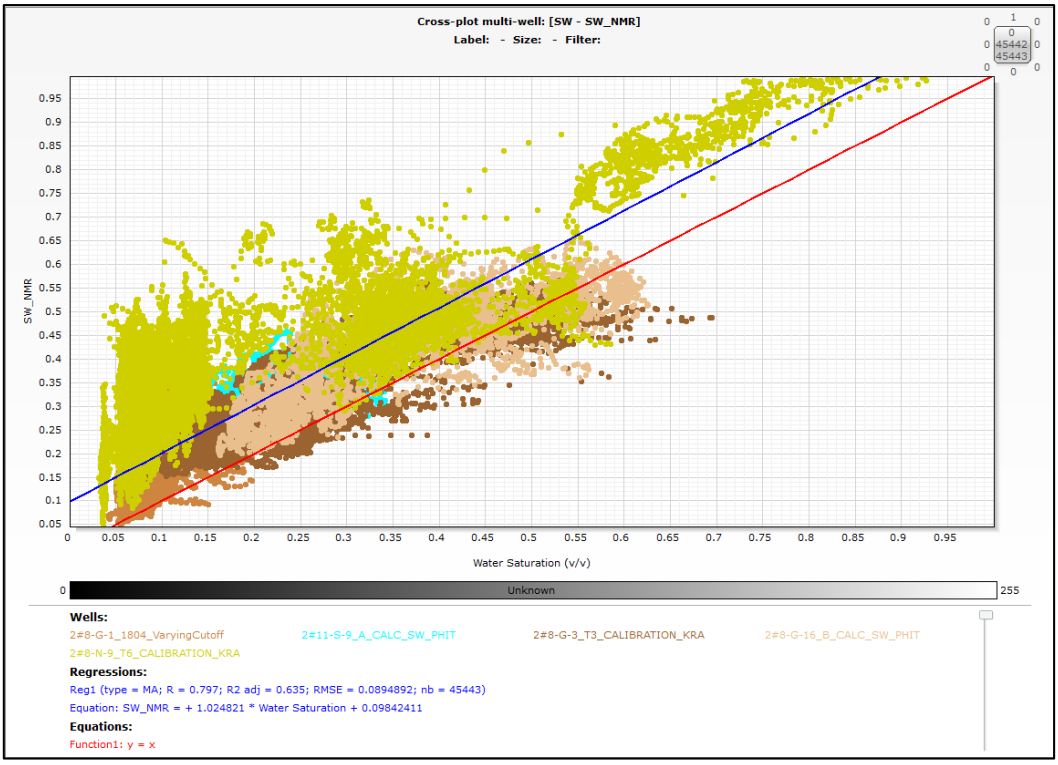

FIGURE 25: CROSSPLOT OF ARCHIE-SW (X-AXIS) VS. NMR-SW (Y-AXIS)

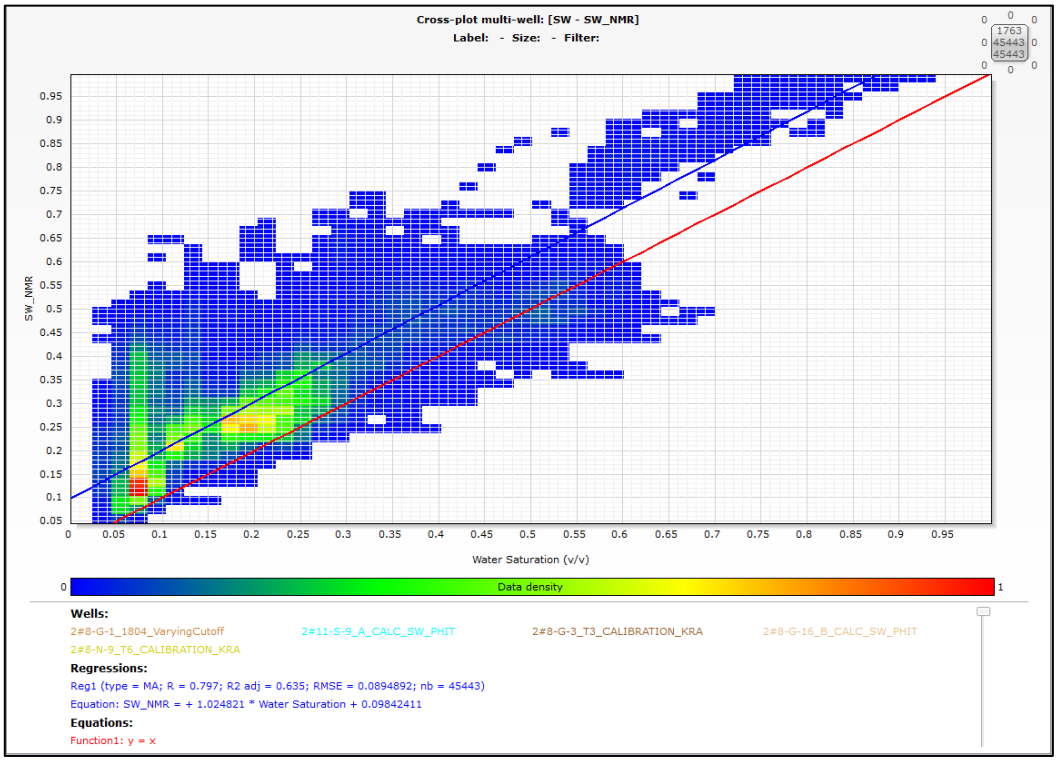

FIGURE 26: THE SAME CROSSPLOT AS FIGURE 24, BUT WITH DATA DENSITY COLOR SCALE

7 NMR APPLIED IN WATER FLOOD SURVEILLANCE

Although Archie's water saturation equation has been used a long time, it cannot distinguish between irreducible formation water and mobile water. This is one of NMR's advantages. By distinguishing between small and large pore sizes as a semi-facies determination; this enables the classification of the nature of the water.

In some newly drilled wells where unexpectedly high water saturation intervals are seen, this has shown to be very useful. Different explanations are proposed; whether it is lithology based effects and irreducible water, or if it is a high-permeability zone with injected water that has experienced a breakthrough. In this chapter some case studies will be presented and the ability of NMR data to provide additional information will be investigated.

7.1 PORE SIZE DISTRIBUTION

The aim for this chapter is that NMR will help understand if the water that is unexpectedly encountered is movable or bound. One easy method is to apply a constant bound fluid cutoff value. It is a straightforward method in fully water-filled formations but becomes more complicated when hydrocarbons are present. This is because the water peak changes both in amplitude and position as a function of the water saturation.

In a fully water saturated formation, the T_2-distribution reflects the pore size distribution (see Chapter 1). The dominant relaxation mechanism is the surface relaxation mechanism. It is proportional to the Surface-to-Volume (S/V) ratio which reflects the pore size distribution. When there are hydrocarbons present, the bulk relaxation of oil is significant and will disturb the T_2-distribution such that it no longer fully reflects the pore size distribution. This is well illustrated in the lower part of Figure 27.

This figure also illustrates that in a water-wet rock, the position of the water peak depends on the water saturation. As the water saturation decreases, the water peak shifts further to the left. The shift happens because the water film is thinning; the amount of water is decreasing, and this is seen by the tool as a reduction in pore size. The amplitude also decreases; this is due to a lower amount of water in the pores to give any signal. Although the water peak

shifts, the oil peak remains at the same position but increases in amplitude as the water saturation decreases. The composition of oil remains constant and the oil is not in contact with the pore walls so there is no surface relaxation mechanism. The total area under the T_2-distribution curve will still give the total porosity regardless of fluid saturations.

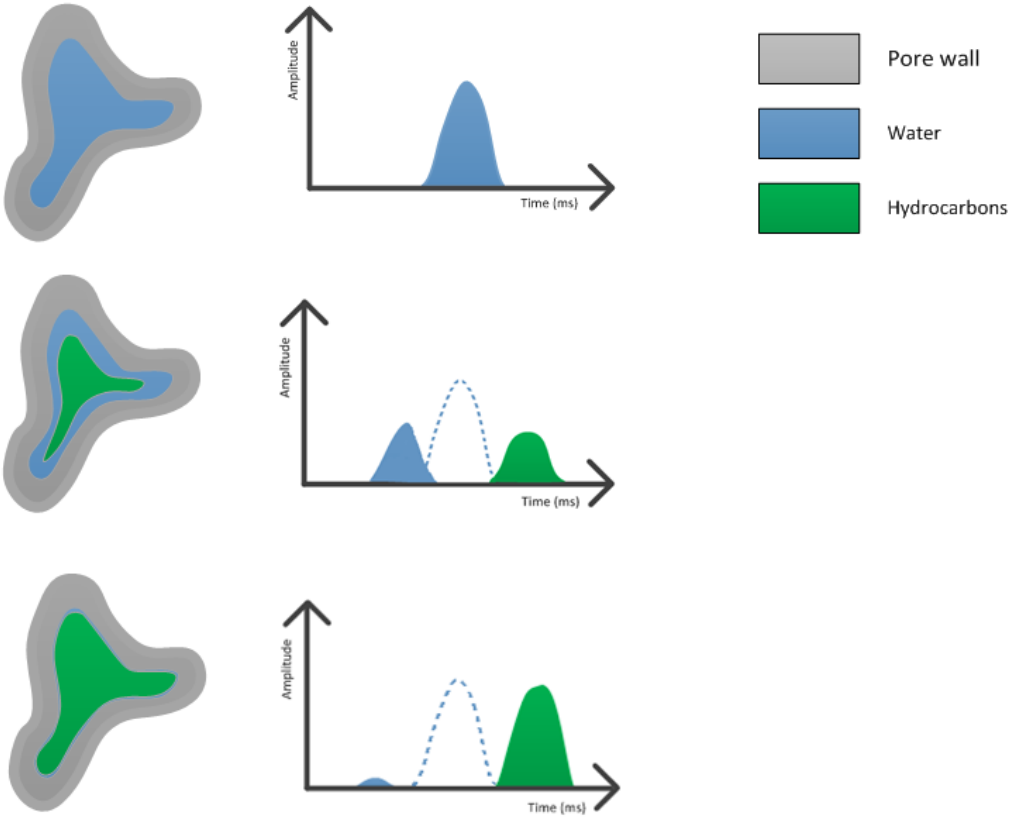

FIGURE 27: ILLUSTRATION OF HOW THE WATER PEAK BEHAVES DEPENDING ON THE WATER SATURATION

This study will assume that the pore sizes are as follows:

- Tor Fm. has a water peak at values of 40 ms
- Hod Fm. has a water peak at values of 15 ms

These values are valid for water saturations sufficiently large so that the water peak is representative for the pore sizes.

First there is the NMR core report from the wells 2/8-F14 and 2/8-A6_A. It specifies that the cores have pore size distributions of 40 and 15 ms for Tor and Hod Fm.

The well 2/8-N3_AY1T2 is not one of the five wells investigated in this study because it does not contain MagTrak data; it contains MRIL data (and T_1 distributions). There is not much difference between T_1 and T_2-distributions because of the lack of diffusion effects in the T_2 distribution. The logs in Figure 28 show that Tor Fm. has values of 40 ms in the water zone and Hod Fm. has values of 1 ms and 20 ms (Track 5).

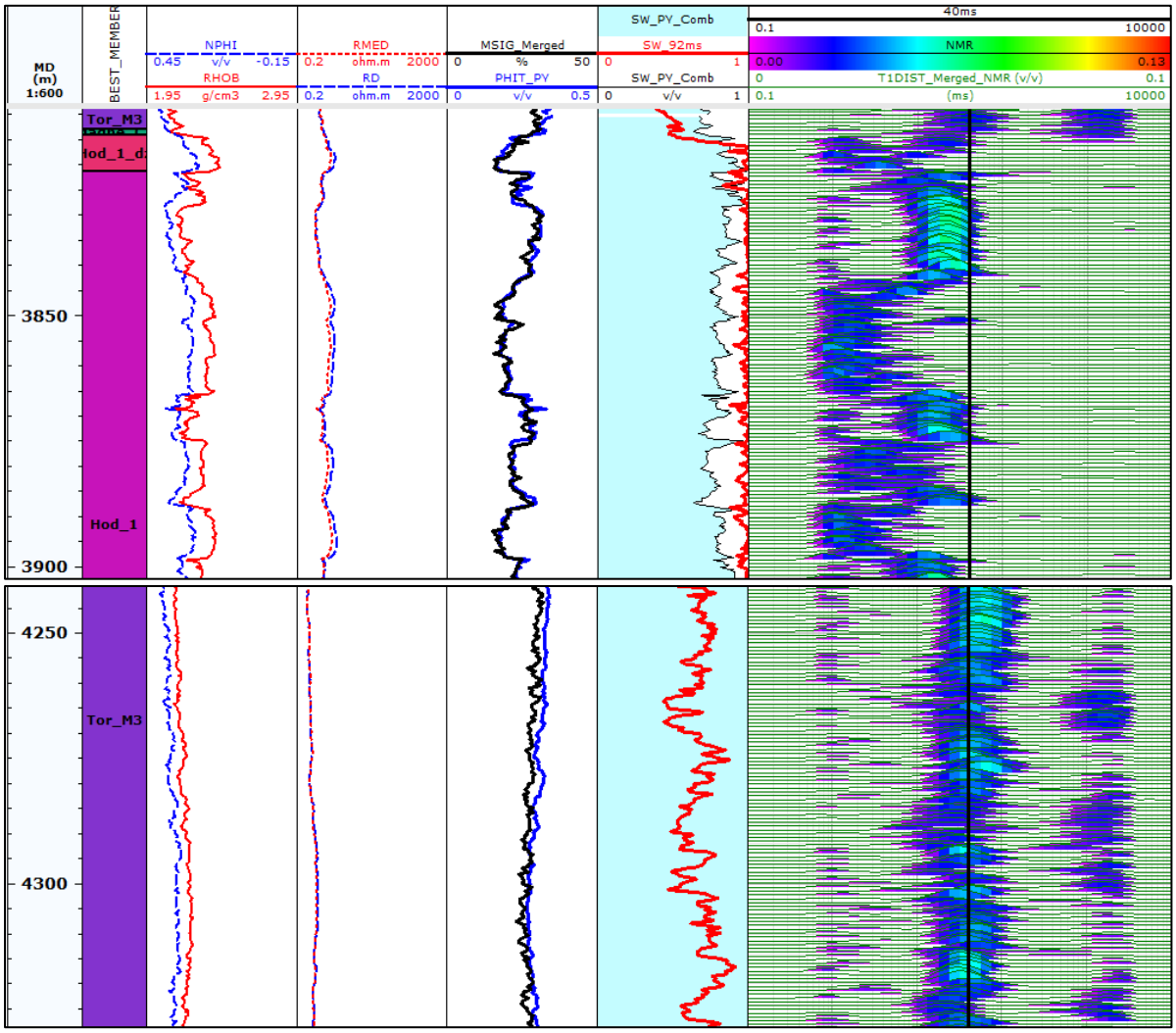

FIGURE 28: WELL 2/9-N3_AY2T2 (MRIL, T_1 DATA), SHOWING THE T_2 DISTRIBTUIONS FOR WATER FILLED FORMATION ROCK

The same values are seen for the well 2/8-N9_T6, in Figure 31 and 32.

To summarize, there is a feature that must be discussed. When high water saturation zones are encountered, they are accompanied by a minor decrease in porosity. This is due to water weakening. When water enters the chalk pores it changes the chemistry and the chalk compacts. This effect is intensified by additional compaction due to pressure depletion which causes mechanical rock compaction.

In the cases presented further on in this chapter the T_2-distribution will be used for classifying the pores into different sizes. The assumption behind this is that in the large pores only a small amount of water is bound whereas in small pores a larger amount of water is bound. The nature of the water in the particular zones will be investigated by analyzing the position of the water peak and thus the size of the pores.

7.2 THE 2/8-N9-T6 CASE

7.2.1 BACKGROUND

This horizontal producer were drilled in 2014 and lies in the northern basin. It lies between the injector 2/8-F16 and the producer 2/8-F2_A as seen in Figure 29. While drilling, a high water saturation zone in the middle of Tor Fm. was unexpectedly detected by the logging tools.

Older Production Logging measurements showed that much of the injected sea water in the injector 2/8-F16 went into the perforation close to the Tor Fm. water zone in 2/8-N9_T6. Furthermore seismic 4D signal shows that there is a change in signal amplitude in this same area.

The contradictory interpretation was the petrophysical. The petrophysical explanation to this larger amount of water was that it was bound formation water due to lithology effects. This was based on the former Archie saturation model which had different exponents according to the formations. This model was investigated and resulted in a new model using the same exponent values for all the formations. Statistically, there were no differences in the formations justifying the former model. This former interpretation did not match what was seen on seismic and other observations.

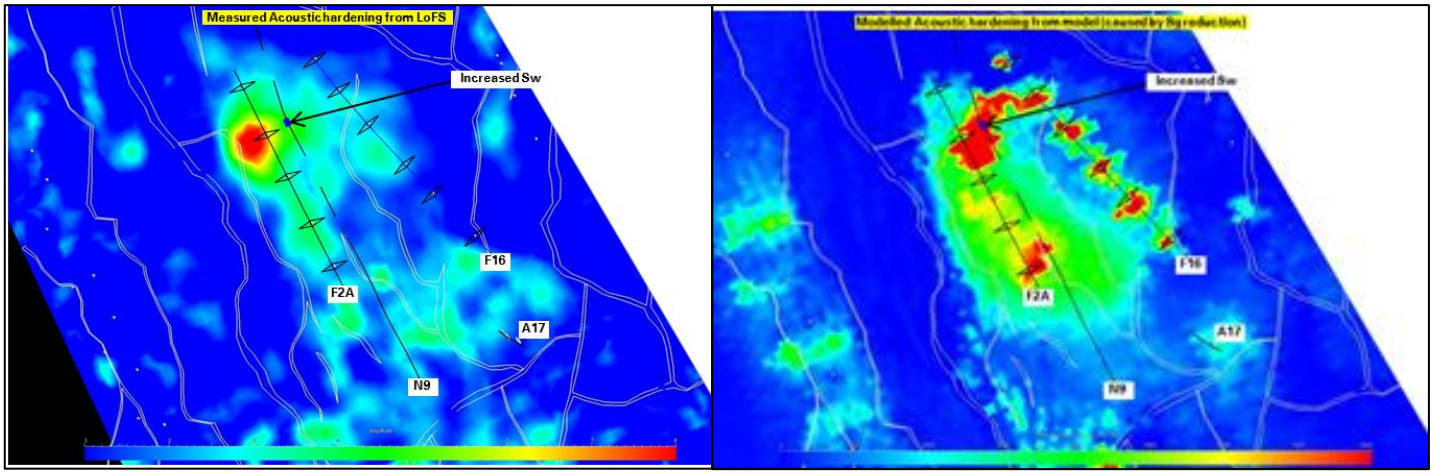

FIGURE 29: SEISMIC IMAGE SHOWING MEASURED (TO THE LEFT) AND MODELLED (TO THE RIGHT) ACOUSTIC HARDENING FROM LOFS DATA

The core study from 2/8-F14 and 2/8-A6_A (Appendix A) indicated that the Tor Fm. has a pore size peak at approximately 40 ms and Hod Fm. has a peak approximately at 15 ms.

Figure 30 shows log curves over the zone of interest. In Track 4 the T_2-distribution is presented. In the same track the green vertical line is the Hod Fm. (15 ms) line and the yellow line is Tor Fm. (40 ms) line. At depth 4100m MD, in the Hod_1 member, the water peak is clearly lying around the 15 ms line (green).

Figure 31 displays the section which contains the water zone further down (marked by a black rectangle). The water peak signal is situated at values of approximately 40 ms. This indicates that this particular zone does not appear to contain smaller pores than the surrounding area. Furthermore, from the density image log (Track 5) bedding dip analyses have been done which show that there is a fault in that zone (red mark in Track 6). This supports the interpretation that it is movable water coming from the injector 2/8-F16 and that it is not irreducible formation water.

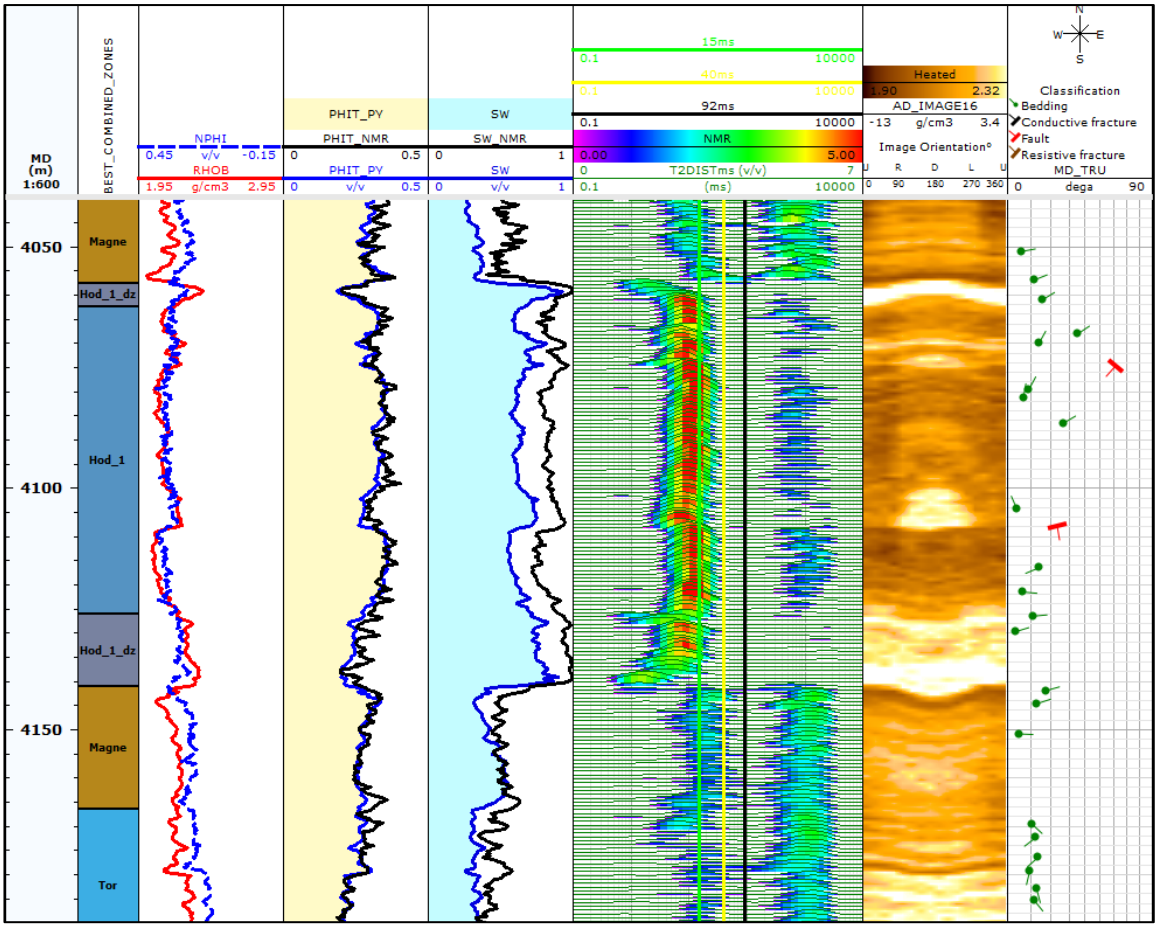

FIGURE 30: LOG CURVES FROM HOD FM. SECTION IN WELL 2/8-N9_T6

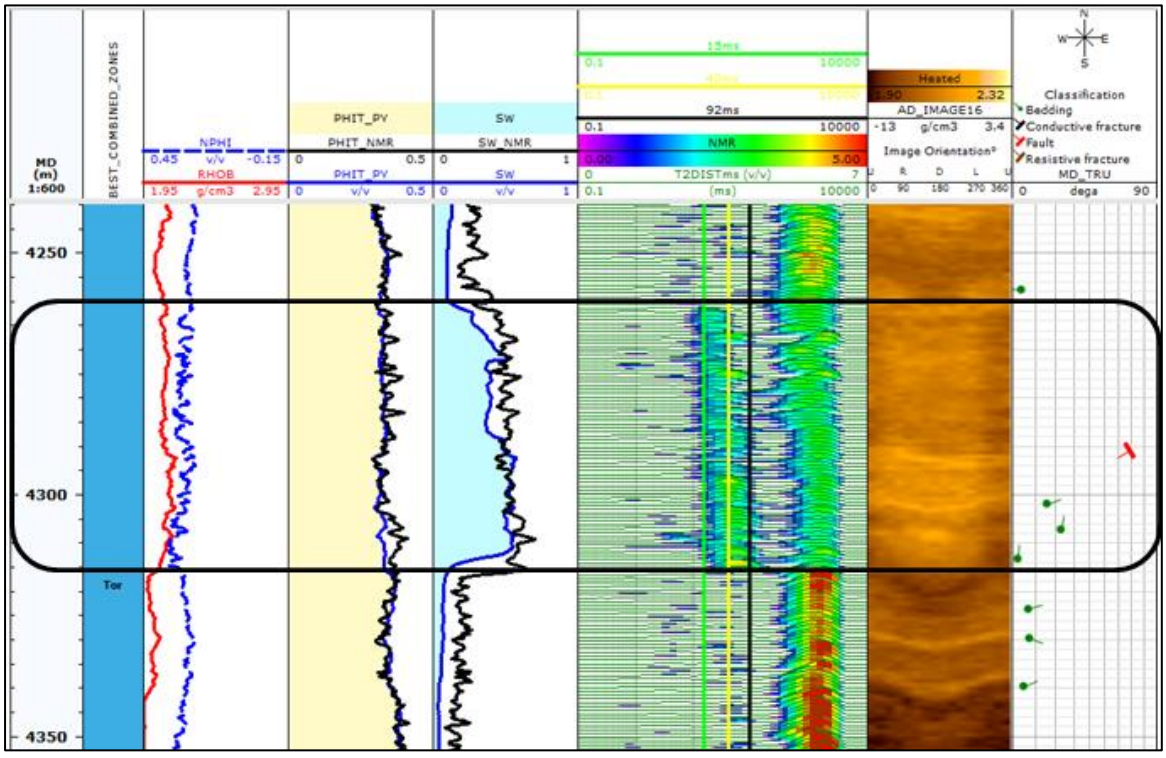

FIGURE 31: LOG CURVES SHOWING THE TOR FM. WATER ZONE IN WELL 2/8-N9_T6

7.3 THE 2/8-G16_B CASE

7.3.1 BACKGROUND

2/8-G16_B is one of many sidetracks before getting to the producer 2/8-G16_BT3 and is situated at the east flank, near the aquifer. Figure 32 is a Hydrocarbon Pore Volume (HCPV) map section of the East Flank. The logs showed several distinct high water saturation zones (Sw above 30%) along the wellpath. The well is horizontal and there are practically no changes in vertical depth. The well has been producing with up to 45% water cut.

The lack of explanation to this is due to the relatively poor understanding of the aquifer and how it is advancing up- and inwards as the reservoir is depleted. Is it a basal water drive, a fault-assisted water drive or possibly an imbibition-driven water front displacement? Other theories suggest a "fingering" water front and advancing through formation layers. It could also be formation water that has been there since the beginning; a higher irreducible water saturation than the surroundings.

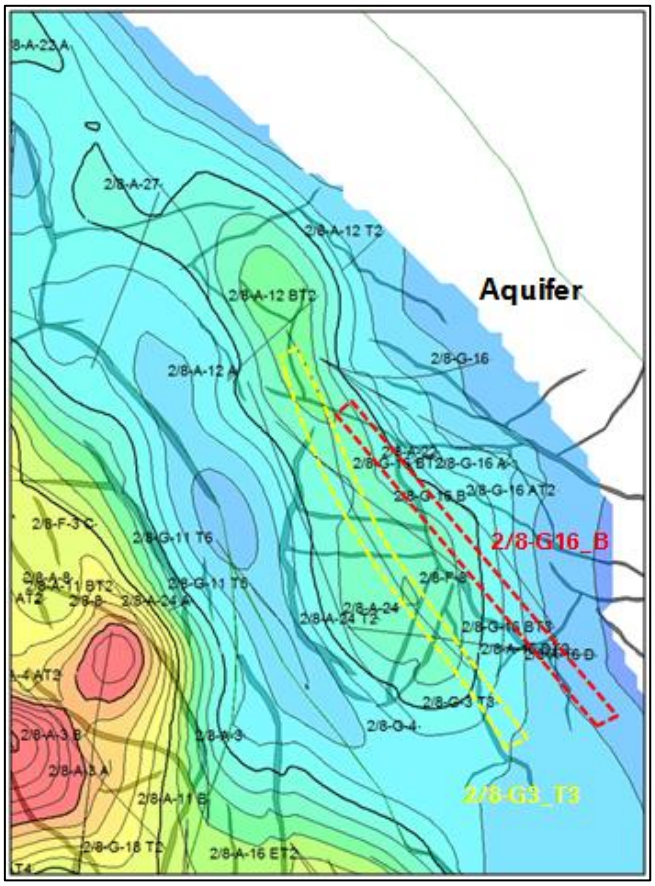

FIGURE 32: HCPV MAP OF THE EAST FLANK, 2/8-G3_T3 (YELLOW), 2/8-G16_B (RED)

7.3.2 INTERPRETATION

Figure 33 displays the main logs required for this interpretation. The yellow line in Track 4 is the 40 ms line. This line is representing the Tor Fm. pore size distribution (see Chapter 6.1 for justifications).

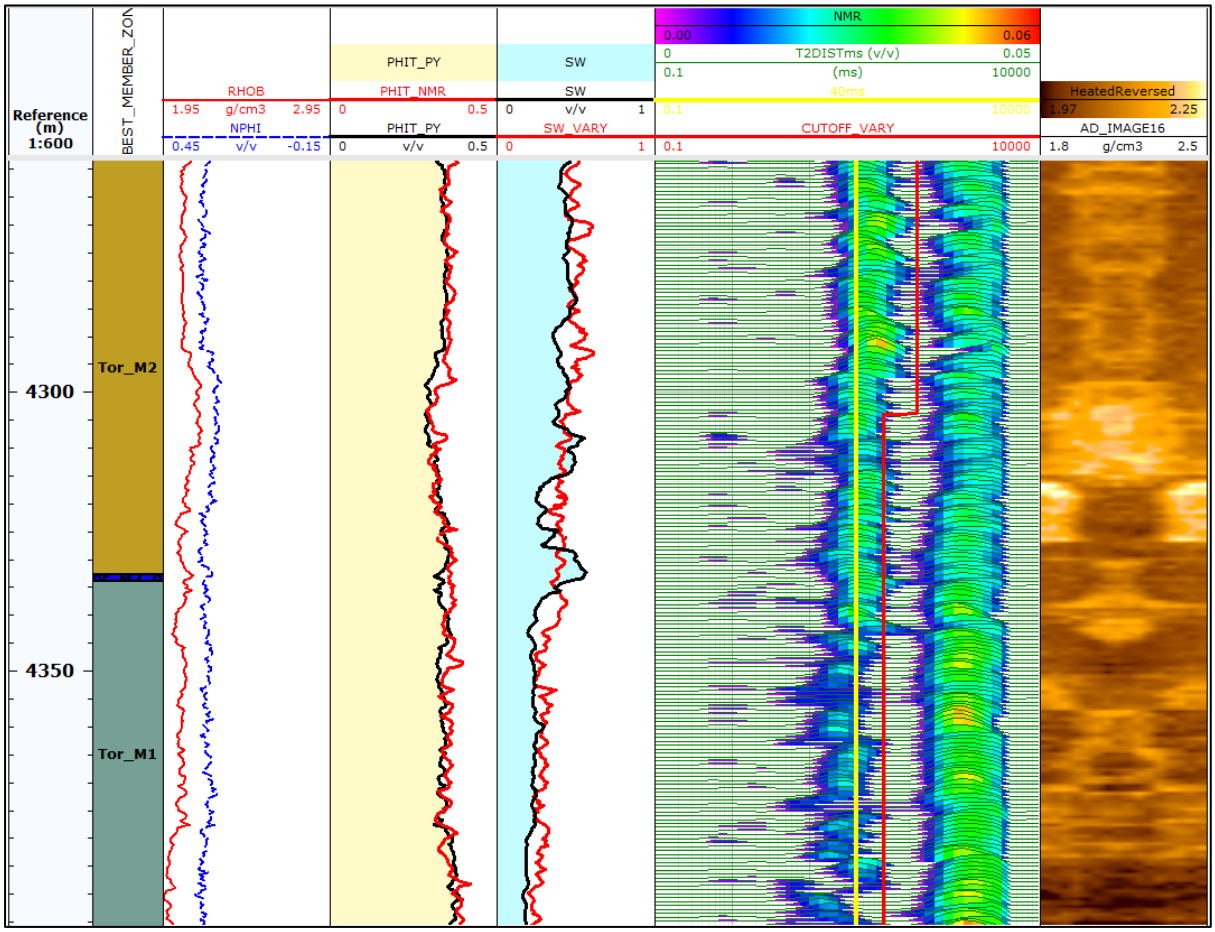

FIGURE 33: MAIN LOG CURVES FROM 2/8-G16_B

There are no important changes in porosity over the different formation members but the Archie-saturation changes from approximately 50% to 20% water downwards from top of the log (4260m MD) to 4330m MD.

Observing the T_2-distribution in Track 4, the water peak (to the left) is strong in amplitude and situated at slower relaxation times. Further down in the wellbore past the water zone the water signal decreases in amplitude and shifts to shorter relaxation time. This implies that there are no clear lithological effects causing the extra amount of water here and that the water is movable.

7.4 THE 2/8-G3_T3 CASE

7.4.1 BACKGROUND

This producer is also situated at the east flank near 2/8-G16_B. It is situated further updip, both toward the central part of the field and upwards in vertical depth. When the reservoir was entered they first encountered a water zone of approximately 100 meters, and then further into the reservoir some very short sections of water and a 100 meter long water zone at 4700m MD. These zones were not expected. Dip interpretations revealed large faults in these areas and the seismic data detects rock compaction.

7.4.2 INTERPRETATION

Figure 34 displays the essential log curves. Track 3 contains density- and NMR-porosity. There are no significant differences between the porosity types. Track 4 displays the Archie-saturation (blue) and the black and red curves are NMR-saturations (black curve is from using the constant cutoff, red curve is from the recommended varying cutoff method).

From 4700-4790m MD the Archie-saturation changes from approximately 20% to 50% water. Over the same interval there is no significant change in either RHOB or NPHI. There is a change in RD which is the main reason for the high Archie-saturation. The porosities both are somewhat lower than in the surrounding areas. This is expected in water zones because there is a water weakening effect as explained previously.

On the T_2-distribution there are two distinct peaks where the peak to left is the water signal peak. Over the particular interval this water peak increases in amplitude as well as it is shifting towards longer relaxation times. The peak lies above 40 ms (yellow line) which indicates that there are no lithological changes here.

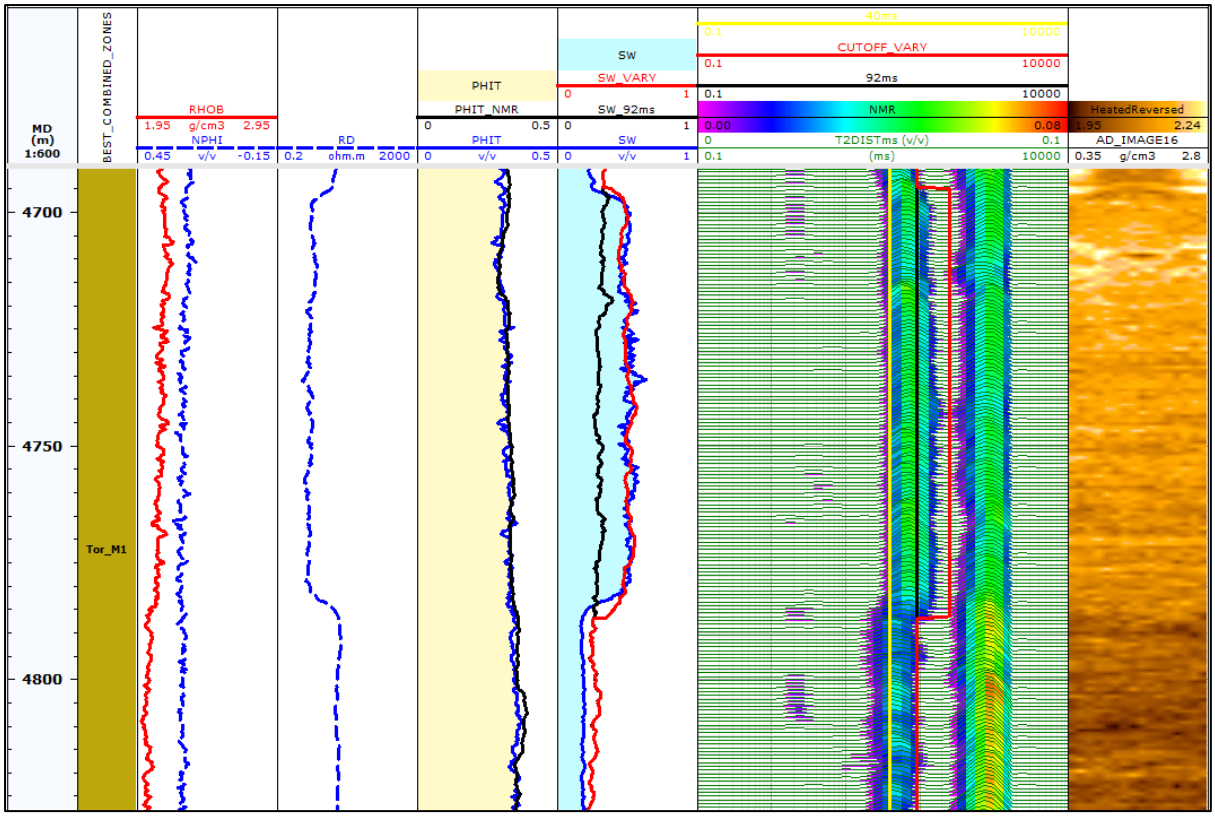

FIGURE 34: MAIN LOG CURVES FROM THE TOR FM. WATER ZONE IN 2/8-G3_T3

8 PERMEABILITY

Permeability estimation is one of the earliest applications of NMR logging and it is widely used. It provides a continuous estimation of the permeability along the wellbore which is preferable to the expensive point by point core analysis. It is one of the outputs from the service company's NMR log report, given as an index. Therefore the usefulness of the NMR-permeability will be investigated in this chapter.

8.1 THE PERMEABILITY EQUATIONS

8.1.1 POROSITY-PERMEABILITY RELATIONSHIP

The permeability prediction for the Valhall field has been based on an empirical relationship between the core porosity and core permeability. A recent study of these relationships revealed an exponential relationship with varied constants according to groups of formation members. To account for some uncertainty there are three cases; base case, low and high case.

$$k_{PORPERM}(md) = b * \exp(a * PHIT) \quad (21)$$

'a' and 'b' are constants depending on the lithological grouping and determined by best fit regression. PHIT is the total porosity.

It is important to specify that these relationships between porosity and permeability are uncertain and that they only represent an estimation of it. Despite the uncertainty the base case PORPERM-relation will serve as the "default" permeability in this analysis. The high and low cases are shifts up and down (by changing the value of 'b') serving as uncertainty range.

8.1.2 THE NMR PERMEABILITY EQUATIONS

NMR logging does not measure permeability directly. It relies on the assumption of a relationship between pore throat and body. It also takes into consideration the T_2-distribution. The parameters are preferably determined by core analysis. There are different equations for predicting permeability from NMR; this thesis will concentrate on the two most common ones.

Coates-Timur Equation

The Coates-Timur equation is the most used NMR permeability equation and shows good results in clastic rocks but rather poor results in carbonates. It is given by Eq. 22

$$k_{Coates}(md) = \left[\left(\frac{MPHS}{a}\right)^2 * \left(\frac{FFI}{BVI}\right)\right]^b \quad (22)$$

MPHS is the NMR-porosity, FFI is the Free Fluid Index and BVI is the Bulk Volume Irreducible. 'a' and 'b' are the Coates parameters.

The service company provides a Coates Equation permeability estimation log in their end-product. Although the parameters can be found by NMR core analysis they claim this estimation should only be used as an indication of high or low permeable zones, not as any definite value. These parameter values have been derived from core study (Appendix A, F14&A6_A) and should give reliable permeability estimations.

Schlumberger-Doll-Research (SDR) Equation

The other permeability equation is the SDR-equation. This equation shows better results in carbonates than Coates Equation but it has issues with hydrocarbon-filled formations. Because it uses the geometric mean of T_2 (T_{2GM}), it will be significantly altered when

hydrocarbons are present because of its particular T_2-distribution. This influences and overestimates the estimated permeability. The SDR equation is given by Eq.23

$$k_{SDR}(md) = \left(\left(\frac{MPHS}{a}\right)^2 * T_{2GM}\right)^b \quad (23)$$

8.2 PROCEDURE

The first step is to determine whether the permeability (MPERM) delivered from the service company (with its default parameters) is reliable as permeability estimation or not. The main formation in the five wells logged with MagTrak is Tor Fm., with only small sections of Magne and Hod Fm. Therefore Tor will be the formation in focus and data from Magne and Hod will be excluded. Crossplots of MPERM and PORPERM will reveal if shifts are necessary, if MPERM is too large or too small or if there is no correlation at all.

Some NMR core studies have been conducted but due to the quality of the cores most core material is from Hod Fm. Only one of the studies have both Tor and Hod cores (F14 & A6_A, see Appendix A for further information), and this study recommended using the values of 'a' and 'b' as given in Table 2. These are values used in the MPERM computations provided by the service company.

TABLE 2: NMR PERMEABILITY PARAMETERS

Equation	Formation	a	b
Coates	Tor	40	0,9
	Hod	40	0,9
SDR	Tor	243	1,6
	Hod	243	1,6

The equations for estimation of the permeabilities in Tor Fm. will then be given by

$$k_{PORPERM-base\ case} = 0.0124 * e^{14.477*PHIT} \quad (24)$$

$$k_{Coates} = \left[\left(\frac{MPHS}{40}\right)^2 * \left(\frac{FFI}{BVI}\right)\right]^{0.9} = \left(\frac{MPHS}{40}\right)^{1.8} * \left(\frac{FFI}{BVI}\right)^{0.9} \quad (25)$$

$$k_{SDR} = \left(\left(\frac{MPHS}{243}\right)^2 * T_{2GM}\right)^{1.6} \quad (26)$$

For the MPERM delivered in the NMR log report, a bound fluid cutoff of 92 ms has been used. This is the carbonate standard cutoff value. The core reports however state that of the homogeneous nature and the micron sized pores this cutoff value is too large. The report proposes a bound fluid cutoff value of 28 ms and 18 ms for Tor and Hod Fm. respectively, with an accuracy of 3 pu. The next step is therefore to recalculate the Coates permeability using the proposed bound fluid cutoff and compare the new k_{Coates} to the PORPERM permeability.

Furthermore the robustness of the parameters ‘a’ and ‘b’ will be investigated. First by keeping everything else but one parameter constant and find the value of this required to obtain the best match between k_{Coates} and PORPERM. Then optimize the values together.

The robustness of the SDR equation will be tested although it is not expected to show good results due to the strong presence of hydrocarbons.

8.3 RESULTS

8.3.1 MPERM

First the robustness of MPERM was examined. The MPERM was computed with a=40 and b=0.9. The crossplot in Figure 35 of Tor Fm. MPERM versus PORPERM shows that the majority of data points lies around the unity slope line (red line). Nevertheless the scatter is large; there are both large overestimations as well as underestimations. There are two different underlying porosities applied; MPERM uses MPHS whereas PORPERM uses PHIT. Although they are considered equal (as discussed in Chapter 4) there are small differences between the two porosities which enhance the difference between the permeabilities.

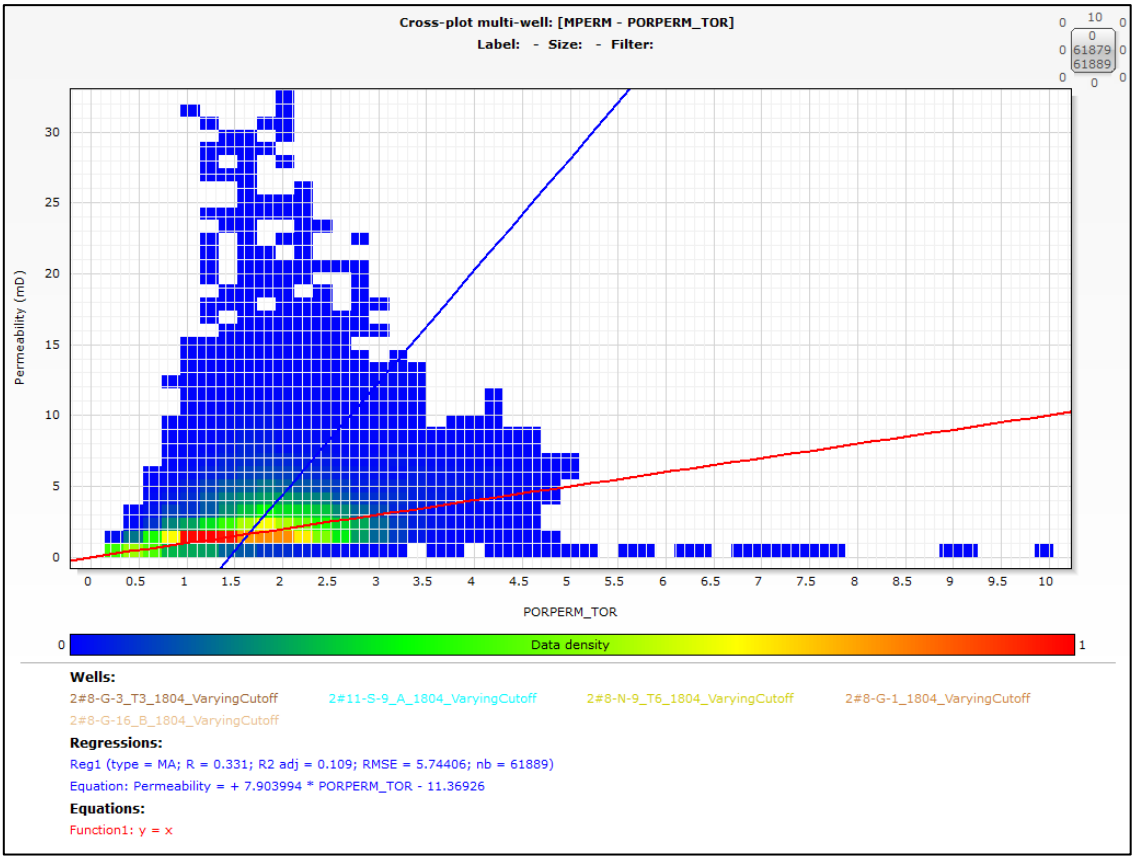

FIGURE 35: CROSSPLOTT OF PORPERM-PERMEABILITY (X-AXIS) VS. NMR PERMEABILITY MPERM (Y-AXIS)

The importance of the use of different porosities was investigated. The PORPERM permeability was recalculated using MPHS in lieu of PHIT (Figure 36). This did not present any important difference in the permeability computations.

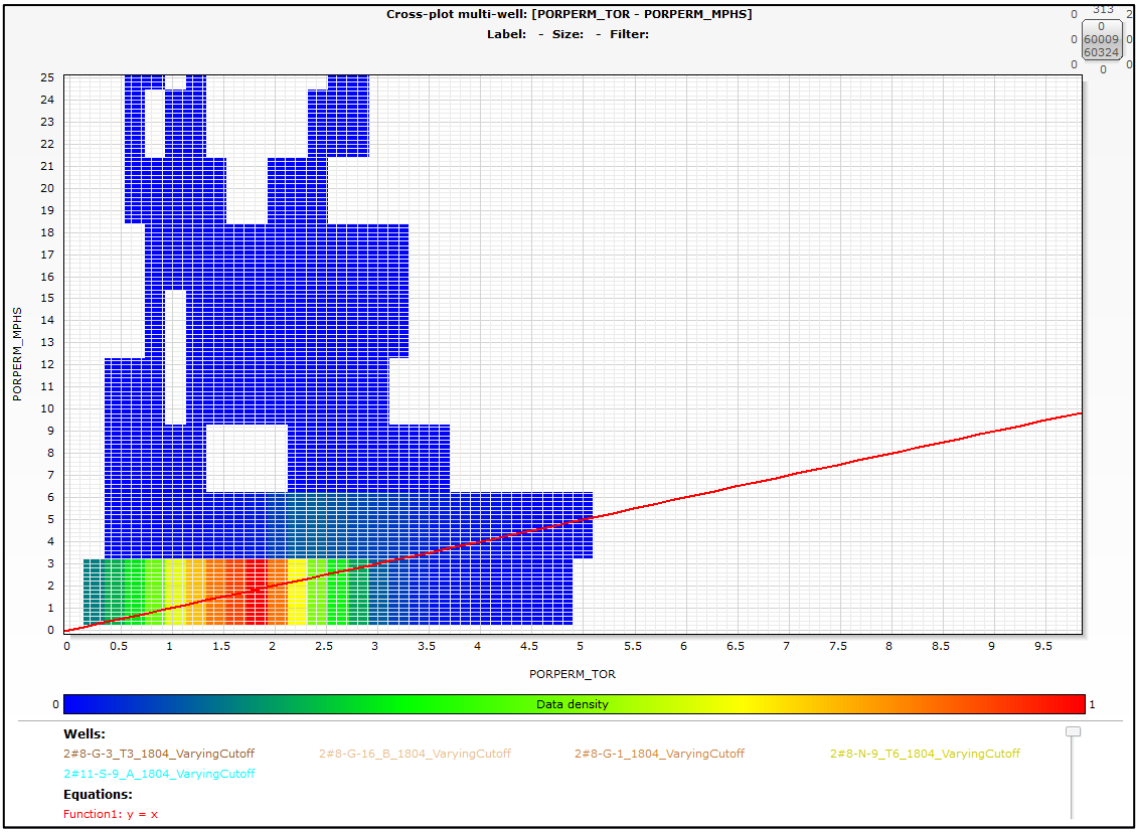

FIGURE 36: PORPERM BASED ON PHIT (X-AXIS) VS. PORPERM BASED ON NMR-POROSITY (Y-AXIS)

8.3.2 Bound Fluid Cutoff

The core report stated that the 92 ms cutoff for bound fluid volume was too high and proposed more suitable values. Therefore the NMR derived permeability has been recalculated with the proposed cutoff of 28 ms for the Tor Fm. and compared to PORPERM (Figure 37). Changing the Bound Fluid Volume Cutoff only changes the Free to Bound Fluid ratio $\frac{FFI}{BVI}$. This exercise only investigated the impact of defining the fluids differently.

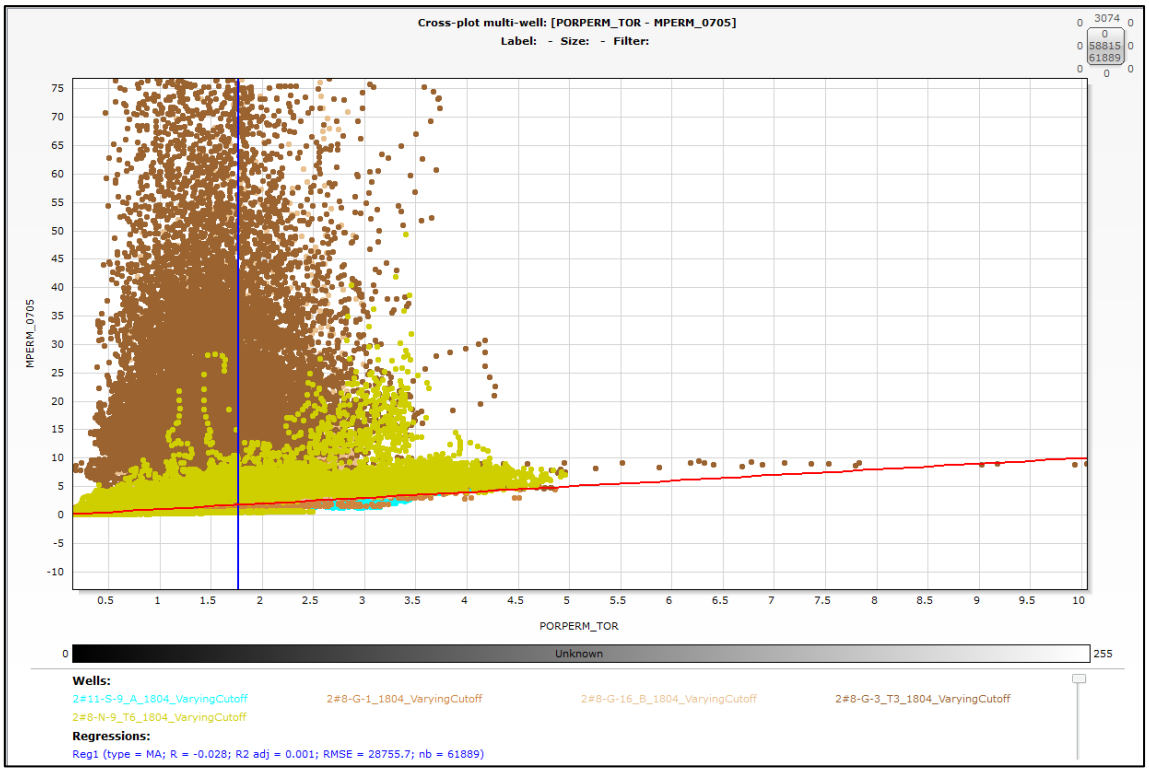

FIGURE 37: PERMEABILITY CROSSPLOT WITH PORPERM (X-AXIS) VS. NMR-DERIVED PERMEABILITY USING BOUND FLUID CUTOFF OF 28MS

The volume of bound fluid varies much and in some wells the bound fluid percentage even decreases to 1% which is unreasonably low. In general the cutoff of 92 ms fits rather well. One possible explanation is that the signal below 92 ms only is water, and for oil-saturated zones the only water present is irreducible water. When there is more water than just the irreducible, 92 ms will give too high bound water volume.

Figure 38 displays the logs from 2/8-G1 where the formation is at its initial oil saturation. There is hardly any difference using the 92 and 28 ms bound fluid cutoff. It is reasonable to assume that the water saturation is at its irreducible saturation. However, at sections where Archie Saturation is higher there is significant difference in the FFI/BVI ratio derived from the two cutoff values.

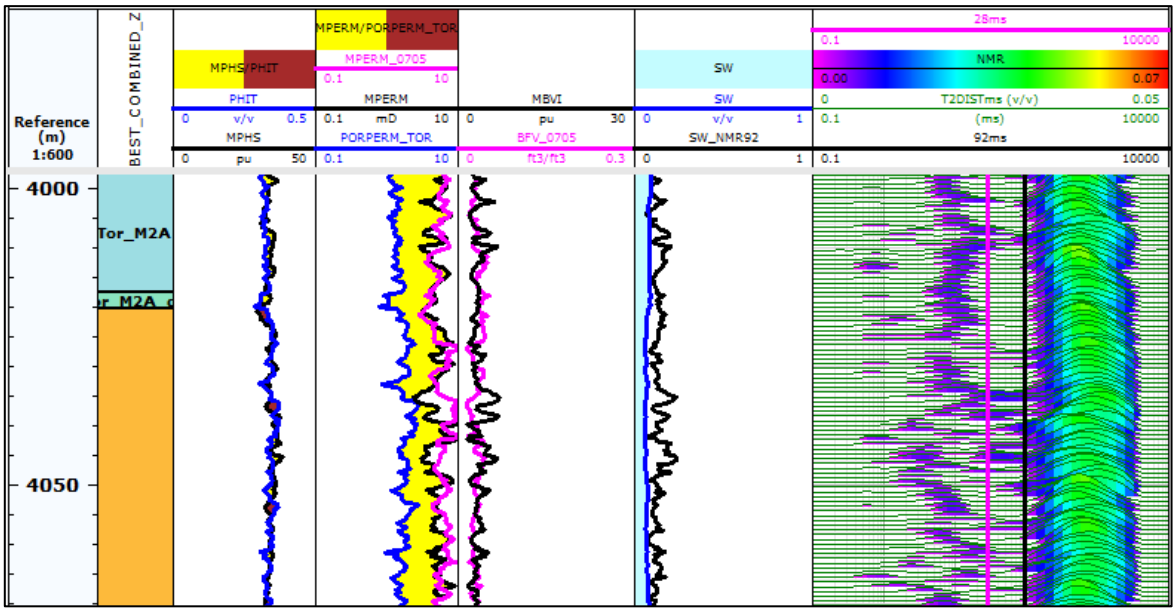

FIGURE 38: LOG CURVES FROM 2/8-G1 SHOWING THE SIMILARITY BETWEEN 92 & 28 MS BOUND FLUID CUTOFFS

This is not the case for other wells. In well 2/8-G3_T3 the difference between the bound fluid volumes is significant, see Figure 39. The 28 ms cutoff predicts an irreducible water saturation of 1-2 % (Track 3, pink curve). Then the free to bound fluid ratio FFI/BVI becomes very high and thus the permeability as well. There is hardly any T_2-amplitude to the left of the 28 ms line (pink) in the T_2-distribution in track 5.

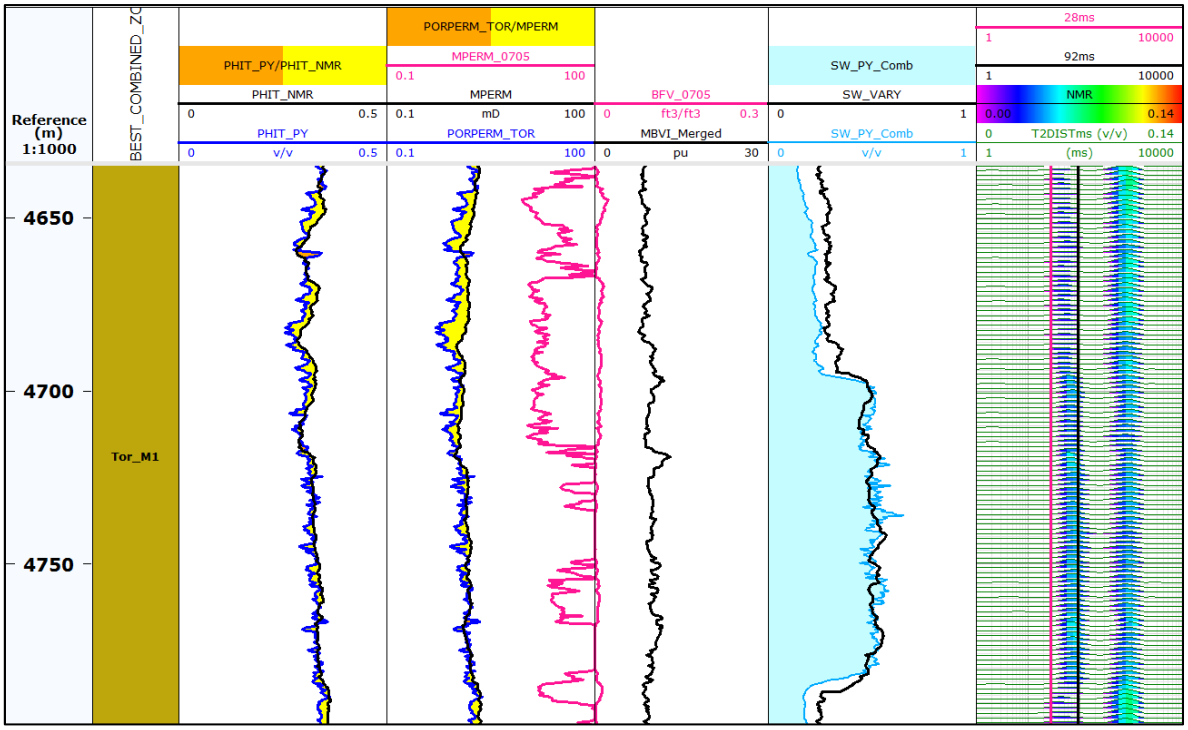

FIGURE 39: LOG CURVES FROM 2/8.G3_T3 SHOWING THE DIFFERENCES THE SAME CUTOFFS CAN PRODUCE

Since the 28 ms cutoff displays such a large diversity in results, compared to the corresponding 92 ms results, to give permeabilities of several thousands of millidarcies, this cutoff does not exhibit ant robustness. It should not be used.

The uncertainty regarding bound fluid volume and defining its cutoff should be investigated further.

8.3.3 THE SDR EQUATION

Figure 40 displays logs from 2/8-N9_T6 with the computed SDR-permeability in Track 2, shown by the black curve. When there is oil present the T_{2GM} in Track 3 is high because of the strong oil signal and therefore the SDR-permeability becomes high. It has values in the range of 100 millidarcies, which is unrealistically high. The conclusion therefore is that the SDR permeability equation is inappropriate for this case.

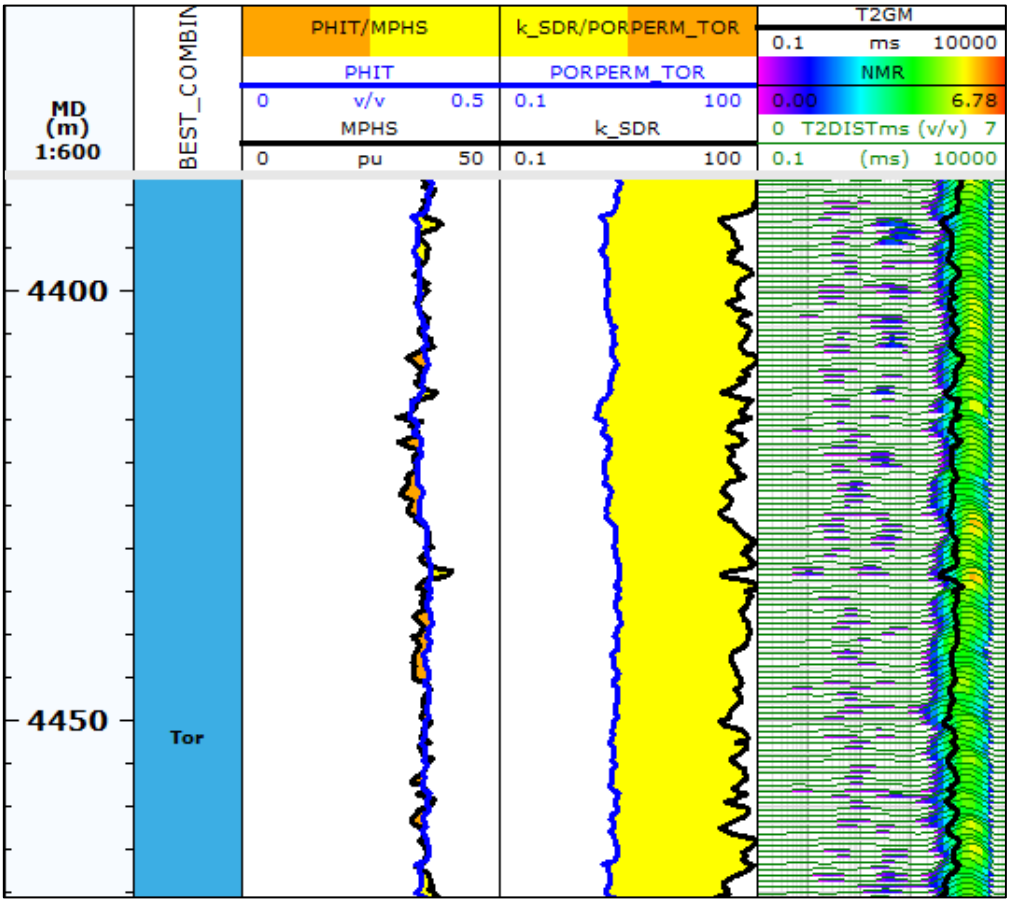

FIGURE 40: LOG CURVES FROM 2/8-N9_T6 DISPLAYING THE DEVIATION OF SDR PERMEABILITY FROM MPERM

8.3.4 THE PARAMETERS A AND B IN COATES EQUATION

The study also investigated the impact of the parameters ‘a’ and ‘b’ in the Coates equation. The parameters were modified in order to try to fit the NMR and PORPERM permeabilities better by decreasing the total difference as much as possible. First, by keeping the ‘b’ constant and varying the ‘a’ the value that minimized the general difference between the two permeabilities was found. Then the same was done for finding a more effective value for ‘b’. Finally, they were simultaneously varied to get a good match.

Various approaches to find ‘b’ values were tried. “Blind tests” were also conducted; finding values of ‘b’, using only four of the five wells and then using the fifth to confirm the reliability. These tests gave values of ‘b’ ranging from 0.38 to 0.43. The parameter ‘a’ was kept constant and equal to 40. All of these ‘b’ values exhibited a better fit to the base case PORPERM relation. By keeping ‘b’ constant at 0.4 a better value of ‘a’ was found to be 33.871. More detailed data are given in Appendix F.

The Coates permeability estimations, with the different values of ‘b’, fitted within the boundaries given by low and high case PORPERM. The curves are given in Appendix F, Figure 50-54. The percentage of data within the boundaries was approximately 60%. An example from a well section is given in Figure 41. This leads to confidence in the optimized ‘b’ value as a better fit than the 0.9 proposed by the core report. The core report has its limitations; a limited number of core from only two wells were used. This does not provide a broad statistical base for analysis. The core quality may also be questionable due to reasons discussed previously.

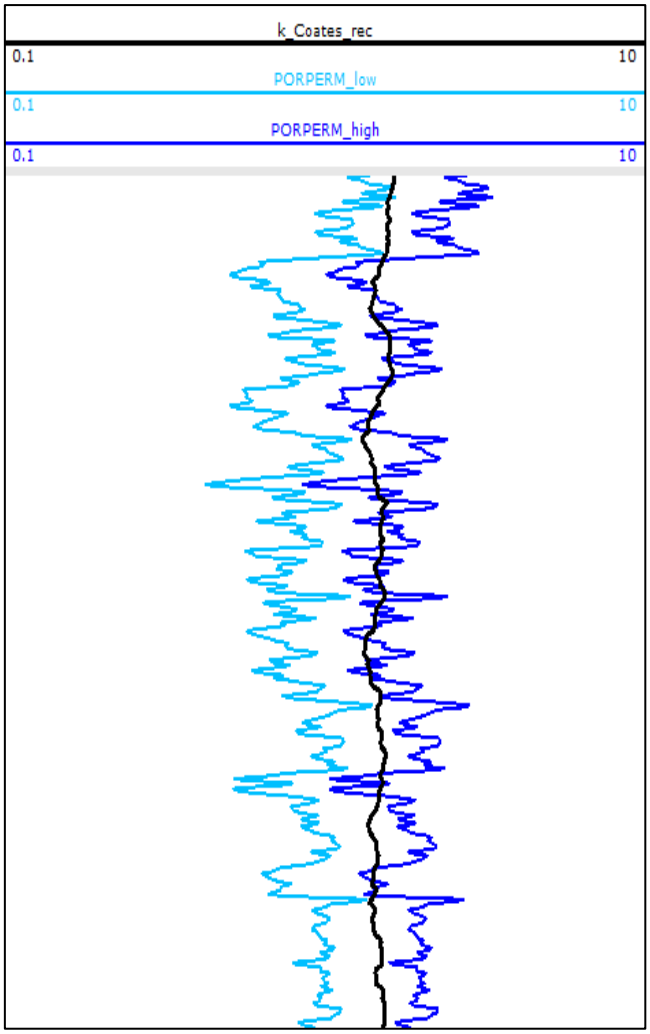

FIGURE 41: EXAMPLE FROM 2/8-G3_T3, PORPERM LOW AND HIGH CASE VS. NMR COATES PERMEABILITY WITH THE NEW, OPTIMIZED PARAMETER VALUES FOR 'A' AND 'B'

9 DISCUSSION

9.1 QC PROCESS

The quality control of the NMR data is, as with other logs, essential. The process aims to weed out data that should be handled with care. It flags the data into three categories according to their believed quality. Preferably this flagging is done with other log data available. If no other data are available this process becomes complicated and more uncertain. One should then look for strange behaviour in the log curves and unrealistic values based on experience.

9.2 CALIBRATION MATERIAL

No core samples for NMR studies were taken from the five wells with MagTrak-data. Core samples have only been taken from wells containing no NMR log data at all or in the case of F14&A6_A where MRIL, the predecessor of MREX the current Wireline NMR tool) was run. The quality of this MRIL NMR data is questionable and the dataset lacks the T_2-distribution. The wells containing cores are situated at the crest so they may not be representative for the entire field. Also, the number of core samples is not considerable enough for a good statistical basis. The parameters derived from these tests should be used with caution. More core studies should be conducted.

9.3 POROSITY

The NMR is a lithology independent porosity tool; it is mainly sensitive to the formation fluids. In addition, this tool does not have a nuclear source and is therefore a preferable choice in a HSSE perspective. The reliability of NMR as a porosity tool was investigated by crossplotting the NMR-derived porosity against the Density-derived porosity after the post-processing QC-process. Figure 14 shows this crossplot. The points do not exhibit any significant scatter and the regression line fits the unity slope line. Particularly in the range of 30 to 40 % porosity which is the typical range of the reservoir. Because of the good fit one can also conclude that the formation is fully polarized.

The NMR tool has a limitation regarding the shallow DOI. Poor borehole conditions often occur because the formation is likely to degrade. In these areas the NMR-porosity tends to become very high whereas no other log seems to capture this change. Poor borehole conditions are not always obvious to detect from the Caliper curve but the density image log indicates more clearly that there are borehole enlargements. These poor borehole conditions should be picked up and marked by a red flag in the QC-process.

9.4 SATURATION

The saturation estimation from NMR is based on the principle that a mixed saturated formation exhibits a bi-modal T_2-distribution where the peak at longer T_2-values is signal from the oil and the other peak is signal from the formation water. A clear separation between the two should therefore give a straightforward saturation computation.

In the pre-computed saturations from the service company different values for the hydrocarbon cutoff were applied. They were ranging from 92 ms to 250 ms. Comparing these to the T_2-distributions showed that the best overall fit with the Archie-saturation was a cutoff of 92 ms. This was also the value that was most centered in the middle of the trough between the two peaks. Although it was mostly between the T_2-peaks, a constant cutoff of 92 ms revealed some limitations. The T_2 water peak sometimes shifted to longer T_2 relaxation times, which made the 92 ms cutoff define some of the water signal as oil. This is described in further details in Chapter 6.1. These areas also showed unexpectedly high Archie-derived water saturation. In order to capture these shifts, the method of varying the cutoff from 92 ms to 250 ms manually according to the position of the trough (or the water peak) was applied and agreed better with the Archie saturation.

Despite this clear separation between the oil- and water-filled porosity, the NMR-derived saturation was far above the Archie-derived saturation in many cases. A difference of 10-15 pu was sometimes observed. An important issue to mention is the different volumes these two saturation methods consider. The NMR tool has a very limited DOI whereas the measurements used in the Archie-equation reach much further into the untouched formation. This means that the NMR tool may see invaded formation while the conventional tools do not. It is unknown how long it takes for invasion to take place, but the MagTrak tool is situated at the end of the BHA to minimize drilling induced movement. This distance is often approximately 10 meters. So the question is if this is enough time for invasion to occur.

There are currently no mud filtrate samples taken for NMR lab experiments. Therefore the signal from mud filtrate is not certain. Though there are indications from poor borehole quality sections that the mud filtrate has a peak around 10 ms. Although it is an OBM it contains in general 20-30% water in addition to emulsifiers. It is highly recommended to take samples for NMR lab tests in the future.

Small amplitudes at very short relaxation times are observed. These could be capillary bound water or artefacts caused by ringing, other noise or the inversion process. The chalk is considered quite homogeneous so one would believe that a signal originating from capillary bound water would be more continuous.

So far the uncertainties related to the NMR-derived saturation have been discussed, but there are also some related to the Archie-saturation. The Archie exponents ‘m’ and ‘n’ may not be correct. The exponents have been calibrated to core samples but there are still uncertainties. There are also large uncertainties around the value of the formation water resistivity R_w. The water flooding program has been ongoing for years and the seawater has a different chemical composition than the formation water. There is a possible effect on the resistivity.

There are lithological effects that have not been accounted for which makes the two estimated saturations differ in some intervals and fit in others. There is also a possibility for presence of gas. The gas signal should appear between the water and oil T_2-peak. In this study this possibility has not been investigated but it is important to have in mind that there could be other fluids than oil and water present. This should be investigated in more detail in the future.

Despite the many uncertainties the NMR-derived saturation demonstrates comparable results with the Archie-saturation.

9.5 PERMEABILITY

The permeability index given in the end product report from the service company has only a qualitative value. It is supposedly only for detection of high and low permeable zones and not a quantification of the permeability. There are two main NMR permeability equations; Coates and SDR. The SDR equation proved to be inappropriate for this case because of the presence of hydrocarbons. An investigation of the impact of the bound fluid volume definition was conducted and revealed that the 92 ms cutoff was better.

An attempt to improve the parameter values of the NMR permeability estimation by comparing it to the PORPERM-permeability values was conducted. This was in order to elaborate a quantitative permeability estimation equation. It was carried out by finding more appropriate values for the Coates permeability equation constants. A function quantifying the difference between the NMR-based and PORPERM-based permeability was defined and minimized (by changing the parameters).

The original 'b' value was found to be too high; a more suitable value would be a value of approximately 0.4 because the blind tests gave a value range from 0.38 to 0.43. Given a 'b'-value of 0.4, the 'a' parameter was optimized to be 33.871.

These values all fitted well within the interval between the low and high case of the PORPERM permeability. However, they are based on only five wells. When more data from new wells come available, this exercise should be redone including all the wells. For now, the recommendation is to use the values of 'a' and 'b' in Table 3 for estimation of the permeability based on NMR data:

TABLE 3: PROPOSED PARAMETER VALUES FOR COATES' PERMEABILITY EQUATION

a	33.87
b	0.4

The recommended equation for permeability estimation is then given by Eq. 27:

$$k_{Coates} = \left(\left(\frac{PHIT}{a}\right)^2 * \frac{FFI}{BVI}\right)^b = \left(\left(\frac{PHIT}{33.87}\right)^2 * \frac{FFI}{BVI}\right)^{0.4} \quad (27)$$

9.6 WATERFLOOD SURVEILLANCE

The method applied in the field cases is not as straightforward as using a constant cutoff for bound fluid calculations. This is because a suitable value has not been found yet. One value that works fine for one well may be misleading for other wells. The lack of core material complicates this method. The standard value is 92 ms for carbonates, but the one core study done on Tor Fm. recommend a value of 28 ms. The bound fluid volume from using 28 ms as cutoff is low, sometimes only 2%. Other times is gives the same values as using 92 ms. It is hard to determine an appropriate Bound Fluid Cutoff based on one data point but it is most likely to be closer to 28 ms than 92 ms because of the very small pores in chalk compared to carbonates in general.

The applied method consists of analyzing the T_2-distribution itself and its behavior. It exhibits two distinct peaks; one from the oil signal, the other from the water signal. The water peak increases in amplitude and shifts to slower relaxation times in these particular intervals. This corresponds to the behavior of the T_2-distribution with varying water saturation discussed more in detail in Chapter 6.1.

The NMR data are not the only argument for the interpretation of movable water. It is supported by geological interpretations. According to these interpretations faults are seen on the Density Image Logs which could increase water movement in the reservoir.

9.7 APPLICABILITY IN GEOSTEERING

The MagTrak tool which has been used for these five investigated wells is a LWD-tool. It is run while drilling the well and can provide real-time data. Because of this it may be used in Geosteering. Traditionally the log data used in Geosteering are Gamma Ray, Resistivity and Neutron-Density porosity. These tools provide information on clay content, porosity and fluid saturations (through the resistivity). Information on permeability may be obtained indirectly through the PORPERM-relation. NMR data also provide porosity, saturation and permeability, but it can also indicate if there is movable water present. It does not require nuclear sources that in some cases cannot be run downhole due to operational risks and HSSE requirements.

A limitation to MagTrak is its shallow depth of investigation of only two inches. This shallow DOI means that the tool is very sensitive to poor borehole conditions. This has been previously observed in some of the wells. Another limitation is the distance to the drilling bit. MagTrak is generally situated at the end of the BHA. As seen in 2/8-G3_T3, MagTrak was situated nearly 50 meters behind the bit behind the other logging tools. A combination of a shallow DOI and a large distance to bit decreases the utility for application in Geosteering. It is possible to shorten this distance but that can possibly sacrifice the data quality due to drilling induced motion. If the data quality is sufficiently good this will add valuable information to the decision making process during Geosteering.

Despite the delay of NMR data while drilling it is useful information that should be acquired. Usually only LWD tools are run in the reservoir sections, therefore it is essential to acquire all important information during drilling, thus also the NMR data.

9.8 OTHER APPLICATIONS

There are several other applications of NMR data. Amongst them are irreducible water saturation, fluid characterization, wettability and capillary pressure curves. This study did not include the investigation of these applications because the study focused on the optimization of the current usage.

Another reason is that some of these applications require diffusion effects as a relaxation mechanism. MagTrak has a constant gradient field; therefore there are no diffusion effects in the T_2-measurements. Currently the only way of getting diffusion effects also, is to use a wireline NMR tool. The diffusion effect can be exploited for fluid characterization and other complex NMR analysis. In the future technological advances may allow for this to be incorporated in the LWD acquisition.

10 CONCLUSION

The current use of NMR data on Valhall has been restricted to a secondary source of porosity. With its potential to do much more, this thesis has now investigated these possibilities and proposed an optimized exploitation of NMR data.

- A workflow for the quality control process has been proposed. This workflow aims to classify the data into three quality categories. The categories are; bad quality(not to be used), yellow (use with care) and green (trusted to be representative)
- The NMR tool proves to be reliable as a porosity tool and can by all means replace the Neutron-Density logging tool if there are HSSE restrictions to the use of this.
- The NMR-derived saturation is reliable though it does not give exactly the same values as the traditional Archie-equation.
- NMR is a powerful tool in the waterflood surveillance. Three case studies were presented to illustrate this. NMR can differentiate between pore sizes when the water saturation is sufficiently high. Thereby it can classify the water as bound or movable which helps the understanding of the water flooding.
- New parameter values for the Coates' permeability equation show good results and should be applied rather than the former ones. They provide a more trustworthy estimation.
- It can provide valuable information for decision making during the Geosteering process. The value of this information increases as the tool is put closer to the bit.
- This study investigated the most applicable utilizations that are currently being used. Future needs may require other applications and they should be investigated.

11 RECOMMENDATIONS AND FURTHER WORK

The applicability of NMR data on Valhall is promising. There are still needs of calibration material and other information. It is recommended to:

- When nuclear sources cannot be used, run the NMR tool as a replacement.
- Use NMR for distinction of bound and movable water in questions related to waterflood surveillance.
- Get NMR core and log data from one and same well. This will increase the confidence in the calibration parameters.
- Take mud filtrate samples for NMR calibration when drilling. It is important information for further work.
- Investigate the possibility of presence of gas as this cannot be ruled out.
- Acquire NMR data with diffusion effects so that fluid characterization (and gas detection) can be conducted.

NOMENCLATURE

SYMBOLS

a	Equation Parameter for Permeability Equations
b	Equation Parameter for Permeability Equations
B_0	External Static Magnetic Field
B_1	Oscillating External Magnetic Field
D	Diffusion Coefficient
f	Larmor Frequency
FFI/BVI	Free to Bound Fluid Ratio
G	Field Strength Gradient
h	Planck's constant
k	Boltzmann's constant
k	Permeability (md)
I	Spin Quantum Number of Nucleus
m	Archie cementation exponent
M_0	Net Magnetic Moment per Unit Volume
$M_z(t)$	Net Magnetization in the z-Direction as a Function of Time
MPHS	NMR Total Porosity
n	Number of Echoes
n	Archie Saturation Exponent
N	Nucleus density in the Formation
PHIT	Total Porosity
r	Pore Radius
R_t	True Formation Resistivity (Ohm.m)
R_w	Formation Water Resistivity (Ohm.m)
S_o	Oil Saturation
S_w	Water Saturation (v/v)
S/V	Surface to Volume Ratio

t	Time
T_1	Longitudinal Relaxation Time
T_2	Transverse Relaxation Time
T_{2GM}	T_2 Geometric Mean
T_K	Absolute Temperature (in Kelvin)
TE	Echo Time
TW	Wait Time

γ	Gyromagnetic Ratio
η	Fluid Viscosity
θ	Angle for which the Protons are flipped when the External Field B_1 is applied
π	Pi (3.1415…)
ρ	Density
ρ_1	Surface Relaxivity for Longitudinal Relaxation
ρ_2	Surface Relaxivity for Transverse Relaxation
ρ_g	Gas Density
τ	Time for which the Oscillating Magnetic Field is applied to the Formation
φ	Porosity

ABBREVIATIONS

4C	Four Components
4D	Four Dimensional (x,y,z direction and time)

ART	Applied Reservoir Technology
BFV	Bound Fluid Volume
CALI	Caliper
CBW	Capillary Bound Water
CPMG	Carr Purcell Meiboom Gill
DOI	Depth Of Investigation
FFI	Free Fluid Index
FID	Free Induction Decay
Fm.	Formation
GR	Gamma Ray
HCC	HydroCarbon Cutoff
HCPV	HydroCarbon Pore Volume
LoFS	Life of Field Seismic
LWD	Logging While Drilling
MICP	Mercury Injection Capillary Pressure
md	millidarcy
ms	unit, milliseconds
m MD	meter Measured Depth
MPERM	NMR-derived Permeability
MPHE	NMR Effective Porosity
MPHS	NMR Total Porosity
MSIG	NMR Porosity (from MRIL tool)
NMR	Nuclear Magnetic Resonance

OBM	Oil Based Mud
OBS	Ocean Bottom Seismic
PAPS	Phase Alternating Pulse Sequence
PHIT	Total Porosity
PORPERM	POR–PERM, relation giving permeability as function of porosity
PP	PoroPerm, MagTrak acquisition mode
PP+LHC	PoroPerm + Light Hydrocarbon, MagTrak acquisition mode
pu	Porosity Units (give in percentage)
QC	Quality Control
RA	Running Average
RF	Radio Frequency
ROP	Rate Of Penetration
SDR	Schlumberger-Doll-Research NMR permeability equation
SW	Water Saturation
SW_VARY	NMR-derived water saturation calculated by a variable cutoff
S/N	Signal to Noise Ratio
WBM	Water Based Mud

REFERENCES

Andersen M., *Petroleum Research in North Sea Chalk,* Amoco Norway Oil Company and Rogaland Research, 1995

Barkved O., Heavey P., Kjelstadli R., Kleppan T., Kristiansen T., SPE, BP, *Valhall Field – Still on Plateau after 20 Years of Production*, Offshore Europe 2003, Aberdeen, UK, 2-5 September 2003

Coates G. R., Xiao L. Z., Primmer M. G., *NMR Logging Principles and Applications*, Houston: Gulf Publishing Company, USA, 2000

Van Gestel J.P., Barkved O., Kommedal J., BP Norge AS, *Valhall Life of Field Seismic Automated Workflow*, SEG Annual Meeting, San Antonio, TX, 2007

Glennie K. W., *Petroleum Geology of the North Sea: Basic Concepts and Recent Advances*, 4th Edition, Blackwell Science ISBN: 9781444313413

Howard J., Hermansen H., Vedvik A., *NMR-Based Water Saturation Estimates in Ekofisk Waterflood Zones,* 6th Nordic Symposium on Petrophysics, Trondheim Norway, May 15-16, 2001

Hürlimann M. D., Venkataramanan L., Flaum C., Speier P., Karmonik C., Freedman R., Heaton N., *Diffusion-Editing: New NMR Measurement of Saturation and Pore Geometry*, SPWLA September 2002

Kenyon W. E., *Petrophysical Principles of Applications of NMR Logging*, appeared in The Log Analyst March-April, 1997

Mao Z., Kuang L., Sun Z. , Luo X., Xiao L., *Effects of Hydrocarbon on Deriving Pore Structure Information from NMR T2 data,* SPWLA 48th Annual Logging Symposium, June 3-6, 2007

McKeon D., Cao Minh C., Freedman R. Harris R., Willis D., Davies D., Gubelin G., Oldigs R., Hürlimann M., *An Improved NMR Tool Design for Faster Logging*, SPWLA 40th Annual Logging Symposium, May 30-June 3, 1999

NMR Carbonate Rock Catalogue, Applied Reservoir Technology (ART), 1998

Timur A., *Nuclear Magnetic Resonance Study of Carbonate Rocks*, the Log Analyst, 1972

Ånensen K., *Application of downhole NMR in chalk reservoirs*, Project report in the course TPG4530 at the NTNU Norwegian University of Science and Technology, Trondheim, 2014

Core Study Reports are all BP internal documents.

APPENDICES

A. CORE STUDIES

Over the years some NMR core studies have been conducted. The objective was determination of calibration parameters. Although core data are considered correct there are limitations to it. Cores are handled roughly, first during the coring process and then when they are brought up to surface and to the lab. Downhole in the virgin formation there is a confining pressure and a pore pressure that exert an effective stress on the rock. This stress "compacts" the rock, so the rock expands when it is brought up to surface and pore collapse due to the pressure relief may occur. In addition, the core is only representative for a very small volume in the reservoir.

Most core material is from Hod Fm. because the Tor Fm. cores are in such a bad condition that lab measurements not are possible.

2/8-A1 and 2/8-A24 NMR Core Study (1998)

This study was the very first NMR study on cores from the Valhall field. The core samples were taken from two wells; 2/8-A1 and 2/8-A24, from the Hod 4 member. The objectives were to find calibration parameters for bound water volume and permeability predictions and to study the relation of the NMR T_2-distributions to capillary pressure curves.

The cores were first cleaned. Then standard porosity and permeability measurements were done. Next they were saturated with brine (20 000ppm NaCl solution) and the NMR measurements were done. Finally Mercury Injection Capillary Pressure (MICP) tests were done on the cores.

The acquisition parameters are given in Table A-1. No partially saturated core measurements were done.

TABLE A- 1: ACQUISITION PARAMETERS FOR NMR CORE STUDY 2/8-A1 & 2/8-A24

TW (ms)	5000
TE (ms)	0.33
NW	2048
NAVG	400

The observations were as follows:

- Relaxivity of 5.6 micron/sec for Hod 4
- Bound water in chalks is more appropriately predicted using a tapered cutoff.
- From the T_2-distribution curves (100% brine saturated), the peak which reflects the pore size distribution, lies around 20ms.

A summary of the calibration values are given below in Table A-2

TABLE A- 2: SUMMARY FROM NMR CORE STUDY 2/8-A1 & 2/8-A24

Function	Parameters	
Relaxivity	ρ (micron/sec)	5,6
Coates-Timur	a	40,1
Permeability Equation	b	0,94
SDR Permeability	a	152
Equation	b	1,4
Fixed T2 Cutoff	T2CF (ms)	16
Tapered Cutoff	T2CT (ms)	5
Minimum Wait Time	TW (ms)	0,4

2/8-F14 and 2/8- A6_A (1998)

This NMR Core study was the first to have NMR data from both cores and well logs. The NMR log data are of the MRIL type, and its quality is questionable. The objectives were to find calibration parameters for NMR bound water and permeability predictions, and to investigate the relations of NMR properties to other petrophysical properties. The core samples were measured in two stages; first a "fresh state" and then a 100% brine-filled state. Firstly, NMR measurements were done on the "fresh state" cores, then they were cleaned and saturated with a 20 000ppm NaCl solution. NMR measurements were then once more conducted on the cores. The acquisition parameters are given below in Table A-3 (fresh-state/brine-filled). At the end MICP tests were conducted.

TABLE A- 3: ACQUISITION PARAMETERS FOR NMR CORE STUDY 2/8-F14 & 2/8.A6_A

TW (ms)	5000
TE (ms)	1.0 / 0.33
NW	2048
NAVG	40
Frequency f (MHz)	5.0 / 2.2

On the fresh state samples a Hydrocarbon Cutoff of 250 ms was applied to separate water from oil in the T_2-distribution. Bound water calibration was derived from MICP. Both fixed and tapered T_2-cutoffs were derived. For the permeability, parameters for Coates-Timur and SDR equations were derived. Table A-4 summarizes the main results:

TABLE A- 4: SUMMARY FROM NMR CORE STUDY 2/8-F14 & 2/8.A6_A

Function	Parameters	Tor	Hod
Relaxivity	ρ (micron/sec)	2.04	2.27
Coates-Timur Permeability Equation	a	40	40
	b	0.9	0.9
SDR Permeability Equation	a	243	243
	b	1.6	1.6
Fixed T2 Cutoff	T2CF (ms)	28	18
Tapered Cutoff	T2CT (ms)	8.7	11
Minimum Wait Time	TW (ms)	1	0.4

The study also stated that the 100% brine-filled samples had peaks centered around 40 ms for Tor Fm. samples and 15 ms for Hod Fm. samples.

NMR Chalk Study for Amoco 2/11-10S(T2) (2004)

A core was drilled in the Hod 2 Formation in well 2/11-S10(T2) for extensive NMR laboratory measurements. The objective was to determine the ability of NMR to provide information regarding porosity, permeability, irreducible water saturation and pore size distribution in the chalk formation. Standard core measurements, NMR measurements and MICP tests were done. The study investigated the NMR responses from brine filled and partially oil filled plugs and the effect of a gradient field. The NMR work was divided in two parts. In the first part NMR measurements were done on 12 brine filled plugs and from those five were selected for further NMR measurements. In this second part measurements were done at irreducible water saturation containing oil as the other pore fluid and at 100% brine. Both with constant gradient field and with zero gradient. The measurements were done on Numar's Core-Spec-100. The acquisition parameters are given in Table A-5

TABLE A- 5: SUMMARY OF NMR CHALK STUDY FOR AMOCO 2/11-10S(T2)

TW (ms)	5000
TE (ms)	0.5 / 1.0 / 2.0
NW	2048
NAVG	400
Frequency f (MHz)	1

The report concluded with

- For oil saturations (S_o) larger than 30% the Coates equation provides a more reasonable permeability.
- A Bound Fluid T_2-Cutoff of 12.91ms should be used.
- The Coates permeability equation with the derived parameters is:
  - $MPERM_{Coates} = \left(\frac{MPHS}{65.5}\right)^2 * \left(\frac{FFI}{BVI}\right)^2$
- The SDR permeability equation with the derived parameters is:
  - $MPERM_{SDR} = 0.0102 * e^{0.0692 * T_{2GM}}$

ART NMR Carbonate Rock Catalogue (1998)

This catalogue is a library of variations in relaxation time responses for different carbonate rocks. Oil companies have provided core material to ART as a joint research project to create this collection. The catalogue enables companies and others to initiate independent research projects on NMR responses in carbonate reservoir rocks. The library does not give any results because it is meant as a tool for research and studies. The samples consist of two small whole-cores of length less than half a meter. From that, three small core samples were taken to do the measurements on. One whole-core is from Tor Fm. and one is from Hod Fm. Both samples are from the well 2/8-F2.

The brine-filled sample T_2-distributions give the pore size distribution. In Figure A-1 the T_2-distributions measured at TE=1ms are for Tor Fm. samples (to the left) and Hod Fm. samples (to the right). Tor Fm. samples demonstrate a peak around 47 ms and Hod Fm. samples a peak around 80 ms.

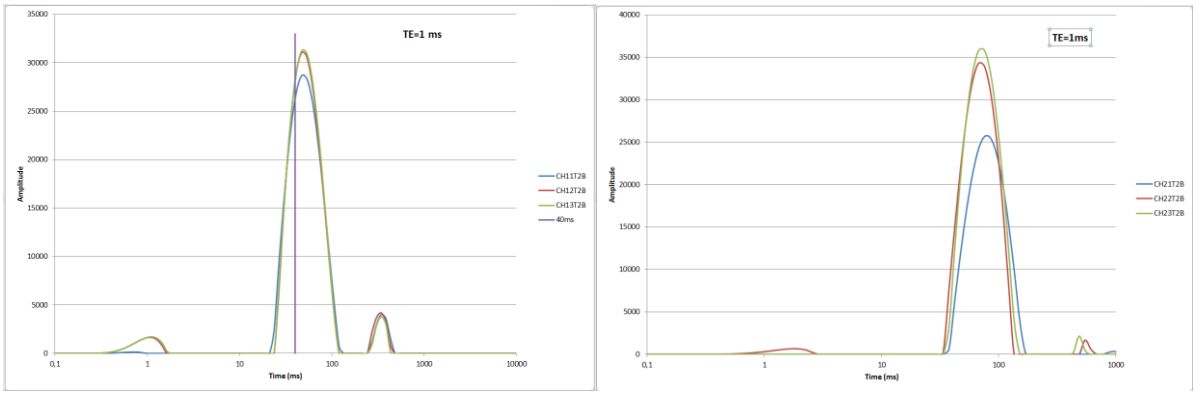

FIGURE A 1: T2-DISTRIBUTIONS FOR TOR FM. (TO THE LEFT) AND HOD FM. (TO THE RIGHT)

This catalogue had no objective of deriving calibration parameters but it can serve for pore size determination and water flooding monitoring.

B. Standard Template for Post-Logging QC

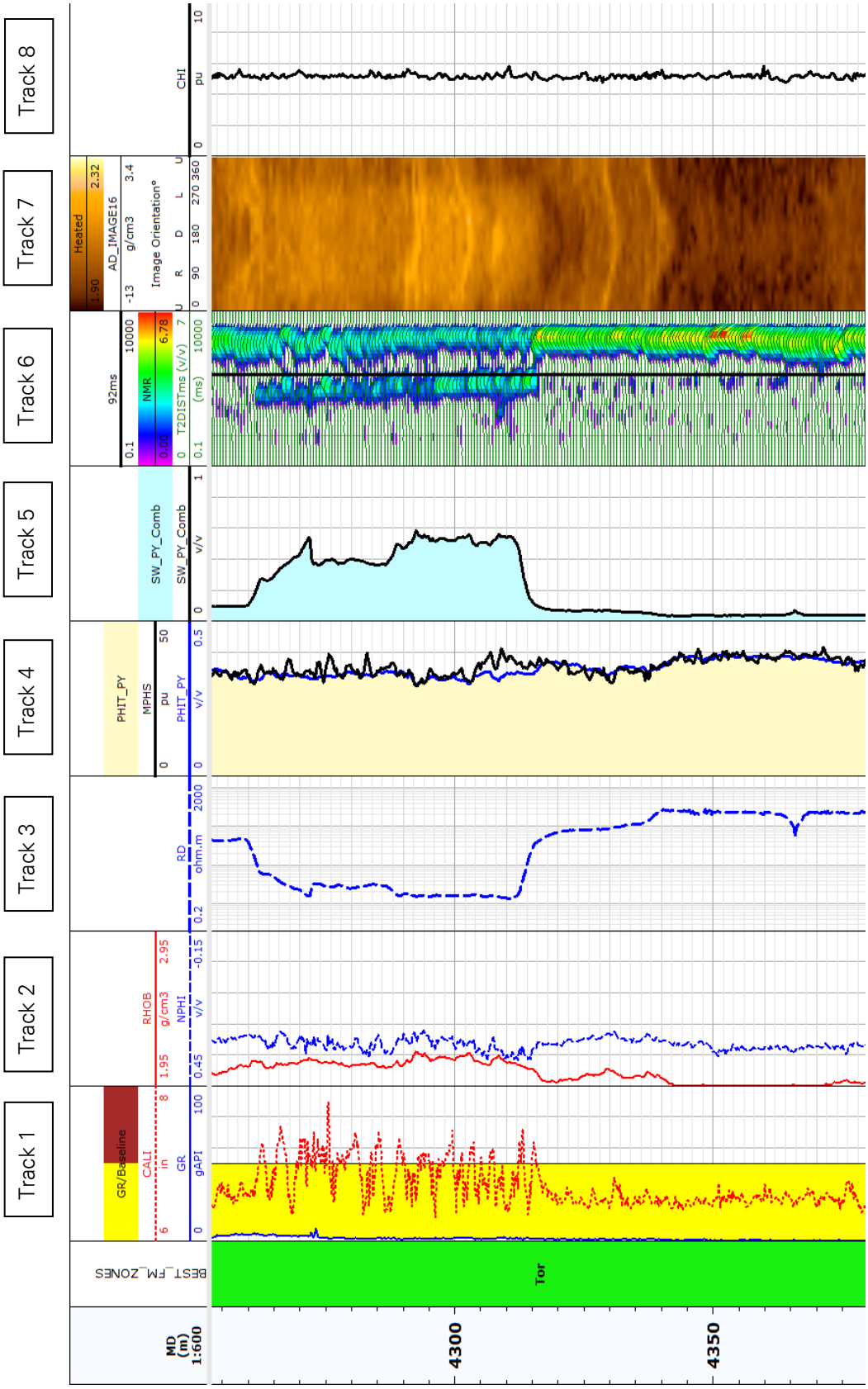

C. Log Curve Abbreviations

The abbreviations may have a suffix added to it with an underscore symbol, those are explanatory

AD_IMAGE16	Image Log based on Density
CALI	Caliper
CHI	Chi factor, NMR Quality Indicator
CUTOFF	Cutoff value which separates T_2-distribution into two separate groups
GR	Gamma Ray
k	Computed permeability
MPERM	Magnetic Resonance Permeability
MPHS	Magnetic Resonance Total Porosity
NPHI	Neutron Porosity
PHIT	Total Porosity (from RHOB)
PORPERM	Permeability from Core Porosity – Permeability calibration study
RD	Deep Resistivity
RHOB	Bulk Density
SW	Water Saturation
T2DISTms	T_2-ditribution given in milliseconds
##ms	Constant line of ## value, used in T_2-distribution

D. QC FLOW CHART

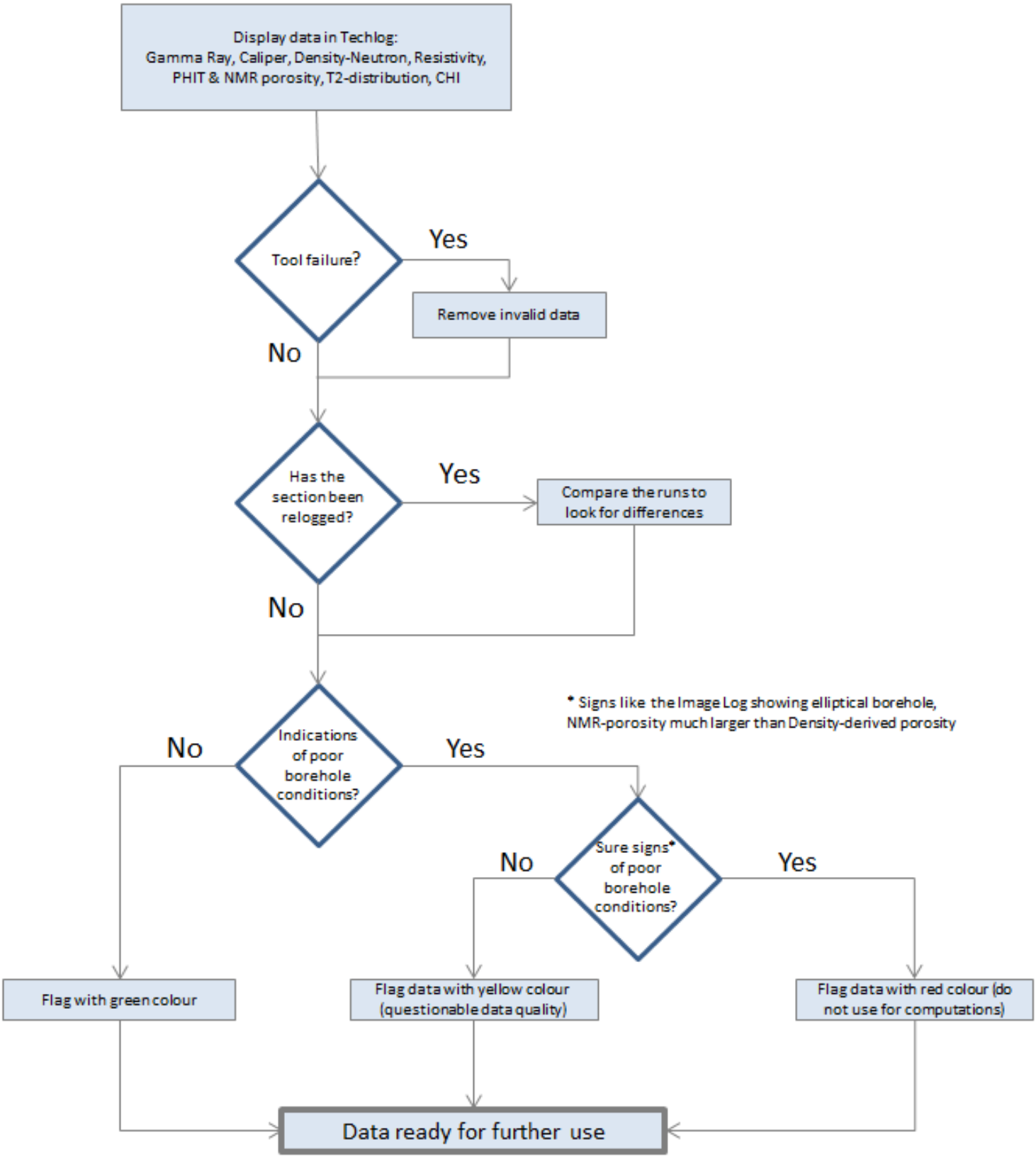

E. SATURATION DATA

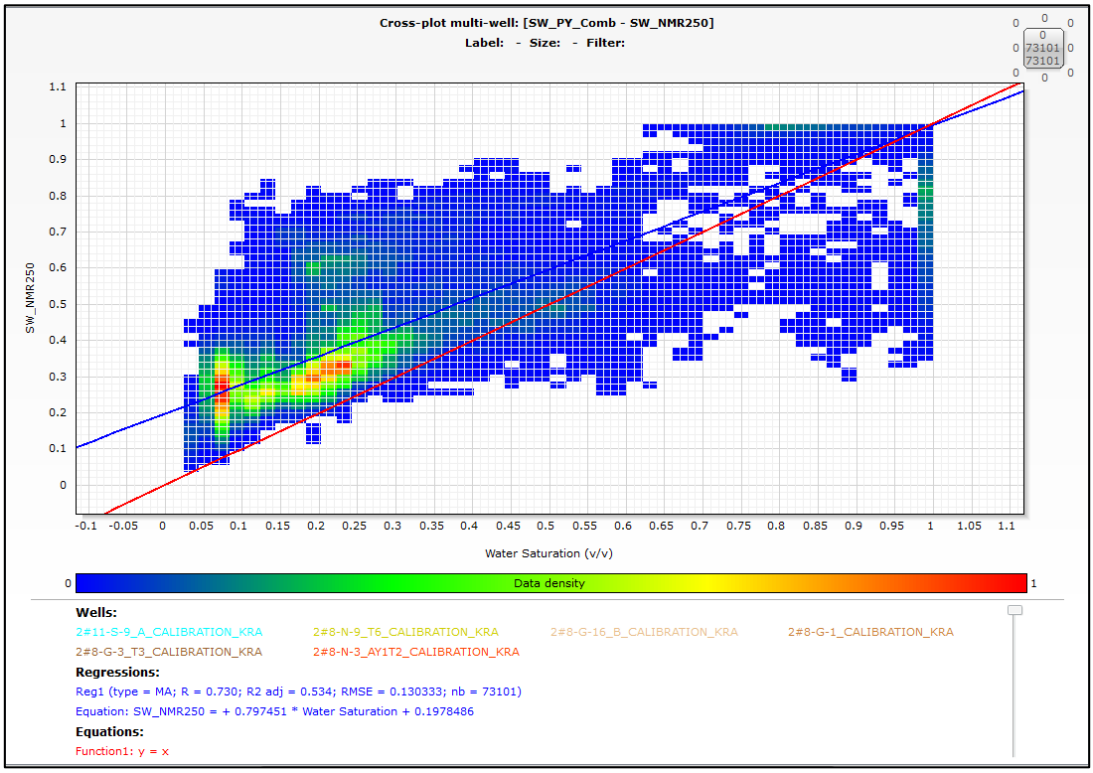

FIGURE 42: MULTIWELL CROSSPLOT OF ARCHIE SW (X-AXIS) VS. NMR SW (250MS CONSTANT CUTOFF)ON THE Y-AXIS, ALL FORMATIONS

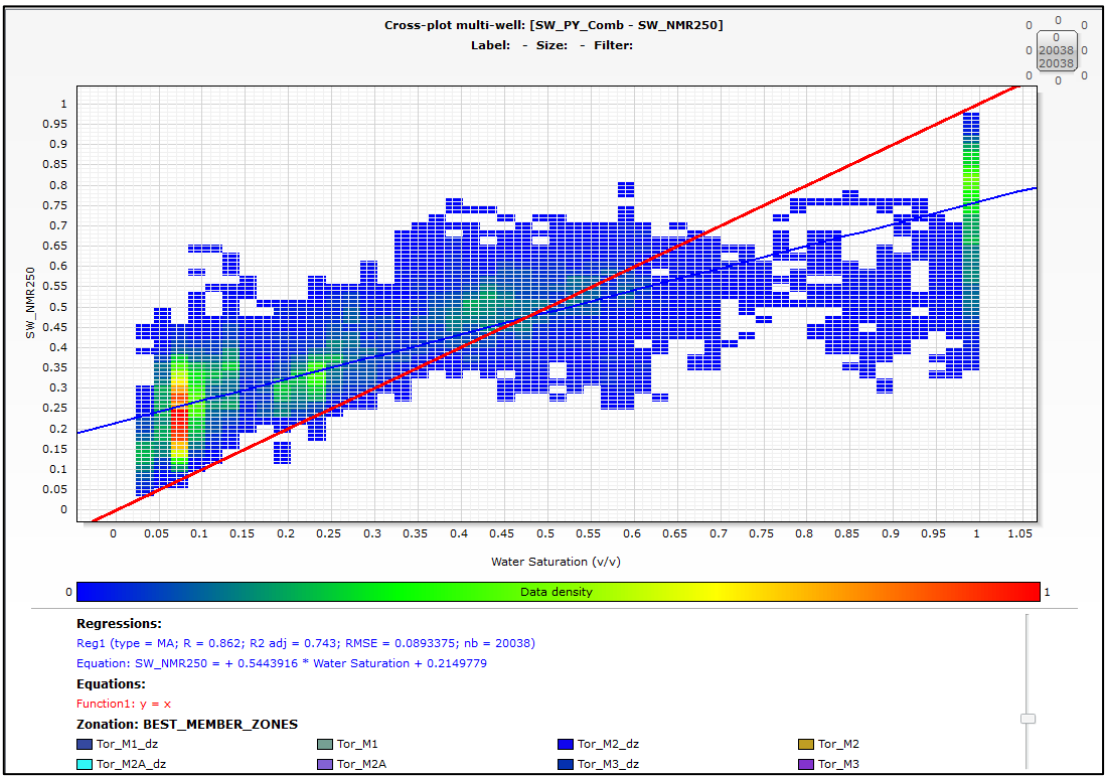

FIGURE 43: MULITWELL CROSSPLOT, ARCHIE SW (X-AXIS) VS. NMR SW (250MS CONSTANT CUTOFF) ON THE Y-AXIS. ONLY TOR FM

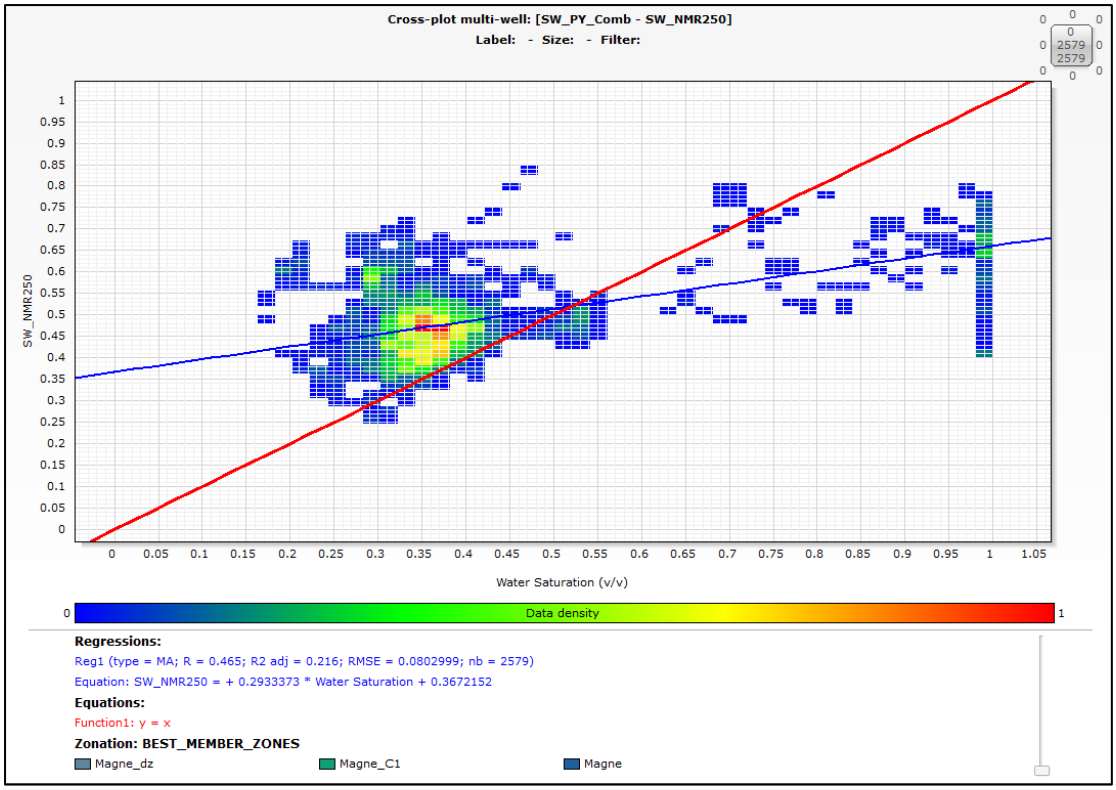

FIGURE 44: MULTIWELL CROSSPLOT, ARCHIE SW(X-AXIS) VS. NMR SW (Y-AXIS) USING 250 MS CONSTANT CUTOFF, ON THE Y-AXIS. ONLY MAGNE FM.

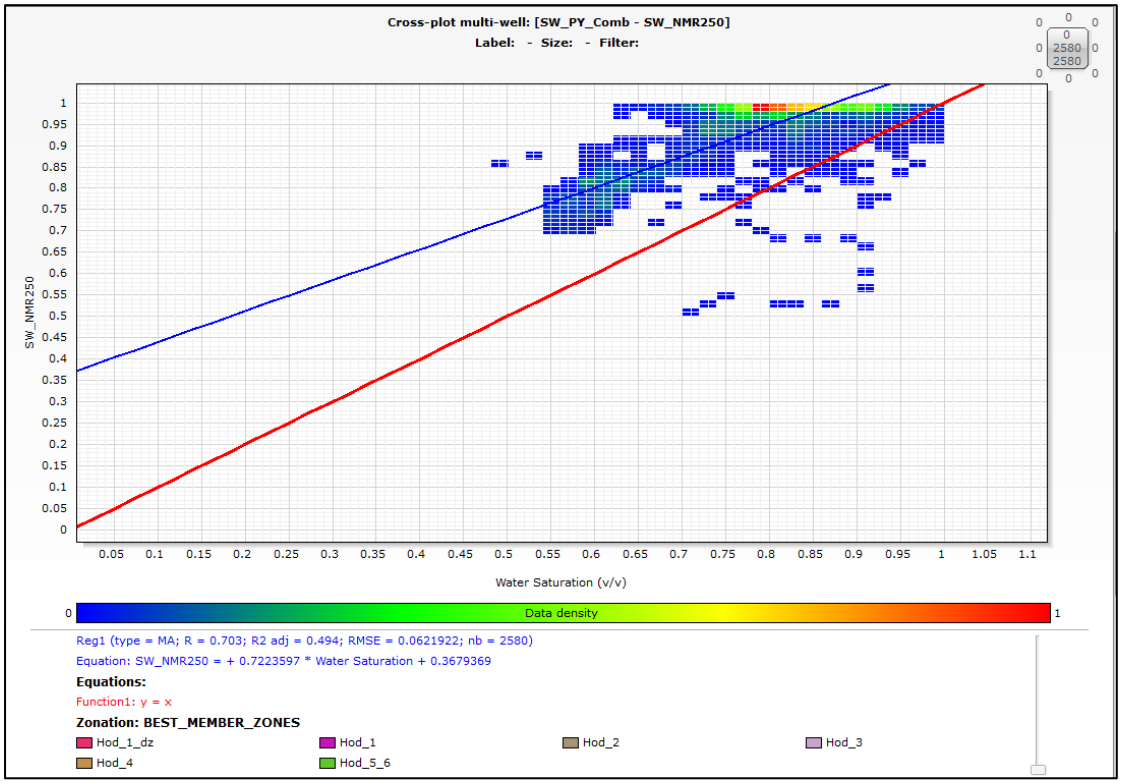

FIGURE 45: MULTIWELL CROSSPLOT, ARCHIE SW(X-AXIS) VS. NMR SW (Y-AXIS) USING 250 MS CONSTANT CUTOFF, ON THE Y-AXIS. ONLY HOD FM.

F. PERMEABILITY DATA

TABLE F 1: OPTIMIZED VALUES OF 'B' EXCLUDING ONE WELL FROM THE PROCESS TO DO A BLIND TEST

Excluded Well	a	b
2/8-G1	40	0,4220
2/8-G3_T3	40	0,3150
2/8-G16_B	40	0,4335
2/8-S9_A	40	0,3822

For Figure 46 to 49 the blue curve is the PORPERM base case permeability, the red curve is the original Coates' Permeability estimation (a=40, b=0.9) and the green curve is the optimized version of Coates' Permeability estimation keeping 'a' constant and equal to 40 and varying 'b' to fit the PORPERM base case permeability the best possible way. Where the curves are a straight line there data points have been removed due to poor borehole conditions.

Figure 50 to 54 contain the Coates' permeability estimation with both 'a' and 'b' optimized. This was done in a two-step process; first by keeping a=40 constant and varying 'b' (using all five wells). The optimized 'b'-value was 0.4. Then keeping b=0.4 and varying 'a' which gave a=33.87. The blue curve is the PORPERM low case permeability, the green curve is the PORPERM high case permeability and the purple curve is the Coates Permeability estimation with the parameter values a=33.87 and b=0.4.

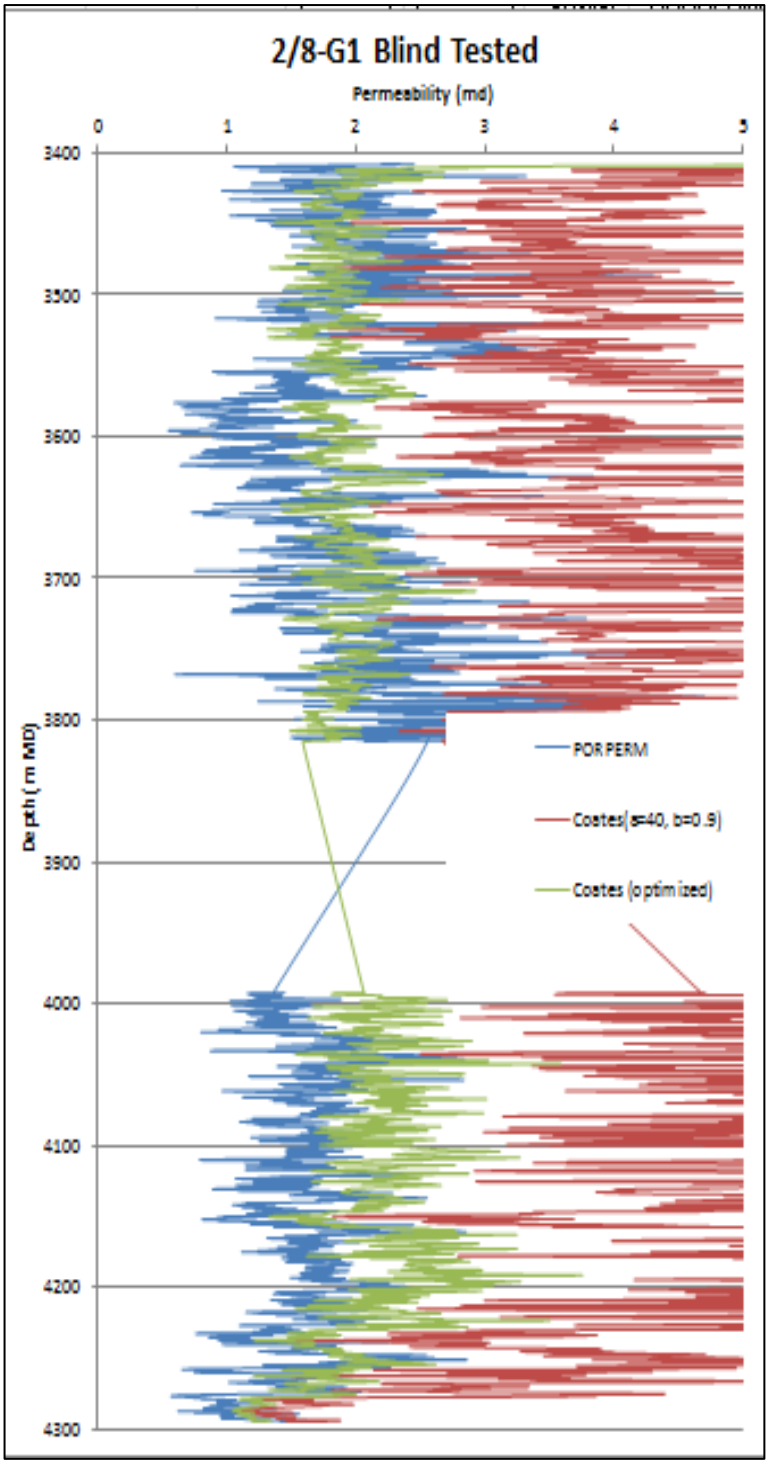

FIGURE 46: 2/8-G1 BLIND TESTED

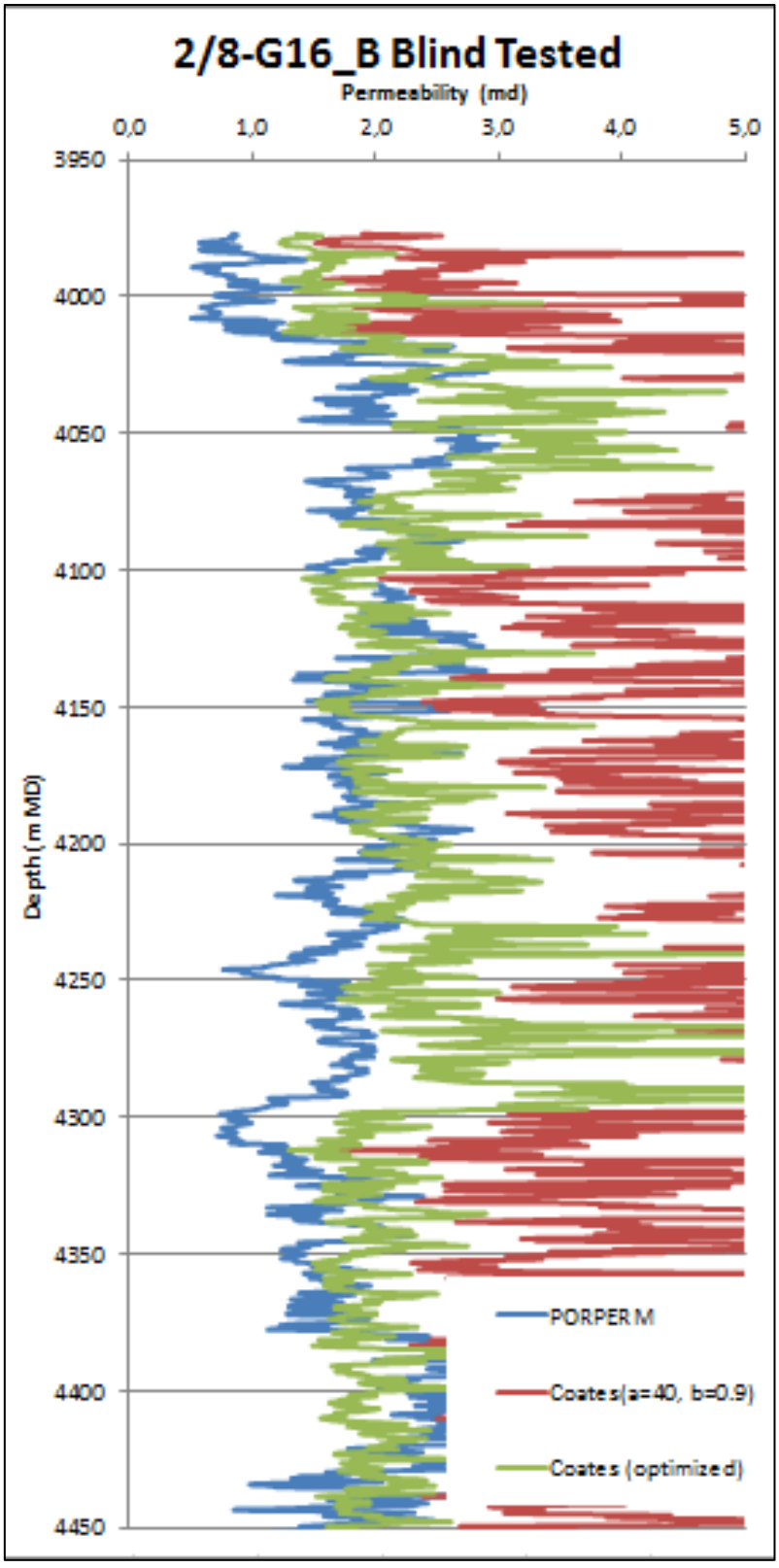

FIGURE 47: 2/8-G16_B BLIND TESTED

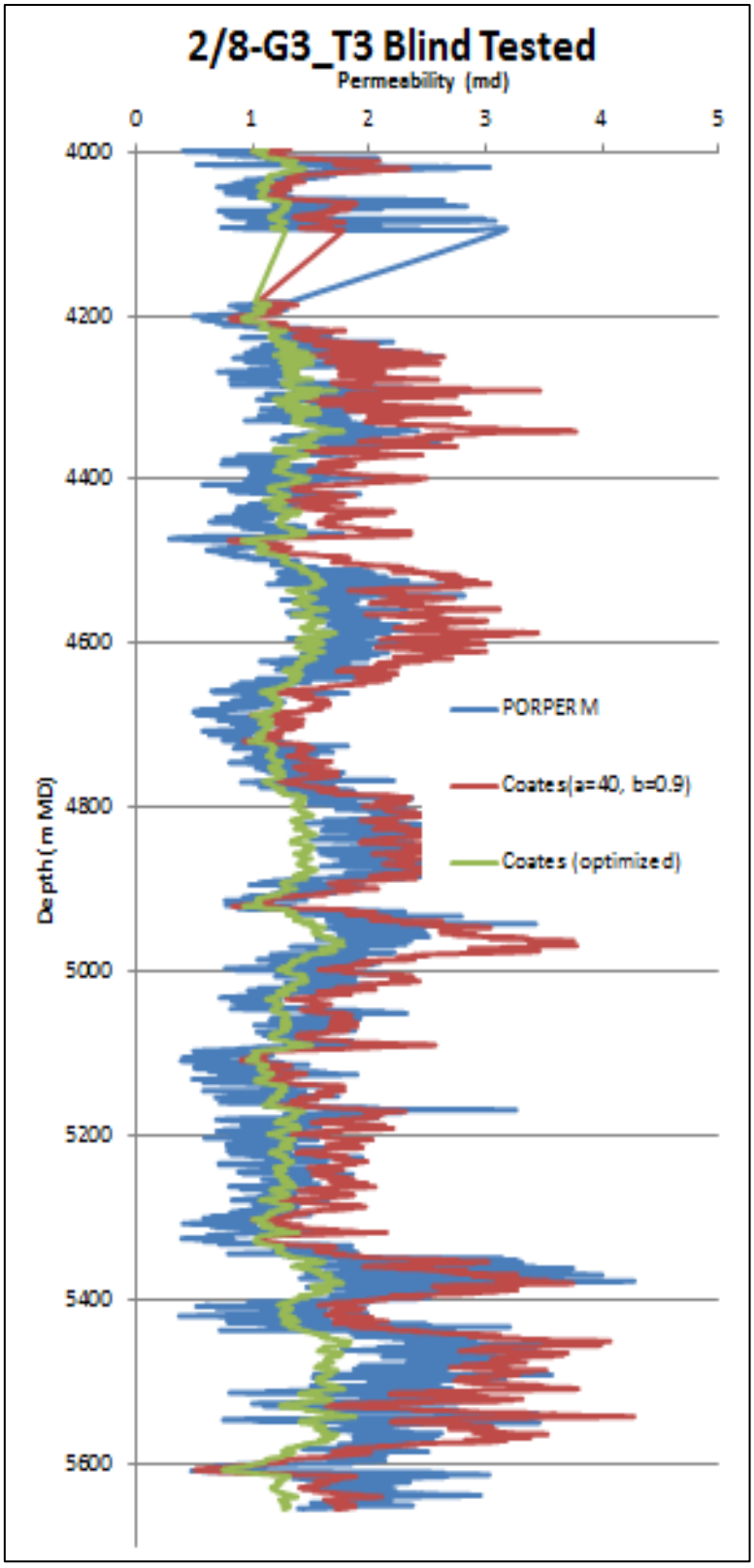

FIGURE 48: 2/8-G3_T3 BLILND TESTED

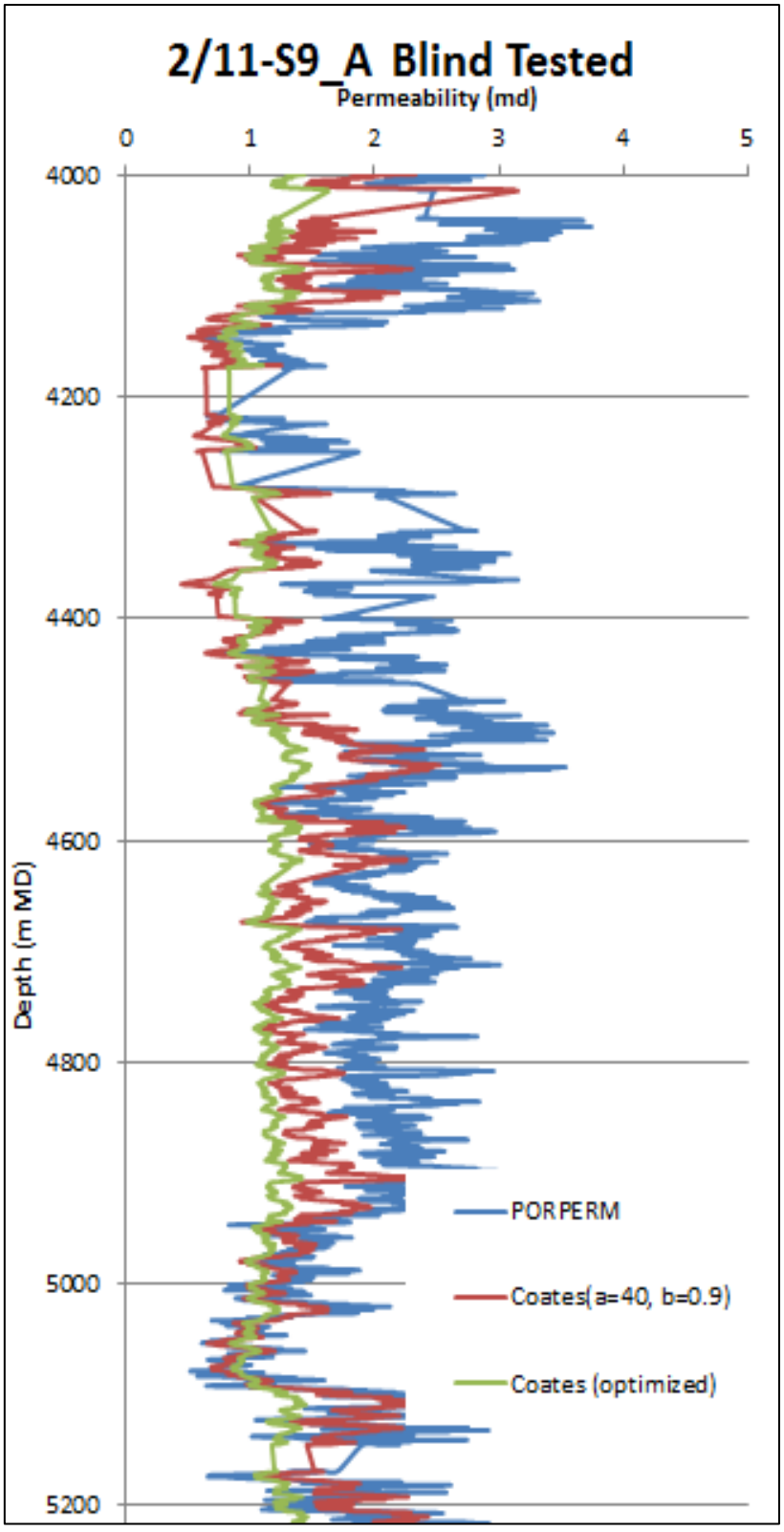

FIGURE 49: 2/11-S9_A BLIND TESTED

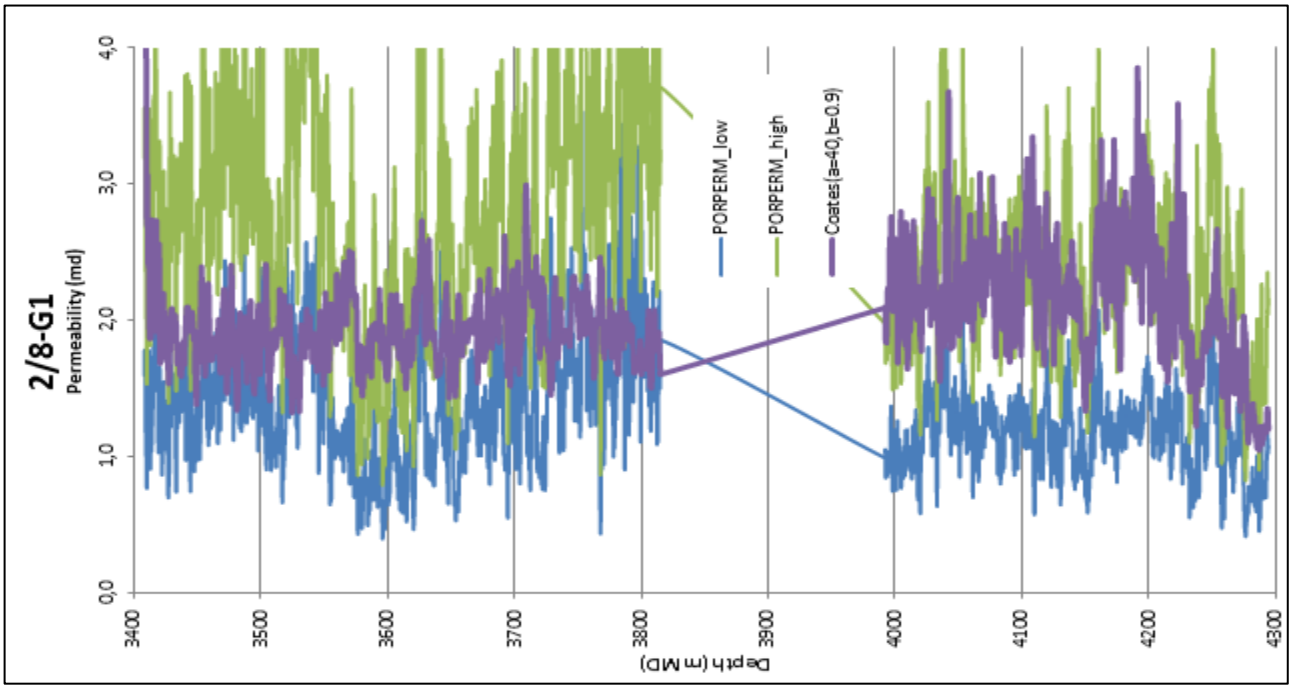

FIGURE 50: 2/8-G1, OPTIMIZED COATES AND HIGH & LOW CASE PORPERM

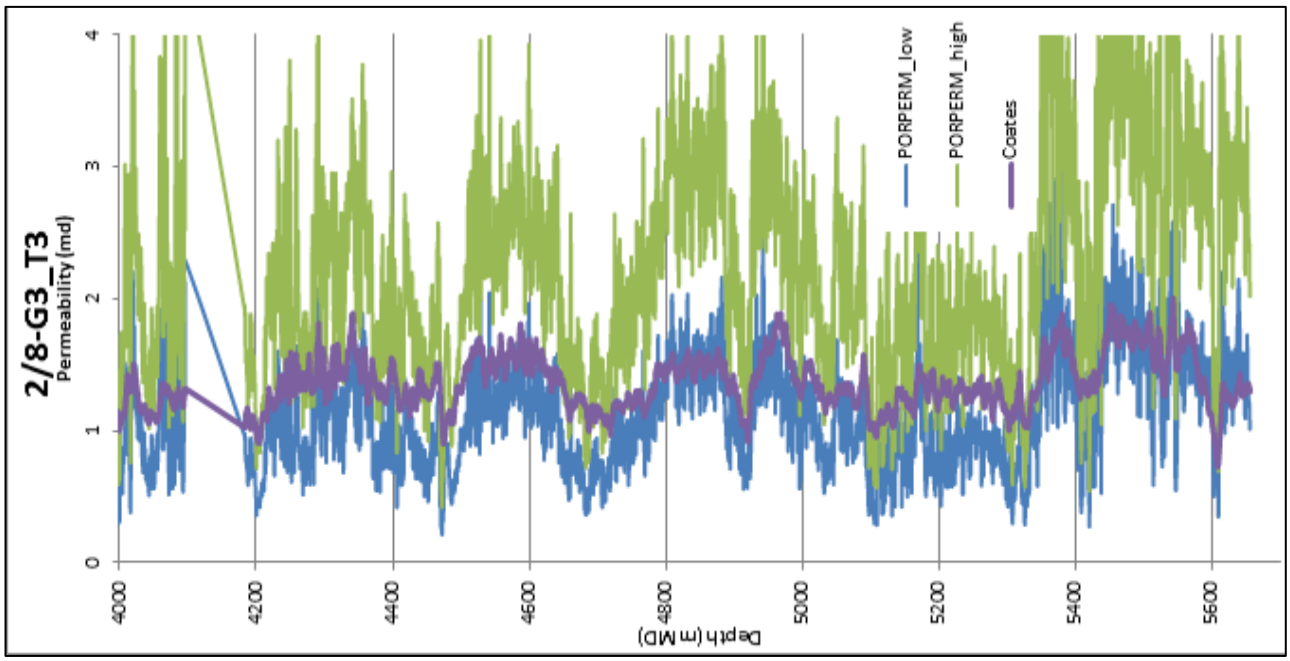

FIGURE 51: 2/8-G3_T3, OPTIMIZED COATES AND HIGH & LOW CASE PORPERM

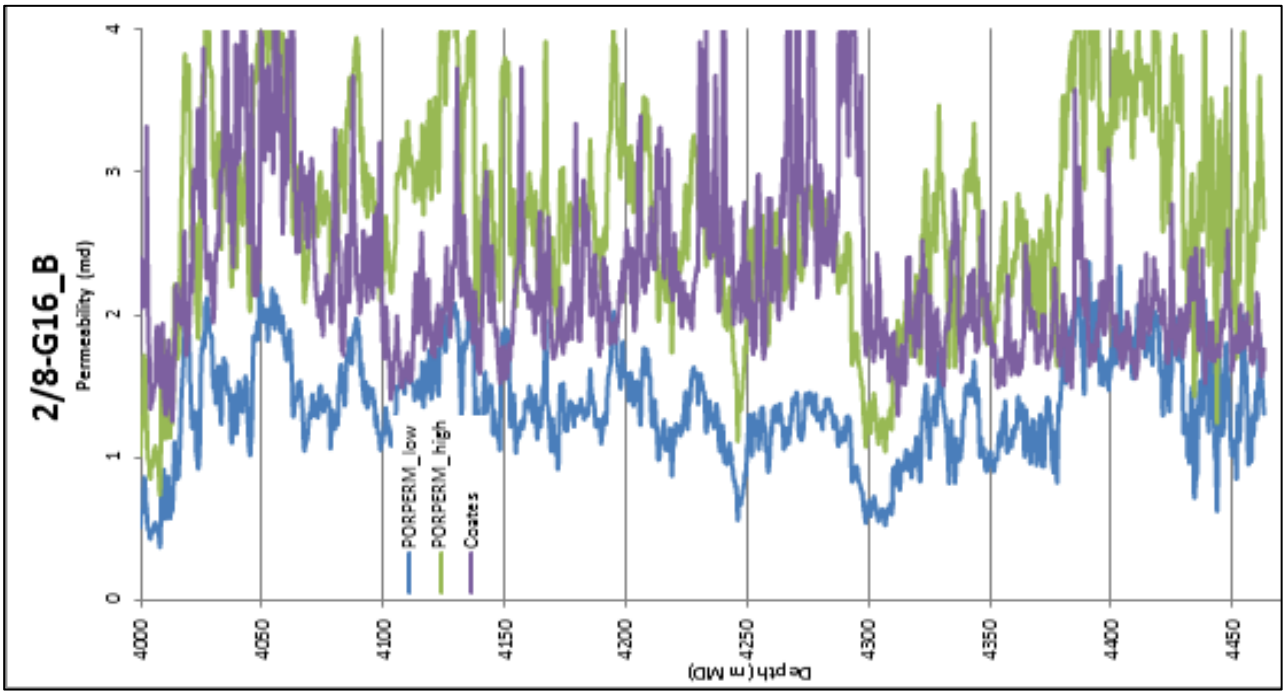

FIGURE 52: 2/8-G16_B, OPTIMIZED COATES AND HIGH & LOW CASE PORPERM

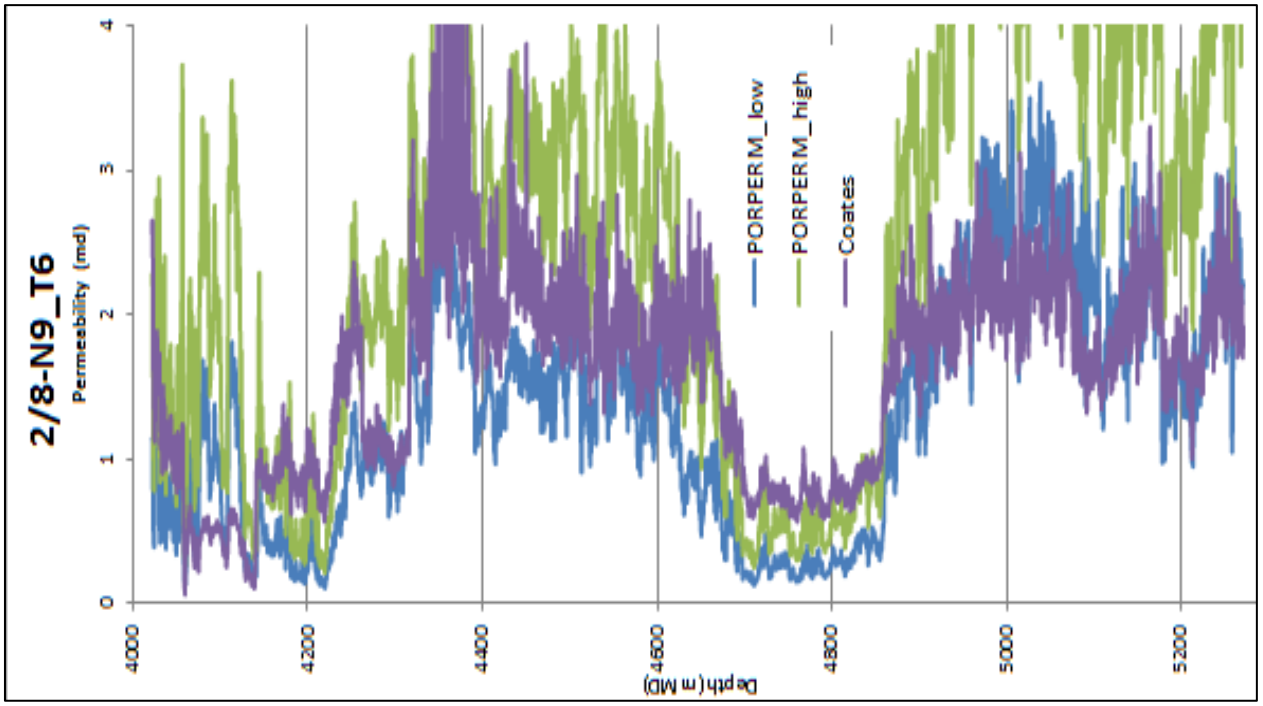

FIGURE 53: 2/8-N9_T6, OPTIMIZED COATES AND HIGH & LOW CASE PORPERM

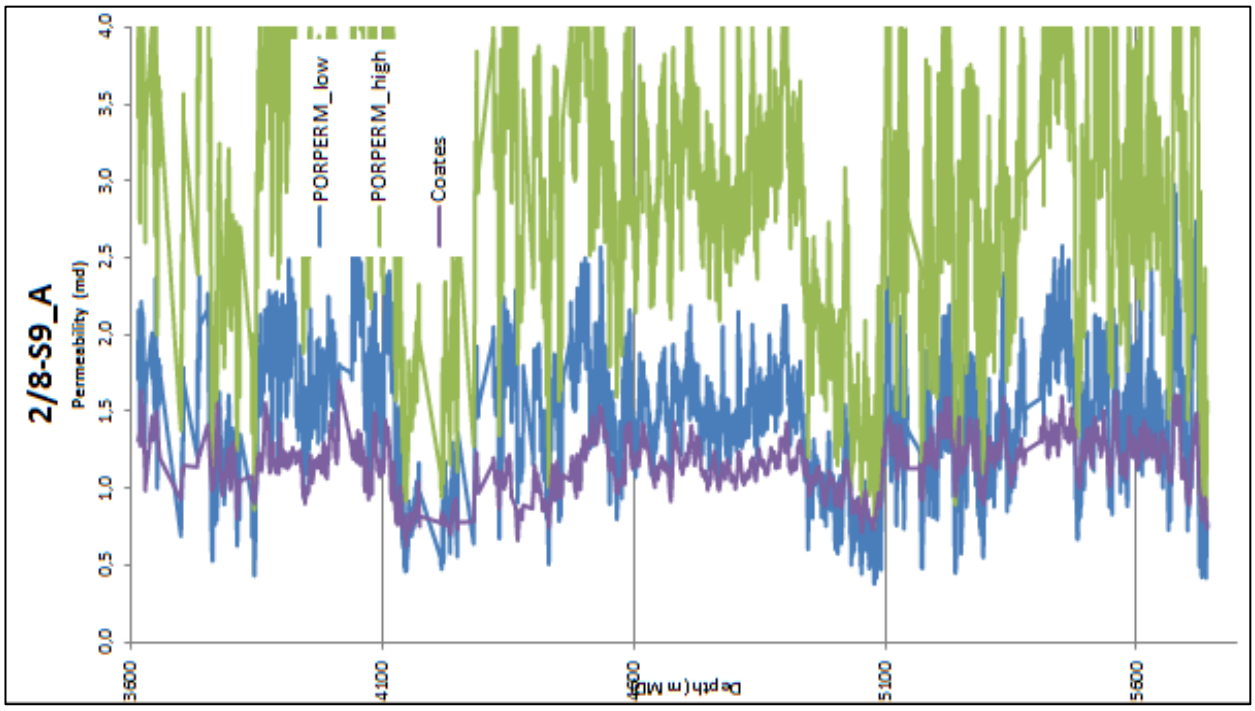

FIGURE 54: 2/11-S9_A, OPTIMIZED COATES AND HIGH & LOW CASE PORPERM